IMPROVED DROUGHT EARLY WARNING AND FORECASTING TO STRENGTHEN PREPAREDNESS AND ADAPTATION TO DROUGHTS IN AFRICA

DEWFORA

A 7th Framework Programme Collaborative Research Project

Downscaled and tailor made hydrological models for the Limpopo and Niger case study basins

WP4-D4.7

October 2012

Coordinator:	Deltares, The Netherlands
Project website:	www.dewfora.net
FP7 Call	ENV-2010-1.3.3.1
Contract no.	265454

Page intentionally left blank

DOCUMENT INFORMATION

Title	Downscaled and tailor made hydrological models for the Limpopo and Niger case study basins
Lead Author	UNESCO-IHE
Contributors	PIK
Distribution	<Please select one of three below> PP: Restricted to other programme participants (including the Commission Services) RE: Restricted to a group specified by the consortium (including the Commission Services) CO: Confidential, only for members of the consortium (including the Commission Services)
Reference	WP4-D4.7

DOCUMENT HISTORY

Date	Revision	Prepared by	Organisation	Approved by	Notes
20/09/2012	1	P. Trambauer	UNESCO-IHE		
09/10/2012	2	S. Fournet	PIK		
14/10/2012	3	P. Trambauer	UNESCO-IHE		
18/10/2012	4	S. Maskey	UNESCO-IHE		
05/11/2012	5	S. Maskey	UNESCO-IHE		
05/11/2012	6	P. Trambauer	UNESCO-IHE		

ACKNOWLEDGEMENT

The research leading to these results has received funding from the European Union's Seventh Framework Programme (FP7/2007-2013) under grant agreement N°265454

Page intentionally left blank

SUMMARY

This report presents the hydrological models that have been developed in the DEWFORA project, which will serve as a tool for hydrological drought forecasting. Two process based hydrological models were chosen to simulate the hydrology of the Limpopo and Niger river basins. The models are adapted to represent some region specific conditions in the basins, e.g. large irrigation areas and wetlands.

For the Limpopo river basin case study, a downscaled version of the global PCR-GLOBWB hydrological model is selected. This is continuous-time simulation, process based distributed model applied on a cell-by-cell basis. The model includes various water storages and flow components including surface, sub-surface and groundwater flows, soil moisture availability, canopy interception and snow storage. New development includes an irrigation scheme to account for the highly modified hydrology in the Limpopo river basin. The model is set up for the Limpopo basin with a spatial resolution of 0.05 x 0.05˚ and simulation is carried out for the past 32 year-period on a daily time step. Runoff data available from the basin are used for the verification of the model results. The model is also tested for identifying historic droughts in the basin and to estimate hydrological drought related indices. The drought identification is done with both a spatially distributed indicator as well as with a runoff indicator in specific discharge stations. The model will be subsequently employed in the project to simulate short to mid-term hydrological drought forecasting.

For the Niger case study, the eco-hydrological model SWIM is selected and tailored to reproduce past drought events with monthly bias corrected reanalysis climate datasets. SWIM is a daily continuous-time, semi distributed catchment model for the coupled hydrological / vegetation / water quality modelling in mesoscale watersheds. The model is set-up and calibrated to represent region specific processes, stocks and fluxes by using regional ground-truth and remote sensing data. The model enables to consider various water storages and flow components such as soil moisture availability, surface, sub-surface and groundwater flows. Further developments integrate now reservoir management, wetlands and inundation plain dynamics to account for specific hydrological patterns encountered in the Niger case study. The advancements of the calibration and validation processes for two model setups are presented in the report. The model will be then employed to simulate short to mid-term hydrological forecast and long term hydrological projections in order to assess drought persistence and risk under a range of upstream water resources management.

Page intentionally left blank

TABLE OF CONTENTS

LIST OF FIGURES

LIST OF TABLES

LIST OF ACRONYMS

BFG	Bundesanstalt für Gewässerkunde
CCAM	Conformal-cubic atmospheric model
CMIP	Coupled Model Intercomparison Project
CORDEX	COordinated Regional climate Downscaling Experiment
CRU	Climate Research Unit
DEM	Digital Elevation Model
DNM	Direction Nationale de la Météorologie, Mali
ECMWF	European Centre for Medium-Range Weather Forecasts
ERAI	ERA-Interim
FAO	Food and Agriculture Organization
GCM	Global Climate Model
GHM	Global Hydrological Model
GIS	Geographic Informaiton System
GLC2000	Global Land Cover 2000
GLCC	Global land cover characteristics
GPCC	Global Precipitation Climatology Centre
GPCP	Global Precipitation Climatology Project
GRASS	Geographic Resources Analysis Support System
GRDC	Global Runoff Data Centre
HRUs	Hydrological Responses Units
HWSD	Harmonized World Soil Databas
IIASA	International Institute for Applied Systems Analysis
ISI-MIP	Inter-Sectoral Impact Model Intercomparison Project
LBPTC	Limpopo Basin Permanent Technical Committee
NBA	Niger Basin Authority
NSE	Nash–Sutcliffe model efficiency coefficient
PCR-GLOBWB	PCRaster GLOBal Water Balance Model
PEST	Model-Independent Parameter Estimation and Uncertainty Analysis
QDR	Direct runoff
QSf	Interflow
QBf	Baseflow
RCM	Regional Climate Model

SAGA	System for Automated Geoscientific Analyses
SRTM	GLC2000
STARS	Statistical Analog Resampling Scheme
SWAT	Soil and Water Assessment Tool
SWIM	Soil and Water Integrated Model
WATCH	Integrated Project Water and Global Change
WMO	World Meteorological Organization

1. INTRODUCTION

The DEWFORA project has several objectives. One of them is to increase the performance of drought forecasting in Africa by implementing state-of-the-art techniques in meteorological, hydrological, and agricultural drought forecasting. Hydrological models are usually used to simulate the effects of periods of precipitation shortfall on water resources (surface or subsurface discharges, groundwater, soil moisture, etc.). The results of such hydrological models can be used to compute spatially distributed drought indicators for different time lengths.

Two hydrological models are developed for the Limpopo and Niger basins in Africa for applying as case studies for hydrological drought forecasting. Meteorological data for these model developments were obtained from European Centre for Medium Range Weather Forecasting (ECMWF), UK – a partner in the DEWFORA consortium. The developed hydrological models will be forced with forecasted meteorology in a following stage of this study to obtain hydrological drought forecasting. This report presents the developments and current results of these models for the Limpopo (Chapter 2) and Niger (Chapter 3) basins. These models will be used in the project for short to mid-term hydrological drought forecasting using meteorological forecasts from ECMWF. If necessary, some adjustments to the current version of the models will be made for applying them in a forecasting mode.

2. HYDROLOGICAL MODEL FOR THE LIMPOPO CASE STUDY BASIN

2.1 DESCRIPTION OF THE BASIN

The Limpopo river basin has a drainage area of approximately 415,000 km^2 and is shared by four riparian countries: South Africa (45%), Botswana (20%), Mozambique (20%) and Zimbabwe (15%) (see Figure 2-1).

The climate in the basin ranges from tropical dry savannah and hot dry steppe to cool temperatures in the mountainous regions. Although a large part of the basin is located in a semi-arid area the upper part of the basin is located in the Kalahari Desert where it is particularly arid. The aridity condition, however, decreases further downstream. Rainfall in the basin is characterized by being seasonal and unreliable causing frequent droughts, but floods can also occur in the rainy season The average annual rainfall in the basin is 530 mm, ranging from 200 to 1,200 mm and occurring mainly in the summer months (October to April) (LBPTC 2010). Two distinct seasons are identified in the basin: a summer and rainy season with about 95% of the annual rainfall, and a winter and dry season.

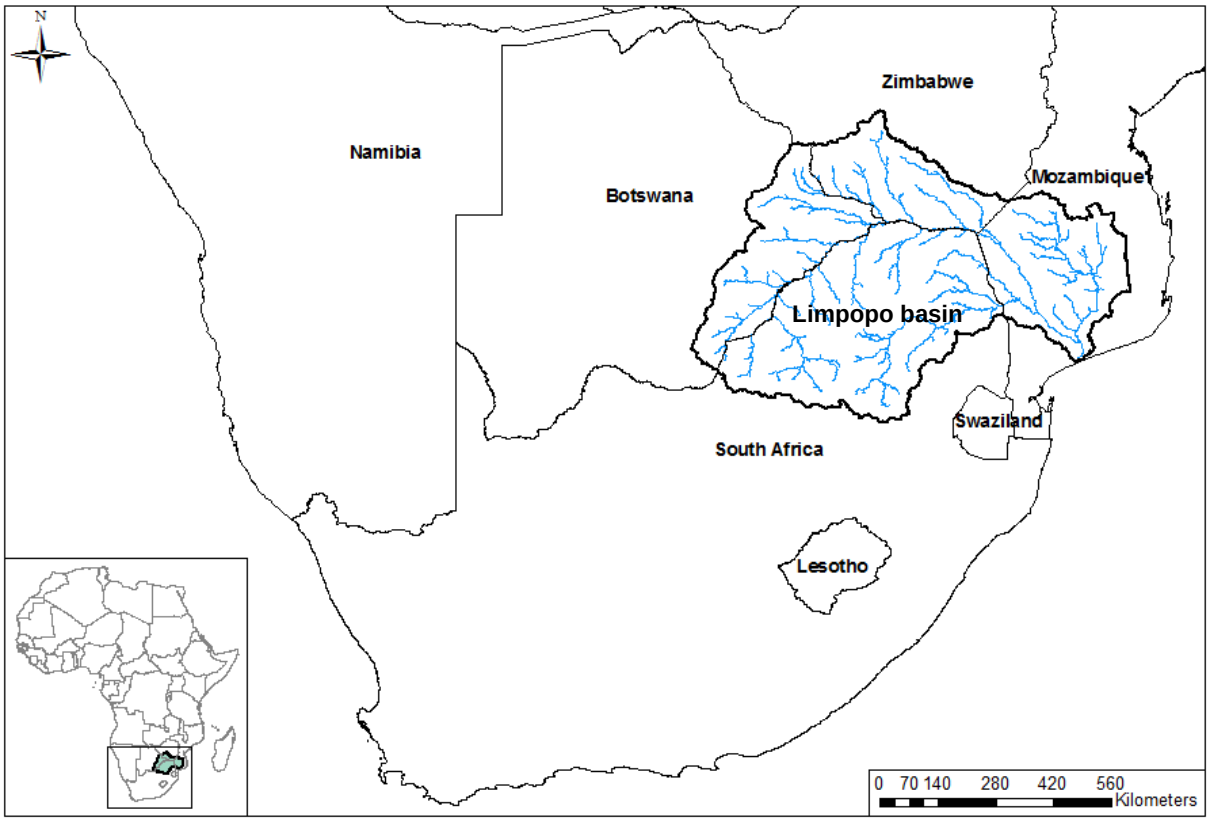

Figure 2-1 Location of the Limpopo river basin

Approximately 14 million people live in the basin and the greatest user of water by sector is irrigation, which takes approximately 50% of the total water demand. In Botswana and Zimbabwe, however, urban supply is the major user. The total estimated present demand is about 4,700 Mm^3/yr, which is almost two thirds of the demand in South Africa, 30% in Zimbabwe, 6% in Mozambique and 2% in Botswana. The total natural runoff generated from rainfall is approximately 7,200 Mm^3/yr showing that a significant portion of the runoff

generated in the basin is currently used. With regards to the water quality, the environmental status of the rivers in the Limpopo River basin varies from natural (in the national parks) to highly modified (e.g. in upper Olifants River) (LBPTC 2010). For a detailed description of the Limpopo River basin the readers are referred to a previous report of this project: Deliverable 6.1, chapter 6 (DEWFORA 2012a).

This basin is particularly challenging for hydrological modeling – which is probably also true for many other arid/semi-arid basins – due to very low runoff coefficient (RC = Q/P) of the basin. Table 2-1 presents runoff coefficients for various parts of the basin based on available observed runoff data and rainfall data (see Section 2.3.2 and 2.3.3) used in this study. For station 24 (Table 2-1), which has the largest drainage area with available discharge data for this study (Figure 2-7), the runoff coefficient is just about 3.1% for the naturalized discharge and merely 0.4% for the observed discharge (without naturalization). Note that the naturalized discharge is estimated as observed discharge plus the estimated extraction. These runoff coefficients are strikingly low: out of 506 mm of annual rainfall only 18 mm (basin average) turned into runoff annually including abstraction. To put it into a perspective, if we neglect storage change in the basin in a long term, one mm error made in the estimate of annual actual evaporation could result in nearly 6% error in the runoff and 1% error in the actual evaporation could cost more than 25% error in runoff estimates. Moreover, the uncertainty in the rainfall input could easily be larger than the runoff coefficient (3.1%) of the basin. As seen in Table 2-1, only 4 stations show runoff coefficients large than 10% and they represent relatively very small sub-basins. Another challenge in modeling this basin is that it is a highly modified basin, which is also clear from the observed and the naturalized runoff from the basin (Table 2-1). For example for the largest drainage outlet available (station 24), the observed annual discharge is just about 12% of the naturalized discharge, which means that the abstraction from the basin is 88% of the total runoff.

Table 2-1 Runoff characterization of the Limpopo basin

Station	Period witout Missing data			Basin Area	Precipitation	Q observed	Abstractions	Q naturalized	Q naturalized /	Q observed /
	From	To	No. Years	(km2)	(mm/yr)	(mm/yr)	(mm/yr)	(mm/yr)	Precipitation * 100	Precipitation * 100
1	01-01-01	31-12-10	10	201,001	494	6.2	8.9	15.0	3.0	1.2
2	01-01-79	31-12-97	19	42,714	648	14.6	25.8	40.3	6.2	2.2
3	01-01-95	31-12-10	16	16,622	694	26.3	28.2	54.6	7.9	3.8
4	01-01-79	31-12-10	32	3,256	748	45.8	2.7	48.5	6.5	6.1
5	01-01-79	31-12-09	31	1,801	627	18.4	18.8	37.3	5.9	2.9
6	01-01-79	31-12-10	32	1,171	667	21.4	30.3	51.8	7.8	3.2
7	01-01-79	31-12-10	32	1,054	556	25.8	5.0	30.8	5.5	4.6
8	01-01-79	31-12-02	24	638	637	74.5	23.6	98.2	15.4	11.7
9	01-01-79	31-12-06	28	517	648	8.1	12.3	20.5	3.2	1.3
10	01-01-79	31-12-00	22	514	791	287.6	18.8	306.4	38.7	36.4
11	01-01-79	31-12-99	21	6,731	538	46.7	46.8	93.5	17.4	8.7
12	01-01-83	31-12-96	14	20,627	633	5.0	47.8	52.8	8.3	0.8
13	01-01-88	31-12-96	9	22,270	651	6.4	48.6	54.9	8.4	1.0
14	01-01-82	31-12-10	29	6,110	611	4.9	49.0	53.9	8.8	0.8
15	01-01-79	31-12-10	32	7,483	625	19.4	20.3	39.6	6.3	3.1
16	01-01-79	31-12-97	19	3,786	630	30.2	28.5	58.7	9.3	4.8
17	01-01-98	31-12-10	13	4,319	589	39.4	25.9	65.3	11.1	6.7
18	01-01-79	31-12-00	22	98,240	539	4.4	14.9	19.3	3.6	0.8
19	01-01-03	31-12-10	8	15,845	478	4.1	8.9	13.0	2.7	0.9
20	01-01-87	31-12-10	24	12,286	713	37.9	6.9	44.8	6.3	5.3
21	01-01-03	31-12-10	8	46,583	601	25.7	30.5	56.2	9.3	4.3
22	01-01-88	31-12-95	8	49,826	602	10.2	29.6	39.8	6.6	1.7
23	01-01-01	31-12-10	10	259,436	500	8.2	9.4	17.5	3.5	1.6
24	01-01-83	31-12-92	10	342,000	506	1.9	14.0	15.9	3.1	0.4

2.2 GENERAL DESCRIPTION OF THE HYDROLOGICAL MODEL

The hydrological model used for the Limpopo river basin is the downscaled and adapted version of the "PCR-GLOBWB-Africa" model. This "PCR-GLOBWB-Africa" is a continental scale version of the distributed global hydrological model PCR-GLOBWB (PCRaster GLOBal Water Balance Model) (van Beek and Bierkens 2009), which was set up for the African continent in an earlier stage of this project. The PCR-GLOBWB was one of the 16 different land surface and hydrological models reviewed earlier in the project - deliverable D4.5 (DEWFORA 2011). The review identified a number of models including PCR-GLOBWB which can potentially be used for hydrological drought studies in large river basins in Africa. PCR-GLOBWB is a grid-based model of global terrestrial hydrology that was developed (and has been continuously updated) in Utrecht University, The Netherlands by R. van Beek and M. Bierkens. On the global and continental scale the model was applied with 0.5˚ x 0.5˚ spatial resolution, which was downscaled to a finer resolution of 0.05˚ x 0.05˚ (approximately 5 km x 5 km) to cover the entire Limpopo basin. A brief description of the model – largely based and extracted from van Beek and Bierkens (2009) and van Beek (2008) – is presented here:

- It is a "leaky bucket" type of model applied on a cell-by-cell basis.
- In many ways PCR-GLOBWB is similar to other Global Hydrological Models, but it also includes some new developed concepts including: new and advanced schemes for sub-grid parameterization of surface runoff, interflow and baseflow, and added explicit routing of surface water flow using the kinematic wave approximation; dynamic inundation of floodplains; a reservoir scheme; and a routine for lateral water

transport of latent heat from which the water temperature and river ice thickness can be calculated.

- PCR-GLOBWB calculates for each grid cell and for each time step (daily) the water storage in two vertically stacked soil layers (max. depth 0.3 and 1.2 m) and an underlying groundwater layer, as well as the water exchange between the layers and between the top layer and the atmosphere (rainfall, evaporation and snow melt). The model also calculates canopy interception and snow storage.
- Meteorological forcings are supplied at a daily time step and assumed constant over a grid cell. Sub-grid variability is taken into account by considering separately tall and short vegetation, open water, and different soil types. Short vegetation extracts water from the upper layer only, while tall vegetation extracts water from both soil layers.
- The total specific runoff of a cell consists of saturation excess surface runoff, melt water that does not infiltrate, runoff from the second soil reservoir (interflow) and groundwater runoff (baseflow) from the lowest reservoir. River discharge is calculated by accumulating and routing specific runoff along the drainage network and including dynamic storage effects and evaporative losses from the GLWD inventory of lakes, wetlands and plain from Lehner and Döll (2004).

2.2.1 Meteorological forcing

PCR-GLOBWB can be directly forced with precipitation and potential evaporation from climate models or re-analysis data. If the meteorological forcing does not include potential evaporation, a separate module is available to prepare potential evaporation input for the model externally.

2.2.2 Surface runoff scheme, vertical fluxes and interflow

Specific runoff from a cell consists of overland flow, runoff from the second soil reservoir (interflow) and groundwater runoff (baseflow). Figure 2-2 presents the model conceptualization.

SURFACE RUNOFF

The input to the first soil reservoir consists of net precipitation (non-intercepted part) and snow melt. The sum of net precipitation and excess snow melt infiltrates into the first soil layer if the soil is not saturated, while surface runoff occurs if the soil is saturated. Variability of soil saturation within grid is accounted for by using the improved Arno scheme of Dumenil and Todini (1992) where the fraction of surface precipitation and excess snow melt turned into surface runoff is related to the fraction of saturated soil.

The fraction of saturated soils is computed from the cell-average water storage in the upper reservoir (W), the maximum average storage (W_{max}), the minimum average storage (W_{min}),

and a parameter that defines the distribution of the soil water storage within the larger cell. These parameters all refer to the pervious area in the cell (i.e. not open water) and are based on the FAO gridded digital soil map of the world (FAO 2003).

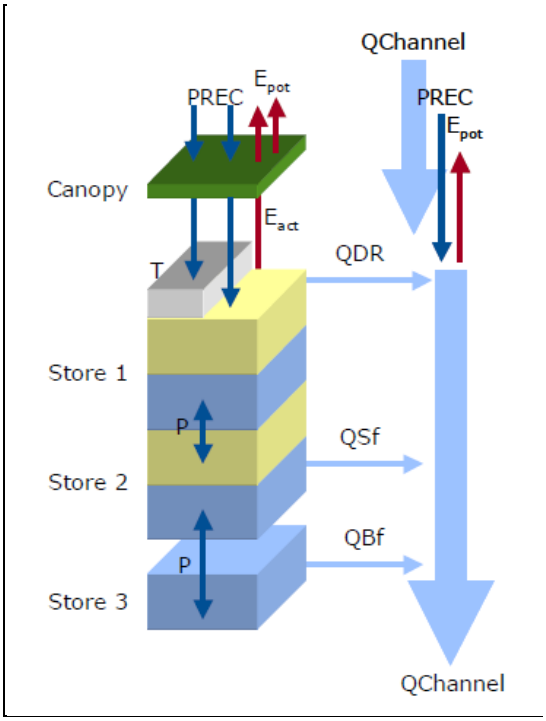

Figure 2-2 Model concept of PCR-GLOBWB: on the left, the soil compartment, divided in the two upper soil stores and the third groundwater store and their corresponding drainage components of direct runoff (QDR), interflow (QSf) and base flow (QBf). On the right the resulting discharge along the channel (QChannel) with lateral in- and outflow and local gains and losses are depicted (van Beek and Bierkens 2009).

VERTICAL WATER EXCHANGE BETWEEN LAYERS

The vertical fluxes (downward fluxes) between the three layers are equal to the unsaturated hydraulic conductivity of the top layer, which is a function of the degree of saturation of the layer. Soil physical relationships for each layer per 0.05˚ x 0.05˚ grid cell were estimated from the distribution of soil types (FAO 2003) and associated tabulated moisture relation and unsaturated conductivity values within the grid cell. For each soil type, the unsaturated hydraulic conductivity and the soil moisture characteristic are modelled according to Clapp and Hornberger (1978) from the derived hydraulic properties (van Beek and Bierkens, (2009).

Capillary rise occurs when the relative degree of saturation of the top layer is smaller than that of the underlying second store. It is driven by the soil moisture deficit in the top layer and is proportional to the unsaturated hydraulic conductivity of the second layer. For the second layer, the capillary rise is described in a similar way, except that the conductivity is the geometric mean of that of the conductivity of the second and the third (groundwater layer), that it only occurs given the proximity of the water table, and that the resulting moisture

content of the second layer cannot rise above field capacity. The capillary rise is therefore a function of the fraction of each cell with a groundwater depth within 5m. It is thus assumed that capillary rise is at maximum if the groundwater level is at the surface and 0 if it 5 m below the surface or below.

INTERFLOW

The interflow occurring in the second soil layer is represented following the simplified approach from Sloan and Moore (1984), which depends on the fluxes from/to first soil layer and groundwater layer, average slope length or drainage distance, saturated and field capacity soil moisture, saturated hydraulic conductivity of the second layer, and average slope. Interflow is only calculated if the soil water content in the second layer is above field capacity. Moreover, the interflow routine is only applied to areas with steep slopes and bedrock, i.e. mountainous areas, and for the fraction of soils with a soil depth smaller than 1.5 m (maximum soil depth in the model) within each grid cell. The soil thickness is derived from the digital soil map of the world (FAO 2003) and is used determine the cell fraction with a soil depth smaller than 1.5m.

2.2.3 Bare soil evaporation and transpiration

To calculate actual bare soil evaporation and transpiration from reference potential evaporation the model follows the following procedure. First, potential reference evaporation E_0 is converted into potential soil evaporation ES_0 and potential transpiration T_0 as:

$$ES_0 = k_{c\,min} E_0 \quad (2.1)$$

$$T_0 = T_c - ES_0 = k_c E_0 - k_{c\,min} E_0 = (k_c - k_{c\,min}) E_0 \quad (2.2)$$

where T_c is the monthly crop specific potential transpiration and k_c and $k_{c\,min}$ are the monthly crop factor and the minimum crop factor for bare soil evaporation respectively. Reductions of the potential bare soil evaporation and the transpiration are directly or indirectly related to the available soil moisture storage. For the bare soil evaporation, no reduction is applicable for the saturated fraction, *x*, of each cell, except that the rate of evaporation cannot exceed the saturated hydraulic conductivity of the upper soil layer. Likewise, the potential bare soil evaporation over the unsaturated area, *1-x*, is only limited by the unsaturated hydraulic conductivity of the upper soil layer:

$$ES = x \min(k_{s1}, ES_0) + (1 - x)\min(k(s_1), ES_0) \quad (2.3)$$

The lack of aeration prevents the uptake of water by roots under fully saturated conditions. Therefore, the fraction of the saturated and unsaturated area within a cell is also considered to determine the actual rate of transpiration.

A climatology of crop factors was developed by van Beek and Bierkens (2009) for the different land surfaces in PCR-GLOBWB that can be used to convert the reference potential evaporation into vegetation specific values. Given the land surface parameterization in PCR-

GLOBWB, these crop factors have to be specified for the fraction open water, short vegetation and tall vegetation respectively, and effective values have been calculated for each 0.05° cell for each month. For the vegetated surface, the GLCC version 2 ((USGS EROS Data Center 2002), mapped at 30 arcseconds) land cover types (Olson 1994a, Olson 1994b) were divided into three categories: natural vegetation, rainfed crops and irrigated crops, where each category was subdivided into tall and short vegetation. Crop factors were calculated from average phenology. van Beek and Bierkens (2009) estimated the Leaf Area Index (LAI) climatology for each GLCC-type, with LAI values per type for dormancy and growing season obtained from Hagemann et al. (1999). An empirical relation by Allen et al. (1998) was used to convert the LAI to crop factors. The effective crop factor for short and tall vegetation per PCR-GLOBWB cell and per month was then calculated by averaging crop factors per GLCC-type based on their areal coverage within the cell. Separate crop factors were used for deep water (channels, lakes and reservoirs) and shallow water (floodplains when inundated). For the computation of monthly open water crop factors, an average $k_{c,wat}$ (values between 1.0 and 1.2) was computed based on the mean fraction of open water in the cell, which was then modified using the mean annual temperature cycle for each grid.

2.2.4 Groundwater storage and groundwater discharge

In PCR-GLOBWB groundwater storage and discharge is modeled by a first order linear reservoir approach. The third (groundwater) reservoir is of unlimited capacity, but the active groundwater storage, which is the part of the groundwater that is being drained by surface water, is computed by assuming a linear relationship between the storage (W_3) and outflow (q_b), i.e. $q_b(t) = W_3(t)/J$ where J is a reservoir coefficient which represents the average residence time of water in the groundwater reservoir.

PCR-GLOBWB uses information about reservoir properties to regionalize the groundwater residence time J, which depends on the saturated hydraulic conductivity of the aquifer ($k_{s,3}$), the drainage porosity (f), the aquifer depth (D_c), and the drainage length (B_c).

A simplified version (7 classes) of the lithological map of the world (Dürr, Meybeck and Dürr 2005) was used to derive the hydraulic conductivity and drainable porosity. By crossing the drainage length map with the lithological map and using the values of drainage parameters derived by van Beek and Bierkens (2009) a global map of the groundwater residence time can be estimated. From this map an average groundwater residence time J can be estimated for each grid cell. This parameterization is used as an initial estimate of global residence time, which can be further calibrated (van Beek and Bierkens 2009).

2.2.5 Surface water and surface water routing

The main processes included in the model are the direct input to or withdrawals from the open water due to precipitation, potential evaporation and water consumption and the resulting lake storage and river discharge. Fundamental to these process descriptions is the

subdivision of surface water into a network with river and lake stretches. In addition to the direct input and losses mentioned above, the total runoff from the land surface is fed to the river network prior to routing for each time step. The river routing is based on the kinematic wave approximation of the Saint-Venant Equation. The lateral inflow in the channel, *q*, is calculated from the total drainage from the land surface and any direct inputs to the freshwater surface.

At the end of the time step, the calculated discharge is used to retrieve a new stage (water level), which is calculated under the assumption of a rectangular channel with a specified channel width. The new stage is passed to the next time step to estimate the wetted perimeter.

Floodplains and through-flow wetlands are treated as regular river stretches except that flooding spans through the entire floodplain normally with higher resistance, which is defined in terms of Manning's *n* separately for the river bed and floodplain.

Like river stretches, lakes and reservoirs can evaporate freely at a rate set by the potential evaporation. Both are treated as a body of water with a variable water depth and surface area. The net influx to the lake is the balance of inflow and outflow if the lake interrupts the river network. The inflow is the incoming river discharge, and the outflow is calculated in analogy to a weir formula as the discharge through a rectangular cross-section. The calculated discharge at the outlet is added to the lateral inflow at the same time step in the kinematic wave approximation of the downstream rivers. To estimate the fraction of the open water surface (lakes and floodplains) the model includes two options: 1) a fixed area option and 2) a variable area option. In this study, we used the fixed area option, in which the areas of lakes and floodplains are kept constant while routing. To derive estimates of surface water areas we used various sources: first, to estimate the channel depth and width we used the hydraulic relationships from Moody and Troutman (2002) which relate channel width and depth with the average runoff. In addition, floodplains, lakes and reservoirs were selected from the GLWD inventory (Lehner and Döll 2004). For the kinematic wave routing scheme the model uses a gradient derived from the Hydro1k dataset (USGS EROS Data Center 2006), the estimated total floodplain width and length and a weighed Manning's *n*.

2.2.6 Reservoirs and reservoir operations

Reservoirs can be viewed as a particular kind of lakes, their main characteristic being that the outflow is controlled to meet certain requirements. A reservoir (or a lake) can occupy multiple cells but should have a single outlet at which the reservoir connects to the downstream network.

In the current version of the model the large reservoirs are only included as lakes where open water evaporation can be sustained. The reservoir scheme included in PCR-GLOBWB could not be applied yet due to missing input data. However, the data is under collection and

it is expected that the reservoir scheme will be included in following deliverables involving the Limpopo model. Small reservoirs are included in the model in the irrigation scheme (see section 2.2.7).

2.2.7 Irrigation

Irrigation is considered in the model in the following way: the irrigation requirement for the irrigated crop area within a cell is supplied through the storage of freshwater in the cell. Thus, for each cell where irrigation takes place, it is assumed that a small farm reservoir is included. The irrigated area within each cell, water requirements and irrigation cropping patterns are extracted from the "Global map of irrigated areas" from Siebert et al. (2007) and FAO (1997).

2.3 MODEL SETUP AND DATA

The Limpopo hydrological model was set up as a downscaled and adapted version of the continental "PCR-GLOBWB-Africa" model. The continental and the original global versions of the model have a daily temporal resolution and a spatial resolution of 0.5˚.

The downscaled model is basically a higher resolution version of the same model, where all the input parameters are derived at a resolution of 0.05˚ (approximately 5 km). Moreover, the small reservoirs in the basin used for irrigation are considered as a small lake from which the irrigation water is extracted and then distributed in the irrigated areas. The Limpopo hydrological model runs also at a daily time step. Results of the hydrological model include: actual evaporation; soil moisture; surface and subsurface runoff, river discharge, root stress, water storage in the three layers, and other hydrological parameters. The following sections describe the collection and preparation of required input data and parameters for the model and some initial model results.

2.3.1 Topographical data

The Digital Elevation Model (DEM) for the Limpopo River basin was produced from the Hydro1k Africa (USGS EROS Data Center 2006) and upscaled to the model resolution of 0.05˚ (approximately 5 km). Figure 2-3 shows the resulting elevations in the Limpopo River basin, ranging from more than 2000 m above sea level in South Africa to elevations close to zero in the plains of Mozambique

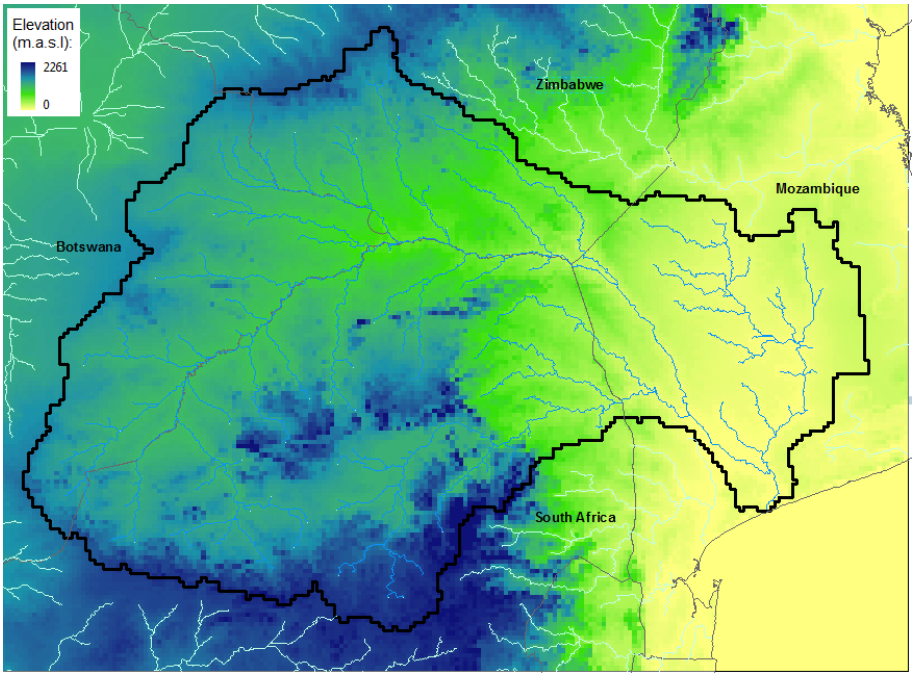

Figure 2-3 Digital elevation model for the Limpopo river basin

2.3.2 Meteorological data

ERA-Interim (ERAI) is the latest global atmospheric reanalysis produced by the European Centre for Medium-Range Weather Forecasts (ECMWF) which covers the period from January 1979 to present date with a horizontal resolution of approximately 0.7 degrees and 62 vertical levels. A complete description of the ERAI product is available in Dee et al. (2011). The ERA-Interim precipitation data used with the present model were corrected with GPCP v2.1 (product of the Global Precipitation Climatology Project) to reduce the bias with measured products (Balsamo et al. 2010). The GPCP v2.1 data are the monthly climatology provided globally at 2.5˚ × 2.5˚ resolution, covering the period from 1979 onwards. The data set combines the precipitation information available from several sources (satellite data, rain gauge data, etc.) into a merged product (Huffman et al. 2009, Szczypta et al. 2011). Besides precipitation, other meteorological data resulting from the ERA-Interim reanalysis data that were used to force the model include: 2 metre daily temperature (minimum, maximum and average) and net radiation. These meteorological variables were collected for the past 32 years (1979-2010) with a daily temporal resolution, and with a spatial resolution of 0.5˚ for the African continent, including the Limpopo river basin. The reference potential evaporation used in this study to force the hydrological model was computed form the re-calibrated form of the Hargreaves equation as suggested by Sperna Weiland et al. (2012). In this formula, the multiplication factor of the equation was increased uniformly from 0.0023 to 0.0031 (Sperna Weiland et al. 2012):

$$ET_0 = 0.0031 R_a (\bar{T} + 17.8) TR^{0.5} \quad (2.4)$$

where, $\bar{T}$=mean daily temperature (˚C), TR = diurnal temperature range (˚C), R_a = extraterrestrial radiation (MJ $m^{-2}d^{-1}$), and ET_0 = potential evapotranspiration in the same units as the radiation.

The seasonal mean (over the period 1972-2010) precipitation and potential evaporation used in this study are presented in Figure 2-4 and Figure 2-5, respectively.

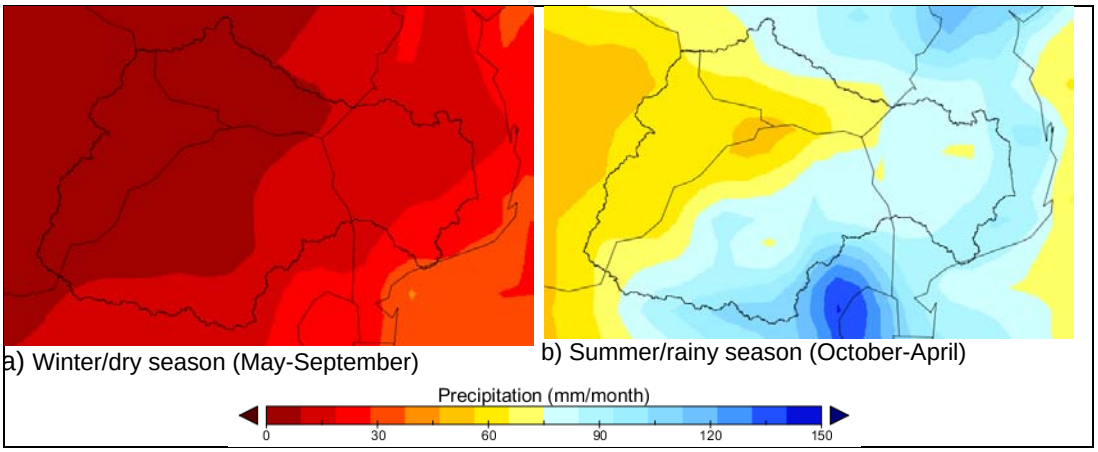

Figure 2-4 Seasonal mean precipitation (1979-2010) from ERA-Interim corrected with GPCP

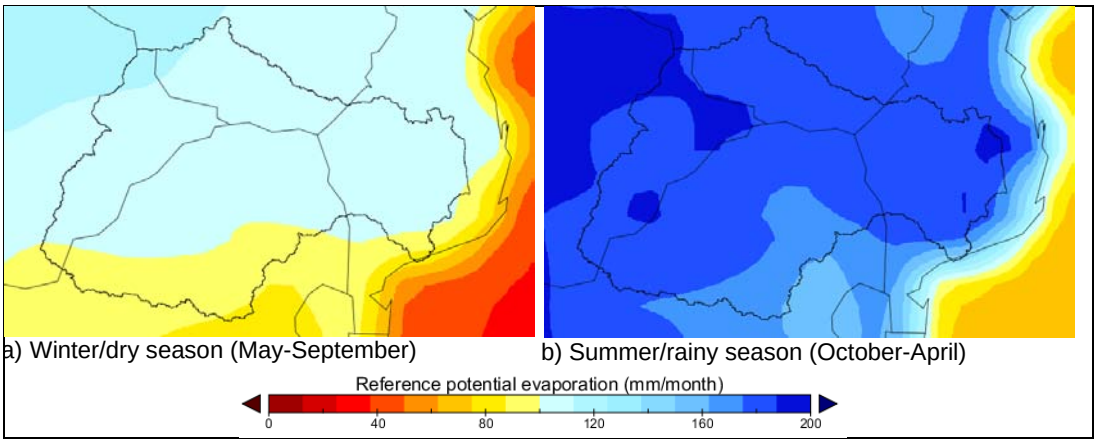

Figure 2-5 Seasonal mean reference potential evaporation (1979-2010) based on re-calibrated Hargreaves equation (Eq 2.4)

The corrected ERAI product (with GPCP) for the Limpopo basin does not differ substantially from the original ERAI. DEWFORA (2012b) compared the mean annual cycle of precipitation of different datasets (ERAI, GPCP, CPCC, CMAP, TRMM) and found a very good agreement between all the datasets in the Limpopo river basin. However, the report (DEWFORA, (2012b) found higher discrepancies between different rainfall products in all other African basins/regions included in the comparison. The mean annual rainfall (1979-2010) over the Limpopo basin computed from the GPCP collected ERAI data is presented in Figure 2-6 . We compared this result with the mean annual rainfall over the Limpopo basin reported in Figure 6-5 of Deliverable D6.1 (DEWFORA 2012a), which is based on the compiled rainfall data within a previous study (LBPTC 2010).

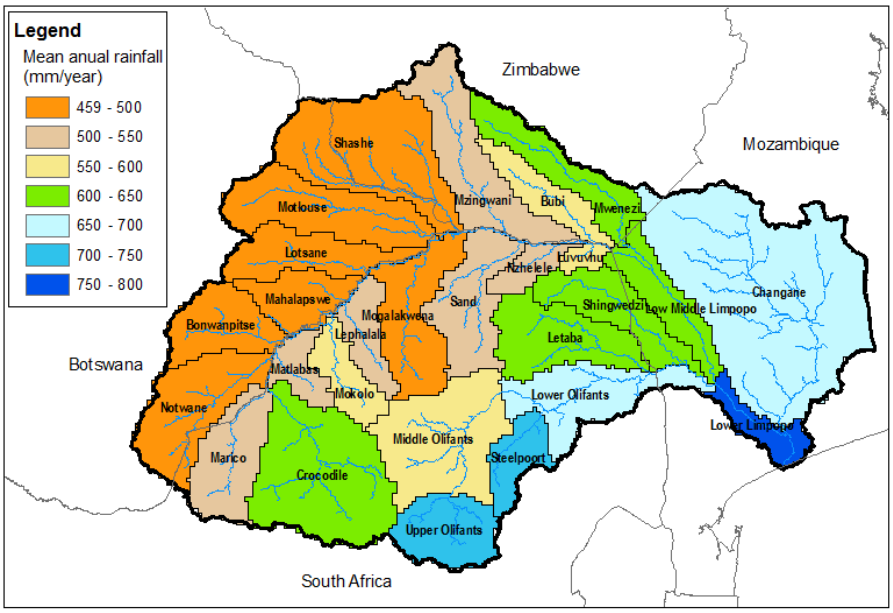

Figure 2-6 Mean annual precipitation (mm/year) for the period 1979 - 2010

In general there is quite a good agreement between the two estimates. Relatively higher discrepancies are observed in parts of Botswana and Mozambique where the ERAI precipitation is higher than the one presented in DEWFORA (2012a).

2.3.3 Hydrometric data

Hydrometric data was collected for calibration/validation purposes mainly from the Global Runoff Data Centre (GRDC) and from the Water affairs, Republic of South Africa (Water Affairs Republic of South Africa). From the available stations, some of them were selected based on the following criteria: availability of data in recent years, and basin greater than 500 km^2. Figure 2-7 presents the selected runoff stations in the basin, most of them in the South African part of the basin as almost no data could be found from stations in the other countries. Table 2-2 present the main characteristics of the selected stations.

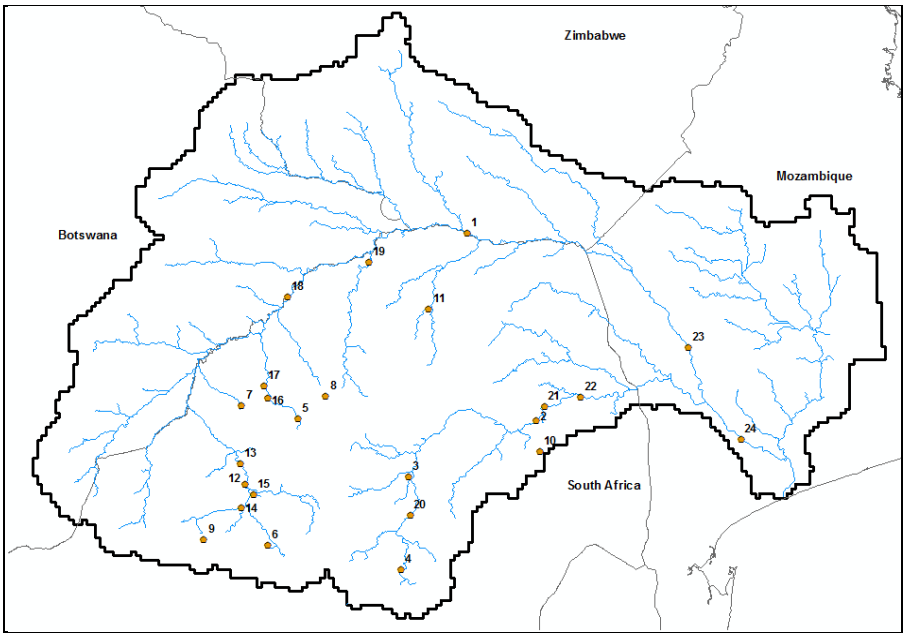

Figure 2-7 Selected hydrometric stations

Table 2-2 Available runoff data from selected hydrometric stations

Id	Station Name	Data Source	Location	Latitude (˚)	Longitude (˚)	Catch. area (km^2)	Data from:	Data until:	Data resolution
1	1196551	GRDC	Limpopo	-22.23	29.99	201,001	07/01/1992	30/08/2011	Daily
2	1196100	GRDC	Olifants River	-24.33	30.74	42,714	01/08/1960	01/12/2011	Daily
3	1196102	GRDC	Olifants River	-24.93	29.39	16,622	01/08/1938	01/06/2011	Daily
4	1196600	GRDC	Olifants River	-26.01	29.25	3,256	01/08/1938	01/06/2011	Daily
5	1196360	GRDC	Mokolo River	-24.28	28.09	1,801	01/03/1948	01/04/2010	Daily
6	1196350	GRDC	Megalies	-25.78	27.76	1,171	01/10/1922	01/12/2011	Daily
7	1196300	GRDC	Matlabas	-24.16	27.48	1,054	01/08/1962	01/11/2011	Daily
8	1196570	GRDC	Lephalala	-23.98	28.40	638	01/12/1955	01/02/2011	Daily
9	1196425	GRDC	Selons River	-25.64	27.03	517	01/09/1963	01/10/2011	Daily
10	1196700	GRDC	Blyde	-24.68	30.80	514	01/11/1909	01/12/2011	Daily
11	1196500	GRDC	Sand River	-23.07	29.58	6,731	01/10/1947	01/08/2001	Daily
12	A2H060	WA-SA	Krokodil River @ Nooitgedacht	-25.06	27.52	20,627	16/08/1982	11/04/2012	Daily
13	A2H132	WA-SA	Krokodil River @ Haakdoringdrift	-24.70	27.41	22,270	14/10/1987	31/10/2007	Daily
14	A2H111	WA-SA	Elands River @ Bulhoek	-25.31	27.48	6,110	17/11/1981	10/04/2012	Daily
15	A2H021	WA-SA	Pienaars River @ Buffelspoort	-25.13	27.63	7,483	01/09/1955	31/07/2012	Monthly
16	A4H005	WA-SA	Mokolo River @ Dwaalhoek	-24.08	27.77	3,786	27/08/1962	25/04/2012	Monthly/daily
17	A4H010	WA-SA	Mokolo River @ Mokolo Nat Res	-23.97	27.73	4,319	01/08/1980	07/03/2012	Daily
18	A5H006	WA-SA	Limpopo River @ Botswana	-22.93	28.00	98,240	12/03/1971	03/03/2012	Monthly/daily
19	A6H035	WA-SA	Mogalakwena River @ Leniesrus	-22.55	28.90	15,845	02/02/1995	08/03/2012	Daily
20	B3H017	WA-SA	Olifants River @ Loskop Nat. Res.	-25.42	29.36	12,286	18/09/1986	03/05/2012	Daily
21	B7H007	WA-SA	Olifants River @ Oxford	-24.18	30.82	46,583	01/10/1955	25/04/2012	Monthly
22	B7H015	WA-SA	Olifants River @ Kruger National Park	-24.07	31.24	49,826	17/11/1987	23/05/2012	Daily
23	E33	ARA- SUL	Limpopo @ Combomume	-23.51	32.46	259,436	02/01/1966	31/08/2011	Daily
24	E35	ARA- SUL	Limpopo @ Chókwè	-24.54	33.06	342,000	19/06/1951	31/05/2011	Daily

2.3.4 Land use, soil, lithology and other derived maps

The majority of the parameter maps required by the model were derived mainly from three maps and their derived properties: (1) the Digital Soil Map of the World (FAO 2003), (2) the distribution of vegetation types from GLCC (USGS EROS Data Center 2002, Hagemann 2002), and (3) the lithological map of the world (Dürr et al. 2005). The maps of soil depth per layer (z_i), maximum soil average storage (W_{max}), and all other soil properties were derived from the FAO "Digital Soil Map of the World" (FAO 2003) (Figure 2-8) and its "Derived Soil Properties". 73 different FAO soil types were distinguished in the basin.

Soil physical relationships at the resolution of 0.05˚ were obtained from the distribution of soil types and associated tabulated moisture retention and unsaturated conductivity within the grid cell, both based on the digital soil map of the world of FAO (2003).

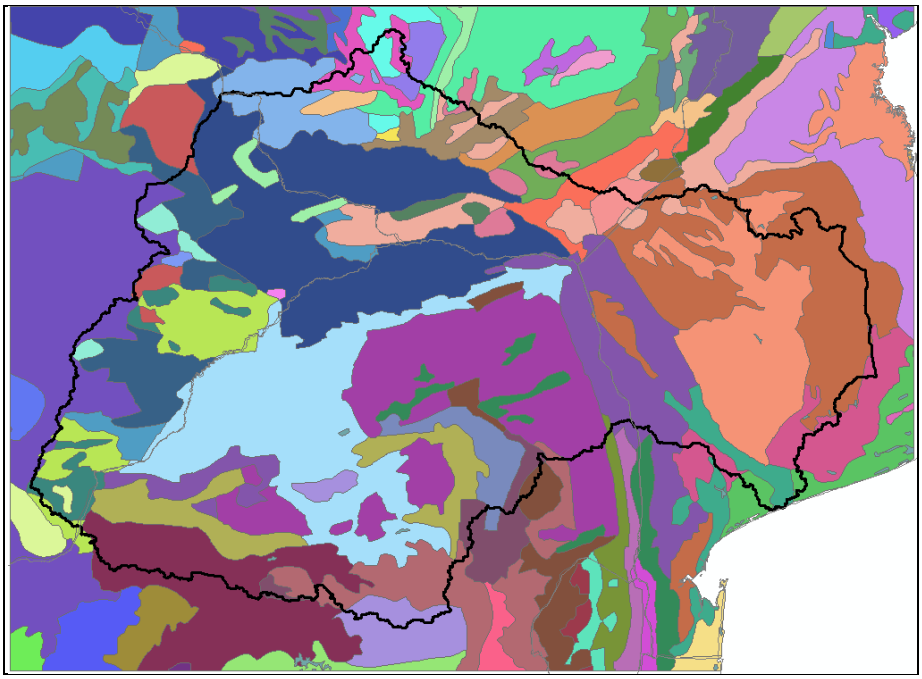

Figure 2-8 "Digital Soil Map of the World" for the Limpopo area (FAO 2003)

The parameter maps related with land cover including: distinction of short and tall vegetation, monthly crop factors, root depth, LAI, and storage capacity of the canopy were derived from the 1x1km distribution of vegetation types from GLCC (USGS EROS Data Center 2002, Hagemann 2002) (see Figure 2-9).

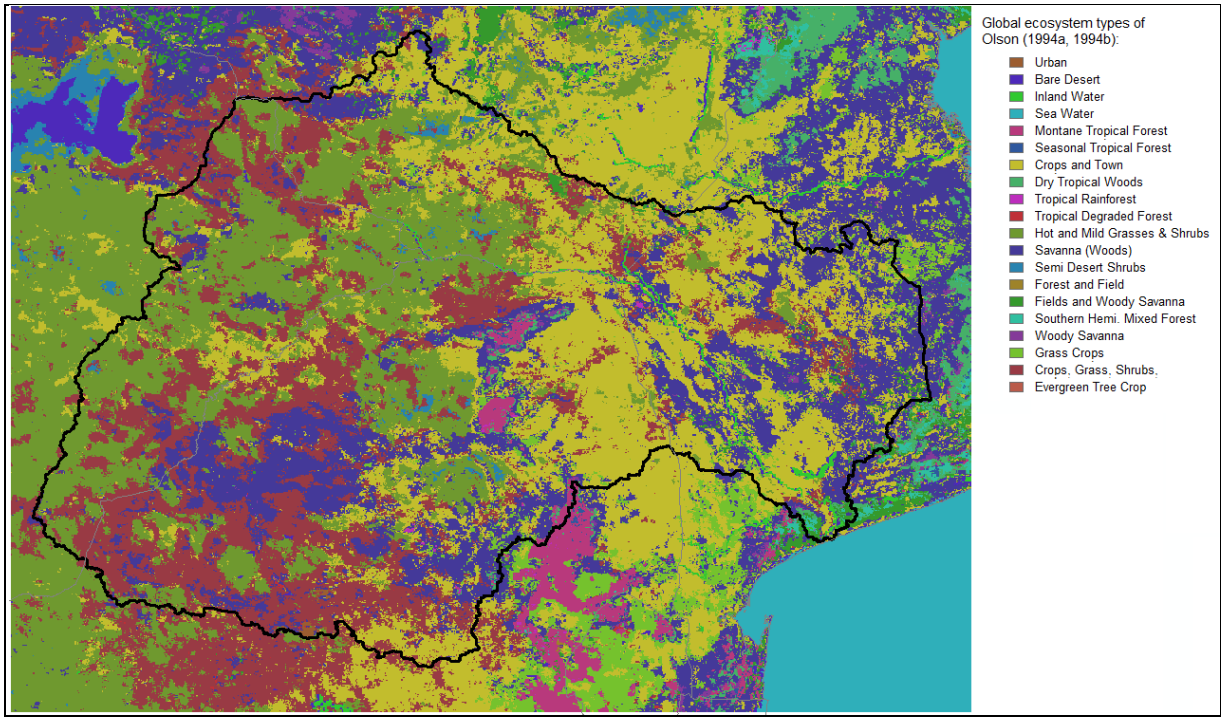

Figure 2-9 Distribution of vegetation types from GLCC in the Limpopo area (USGS EROS Data Center 2002, Hagemann 2002)

Figure 2-10 shows the lithological map for the Limpopo river basin according to Dürr et al. (Dürr et al. 2005) from which the groundwater residence time was calculated.

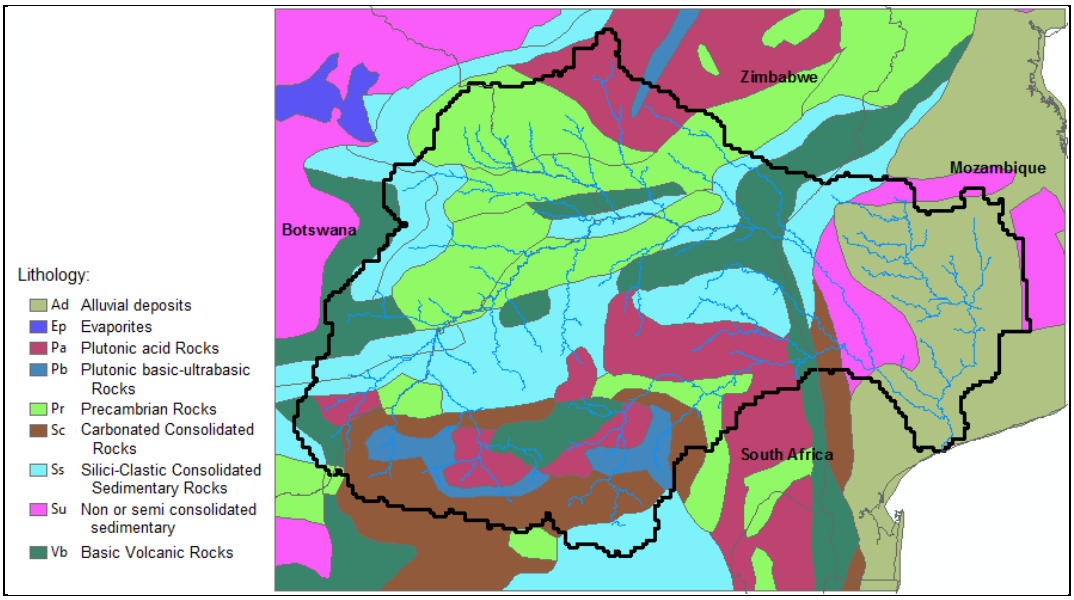

Figure 2-10 Lithologic map of the Limpopo river basin, modified from (Dürr et al. 2005)

For the routing scheme, the Manning coefficient (*n*) was computed assuming a coefficient *n* for the floodplains of 0.1 and a coefficient *n* for the channels of 0.04 (Sperna Weiland et al. 2011). To estimate the channel width W (m) and depth D (m) from the average annual flow Q (m^3/s), the following formulas from Moody and Troutman (2002) were used:

$$W = 7.2Q^{0.5} \quad (2.5)$$

$$D = 0.27Q^{0.39} \quad (2.6)$$

The fraction of the channel in each pixel was computed by dividing the surface area of the channel by the pixel area.

IRRIGATION

The irrigated area was obtained from the Global map of irrigated areas in 5 arc-minutes (0.083333 decimal degrees) resolution based on Siebert et al.(2007) and FAO (FAO 1997) (see Figure 2-11). From the same dataset (FAO 1997, Siebert et al. 2007) and data presented in Table 6-9 of the Inception Report (DEWFORA 2012a) we computed the water requirements for irrigation per country based on the irrigated area. We then converted the annual water requirements for the irrigated areas to monthly irrigation intensities based on the "Irrigation cropping pattern zones" (FAO 1997) (see Figure 2-12 and Figure 2-13).

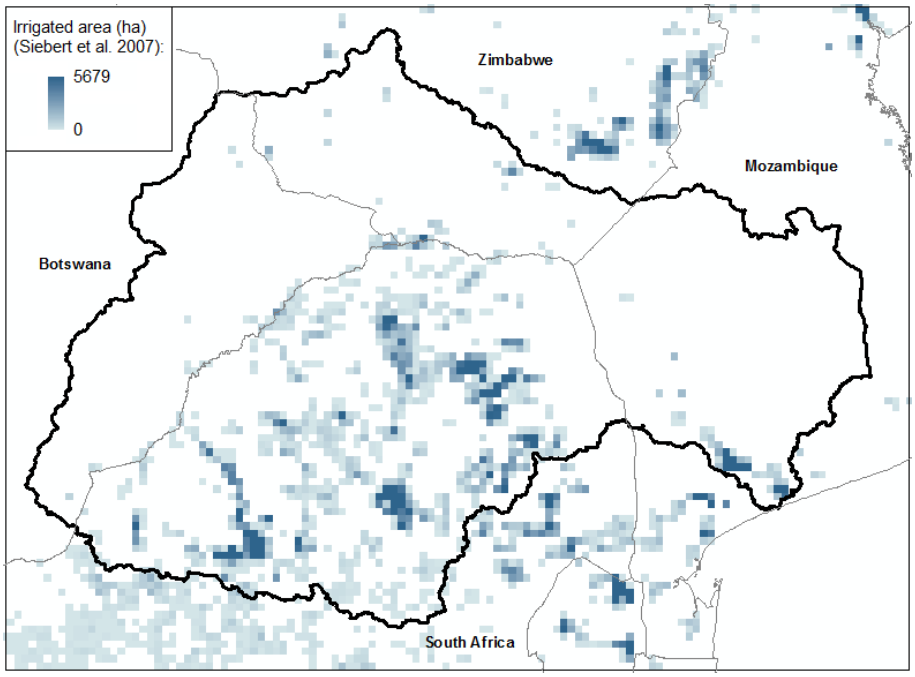

Figure 2-11 Global Map of Irrigation Areas (Siebert et al. 2007)

Table 2-3 Irrigation in the Limpopo basin

County	Water requirements (mm/day)	Irrigated area (ha)	Water requirements (Mm^3/year)
Botswana	2.9	1,381	14.6
Mozambique	3.2	40,000	460
South Africa	3.3	198,000	2,376
Zimbabwe	3.0	4,000	44

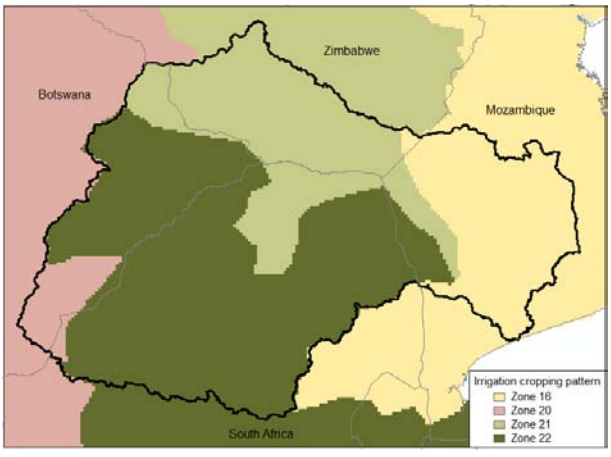

Figure 2-12 Irrigation cropping pattern zones (FAO 1997)

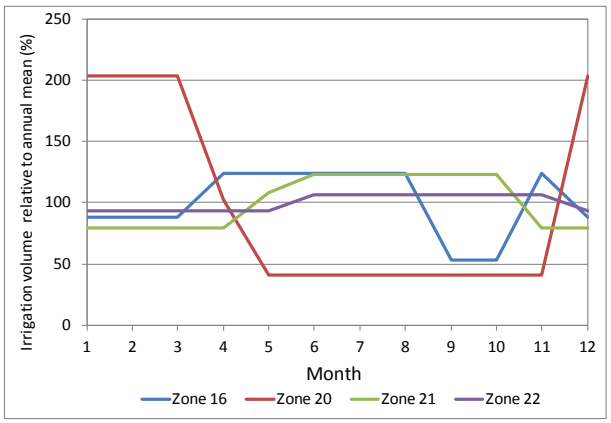

Figure 2-13 Monthly cropping intensities (%) for each zone (FAO 1997)

In the current version of the model the irrigation requirement for a cell is supplied through the storage of freshwater in the cell. If the information on groundwater extraction for irrigation is available, the model can be extended to take in to account the groundwater supply for irrigation.

2.4 MODEL RESULTS

In the current version of the model no calibration has been applied. PCR-GLOBWB is a process based distributed model and such a model should be applied with minimal calibration, particularly when they are applied in a large basin. The focus in this report is to show how good this model can simulate hydrological drought related indices without doing any calibration of the model parameters but making use of the best available input data. In the future work of the modeling, we will assess if there is reasonable room to improve the model results by re-assessing or calibrating on some of the relatively more empirical or lumped parameters of the model, e.g. the groundwater residence-time. It is also important to note that the final objective of this model is to use for hydrological drought forecasting with forecasted meteorological forcing. In such a forecasting scheme, the difference that different ensembles of meteorological forecasts may bring in hydrological model results can be expected to dominate any gains that may be achieved by calibrating the model with one set of historic data. The runoff data available are used for the verification of the model results.

2.4.1 Verification with runoff data

Here we provide a comparison of the simulated discharge from the PCR-GLOBWB based hydrological model of the Limpopo basin with the runoff data. We present this comparison for some of the stations presented in Table 2-2, specifically the ones with large drainage areas.

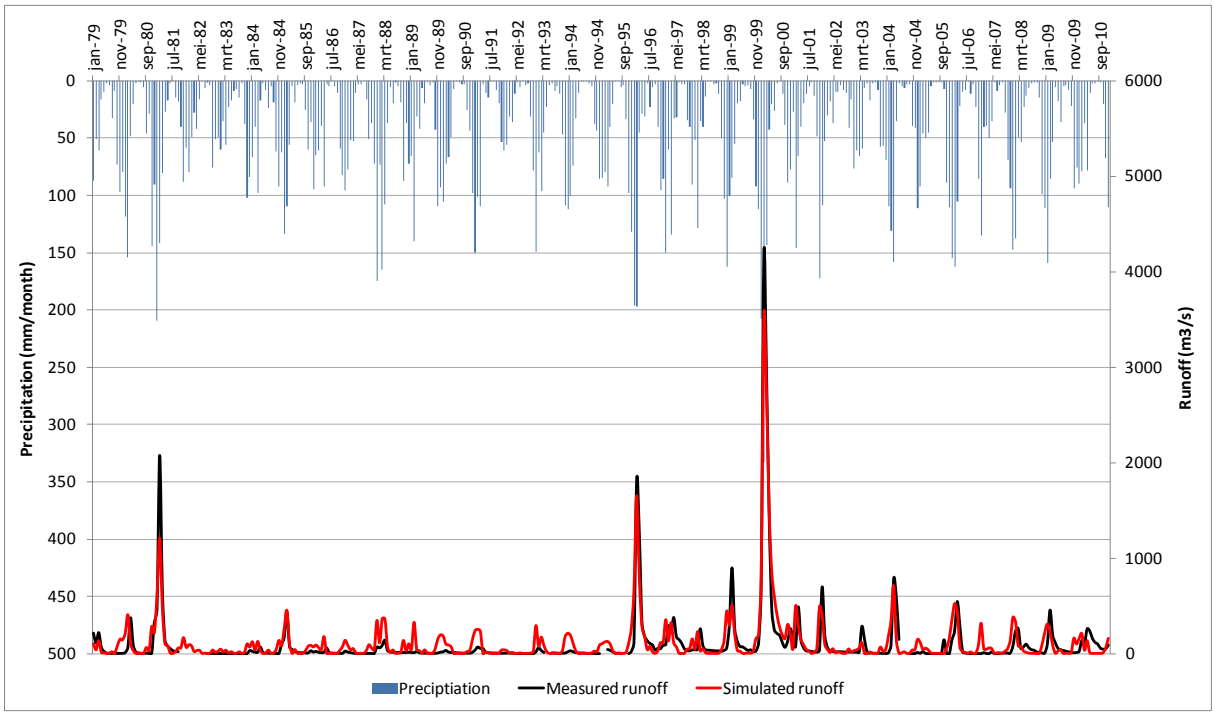

Figure 2-14 Runoff at gauge 24 (ARA- SUL: St No. E35)

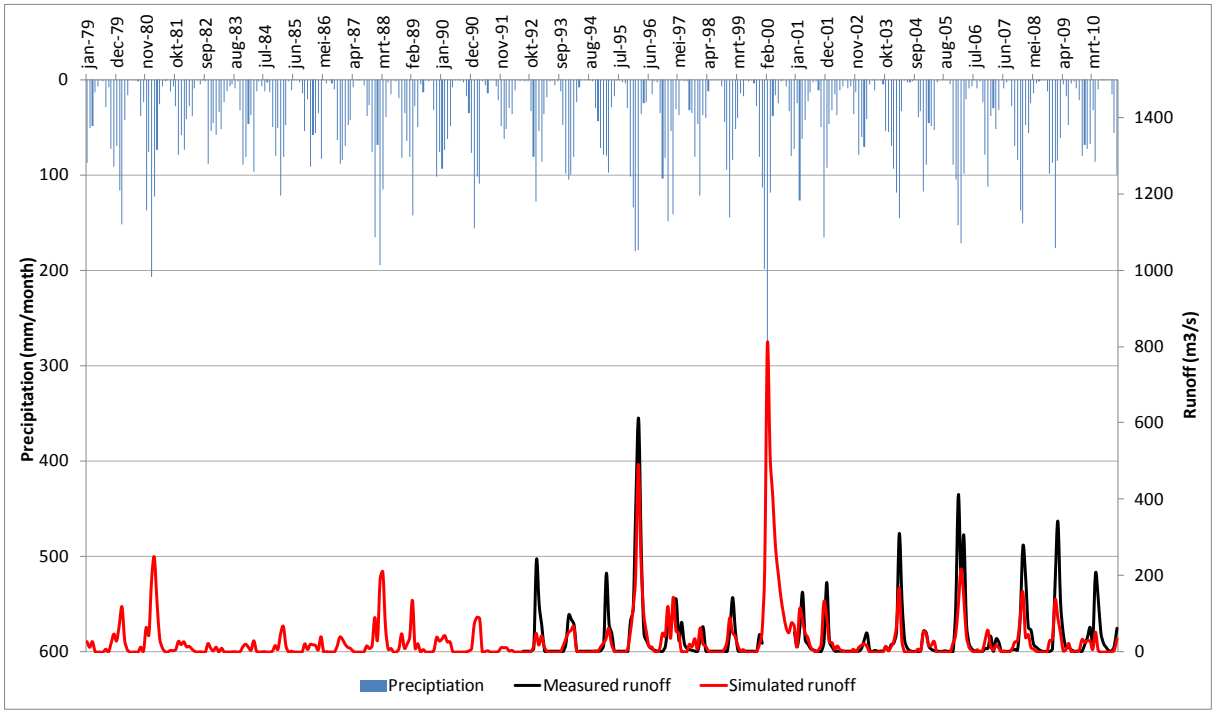

Figure 2-15 Runoff at gauge 1 (GRDC: St No. 1196551)

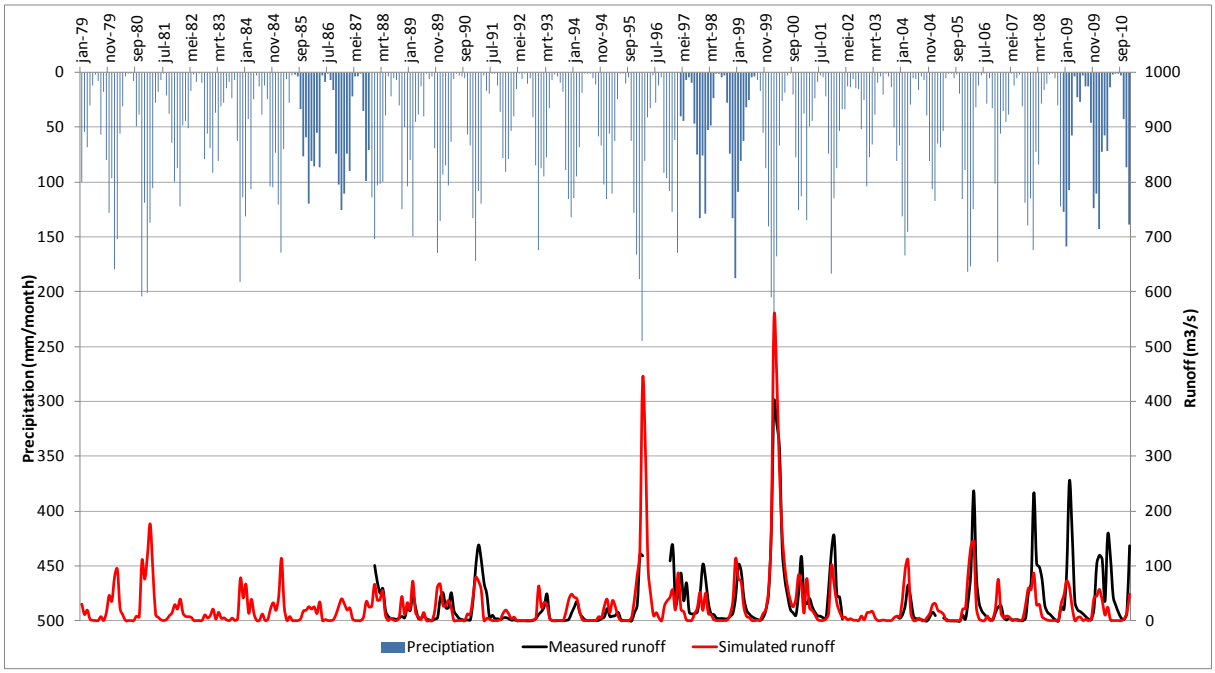

Figure 2-16 Runoff at gauge 22 (WA-SA: St No. B7H015)

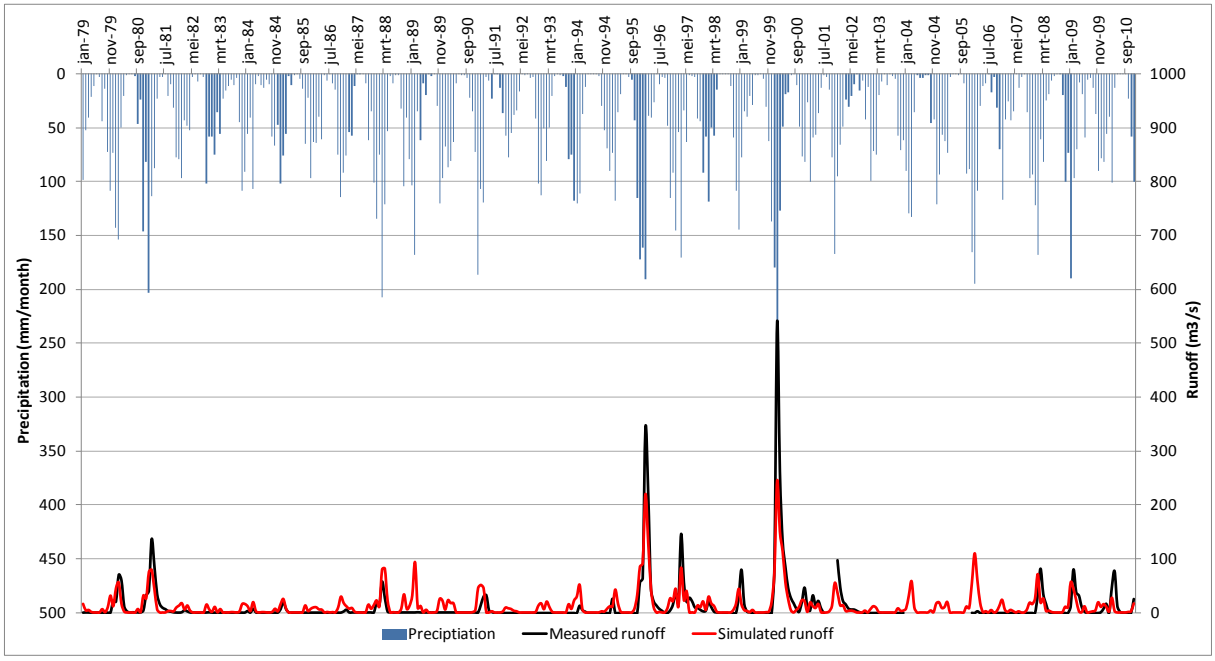

Figure 2-17 Runoff at gauge 18 (WA-SA: St No. A5H006)

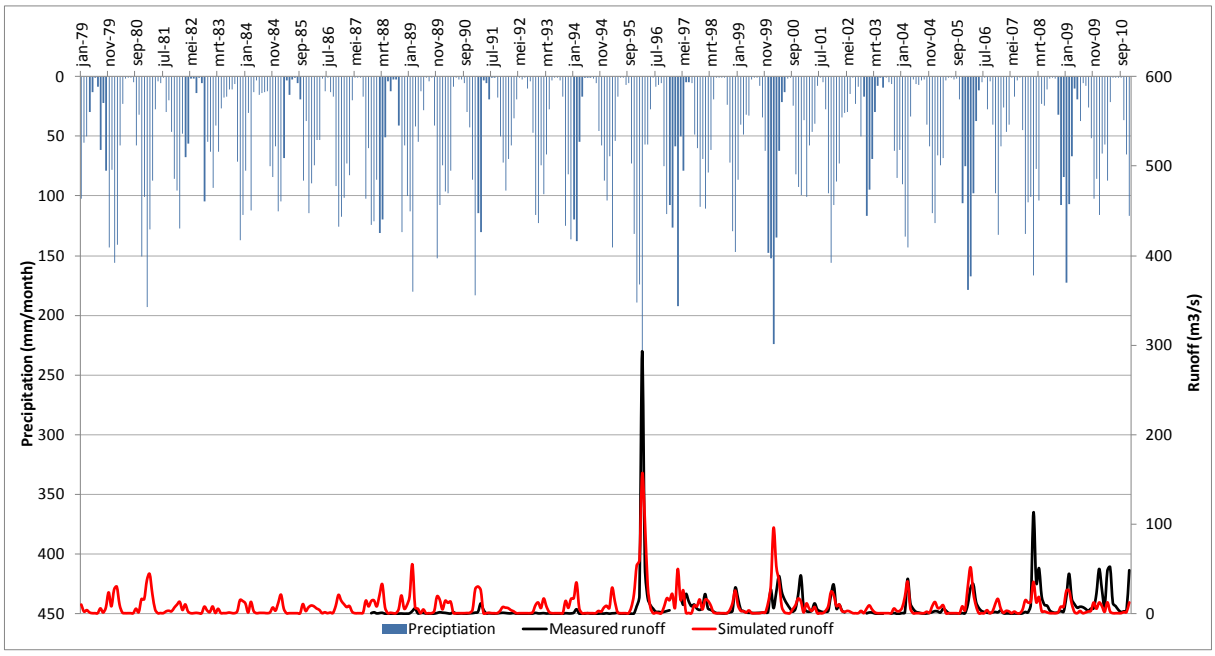

Figure 2-18 Runoff at gauge 13 (WA-SA: St No. A2H132)

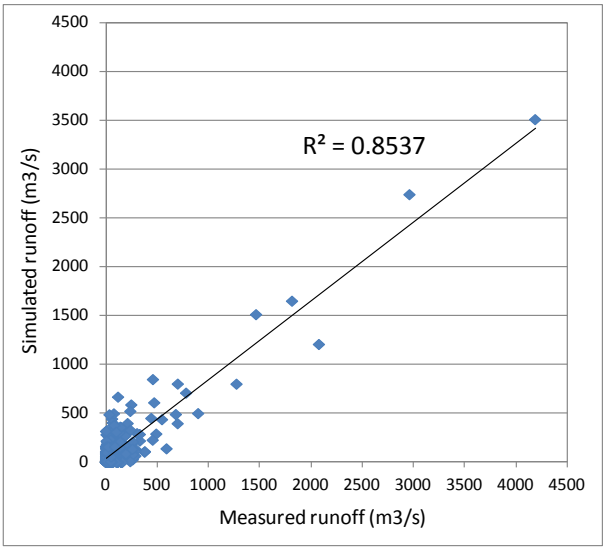

Figure 2-19 Fit between measured and simulated runoff (ARA- SUL: St No. E35)

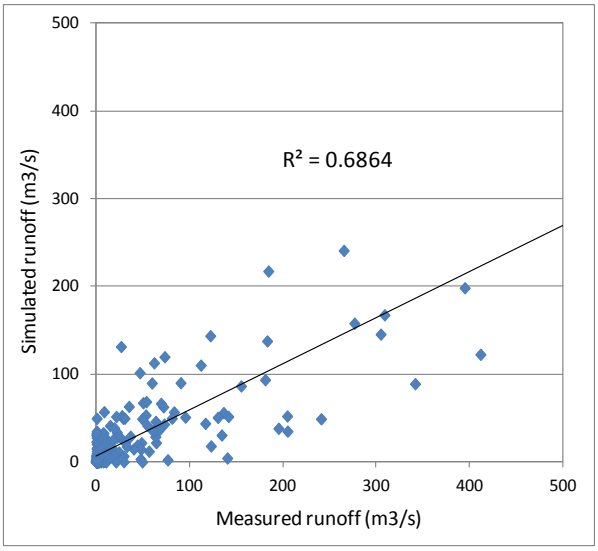

Figure 2-20 Fit between measured and simulated runoff (GRDC: St No. 1196551)

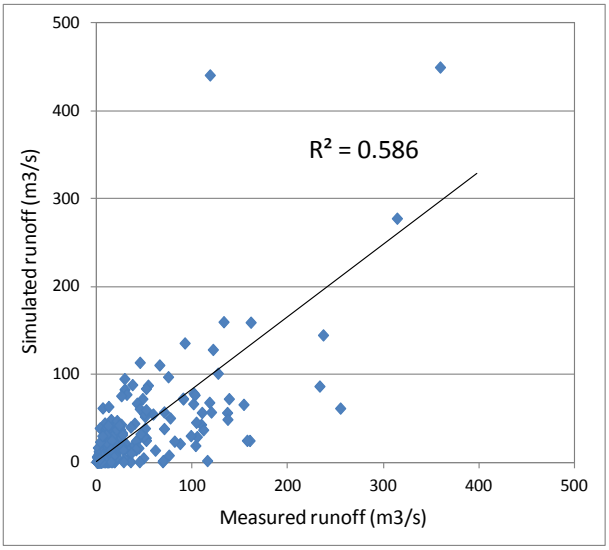

Figure 2-21 Fit between measured and simulated runoff (WA-SA: St No. B7H015)

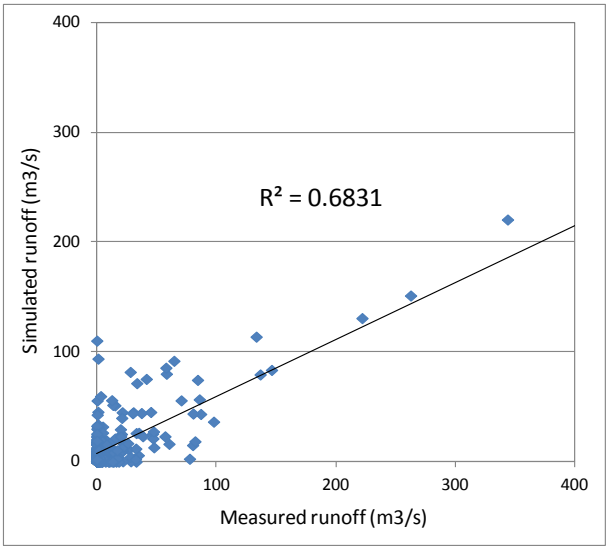

Figure 2-22 Fit between measured and simulated runoff (WA-SA: St No. A5H006)

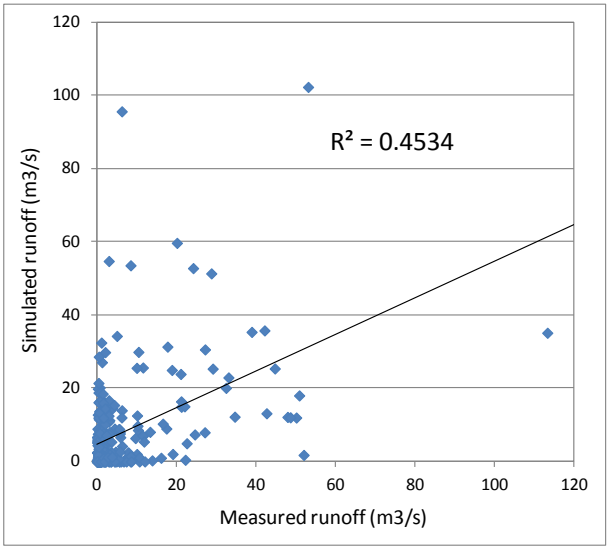

Figure 2-23 Fit between measured and simulated runoff (WA-SA: St No. A2H132)

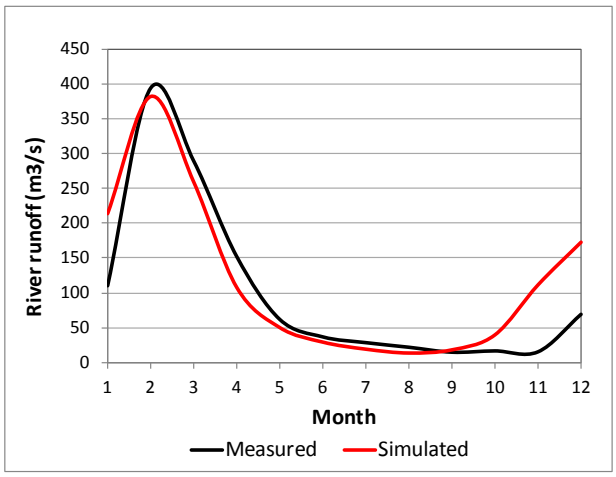

Figure 2-24 Mean annual runoff at gauge 24 (ARA-SUL: St No. E35)

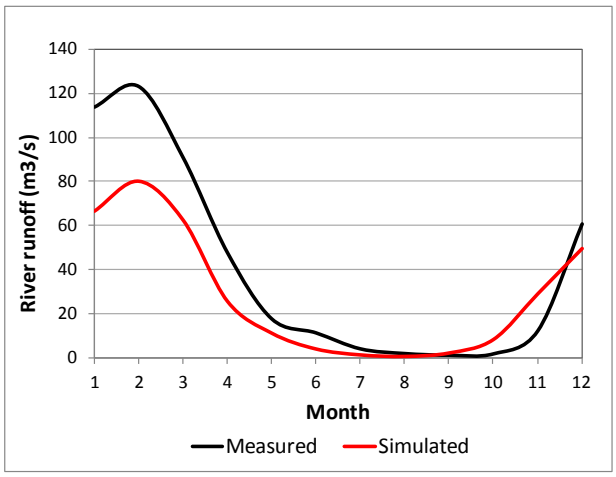

Figure 2-25 Mean annual runoff at gauge 1 (GRDC: St No. 1196551)

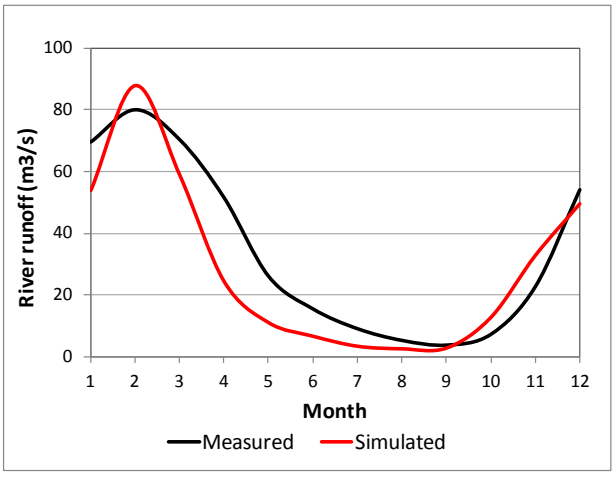

Figure 2-26 Mean annual runoff at gauge 22 (WA-SA: St No. B7H015)

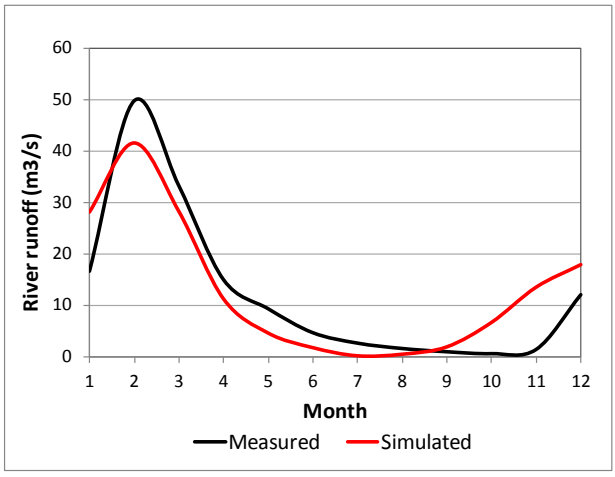

Figure 2-27 Mean annual runoff at gauge 18 (WA-SA: St No. A5H006)

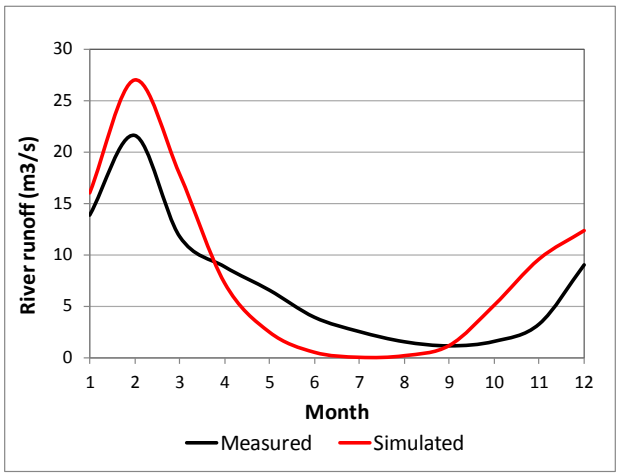

Figure 2-28 Mean annual runoff at gauge 13 (WA-SA: St No. A2H132)

2.4.2 Identification of historic droughts in the basin using the hydrological model

Given that the purpose of this model is the forecasting of droughts, it is important that the model captures the most important droughts in the simulated period 1979- 2010.

One of the model outputs is the daily 'root stress', which is a spatial indicator of the available soil moisture, or the lack of it, in the root zone and the stress of the plants in the case of drought. This indicator ranges from 0 to 1, where 0 indicates that the soil water availability in the root zone is at field capacity, and 1 indicates that the soil water availability in the root zone is null and the plant is therefore under stress.

Moreover, a commonly used indicator for hydrological droughts is the Standardized Runoff Index (SRI) varying between 2.0 (extremely wet) and -2.0 (extremely dry). This indicator is computed both from the model results (simulated runoff) as well as from the observed runoff.

ANOMALY OF ROOT STRESS

We computed the root stress indicator as anomaly of its long term average at a monthly time step. Figure 2-29 a) presents the anomaly of root stress for the most severe drought in the recent history; and b) presents the anomaly of root stress for a particular wet year in the Limpopo river basin. Root stress anomalies of 0.5 indicate that the root stress of that month is around 50% higher than the long term average of that month and root stress anomalies of -0.5 indicate that the root stress of that month is around 50% lower than the long term average of that month. High positive anomalies can be observed for the drought of 1991-92 and high negative anomalies can be observed for the flood of 2000.

Figure 2-29 c) shows a "normal" year in the Limpopo basin with anomaly values close to zero; and d) illustrates the spatial variability of root stress anomaly within the basin.

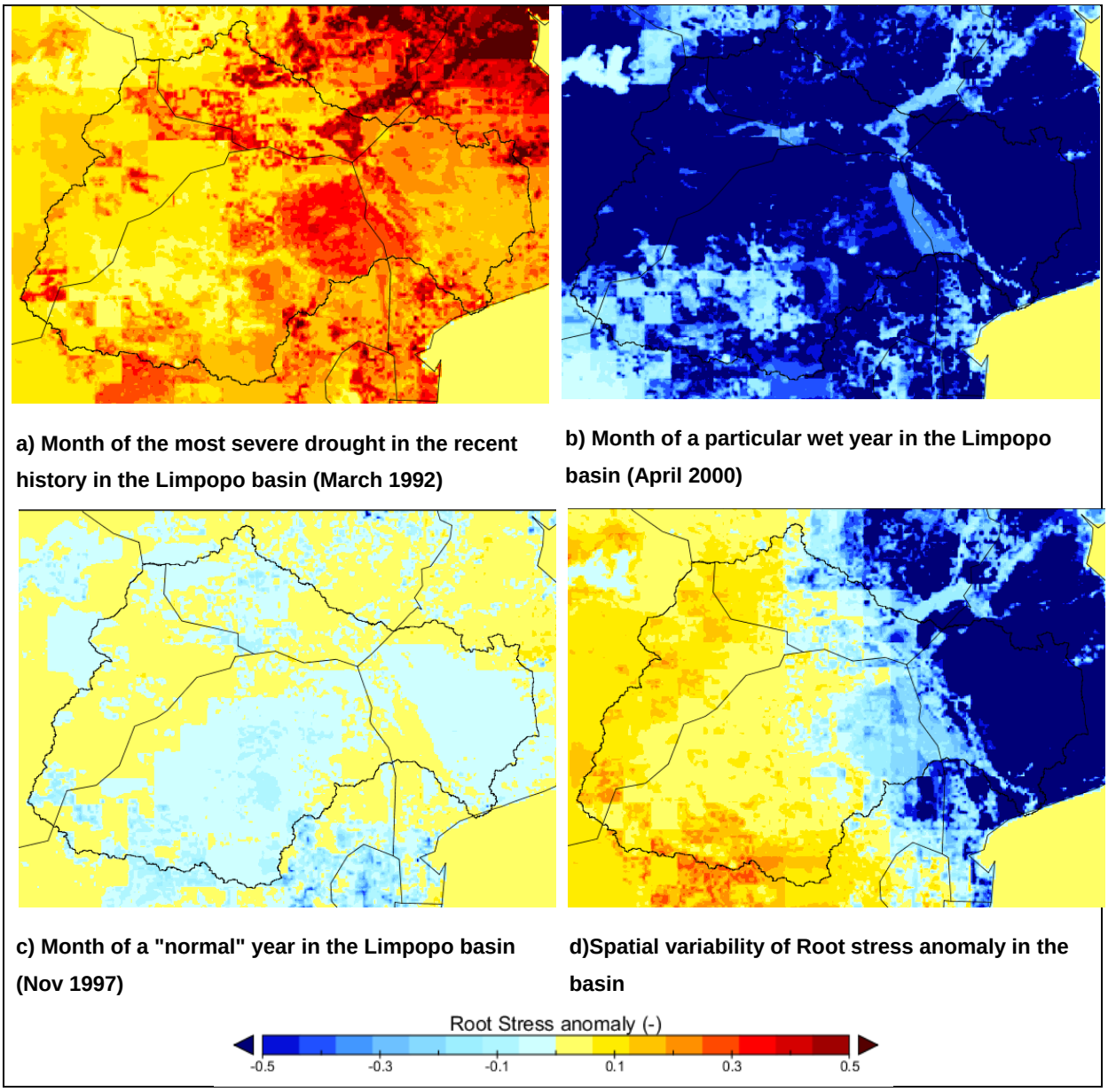

a) Month of the most severe drought in the recent history in the Limpopo basin (March 1992)

b) Month of a particular wet year in the Limpopo basin (April 2000)

c) Month of a "normal" year in the Limpopo basin (Nov 1997)

d)Spatial variability of Root stress anomaly in the basin

Figure 2-29 Root stress anomaly in particular months in the Limpopo river basin

Figure 2-30 present the anomaly of the root stress for two other of the most severe droughts in the recent history (1982-83 and 1994-95). In both cases the anomaly root stress is highly positive.

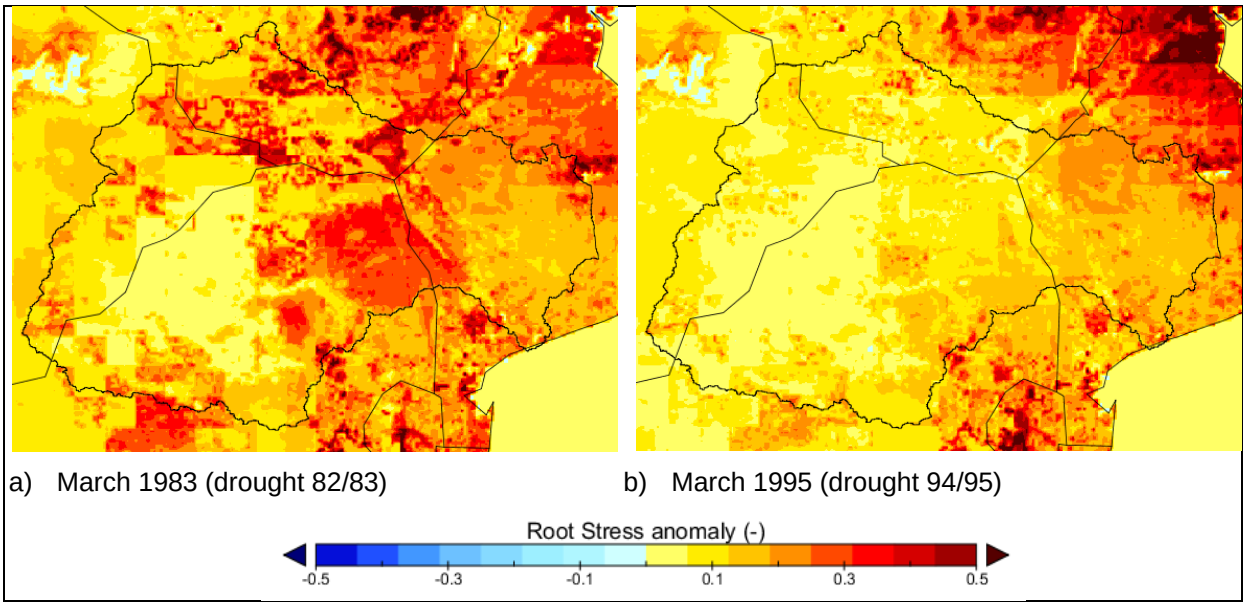

Figure 2-30 Other major drought in the Limpopo basin

STANDARDIZED RUNOFF INDEX (SRI)

The Standardized Runoff Index (SRI) is a commonly used index for the characterization of hydrological droughts. It is based on runoff data but is computed using a similar approach as the well known Standardized Precipitation Index (SPI). These indicators are attractive due to their ease of computation.

The computation of the SRI (McKee et al. (1993) involves the following steps: a monthly runoff data set of a continuous period of at least 30 years is used to compute time series of runoff moving averages for selected time scales periods: 3, 6, 12, 24 or 48 months. These time scales are defined by McKee et al. (1993) as typical time scales for precipitation deficits to affect the five types of usable water sources. The computed data sets are fitted to the Gamma function to define the historic relationship of probability to runoff. The cumulative probability of any observed runoff data point is calculated and transformed to a standard normal random variable with a mean of zero and standard deviation of unity. This value is the SRI for the particular runoff data point (McKee et al. 1993). We computed the SRI using the software SPI SL6 developed by the National Drought Mitigation Center (NDMC) at the University of Nebraska-Lincoln, US (freely available at http://drought.unl.edu/MonitoringTools/DownloadableSPIProgram.aspx).

Although this index is very simple to calculate, it requires a monthly runoff data set for a continuous period of at least 30 years without missing data. This makes it basically impossible to compute SRI for the observed runoff in the stations of interest, which contain gaps of missing data reducing the continuous measured data in general to about 10 years. Because of this limitation in the runoff data availability, we computed SRI only for the simulated runoff for the 32 year period 1979-2010 and we compared these results with a

variation of the SRI, called the Streamflow Drought Index (SDI) proposed by Nalbantis and Tsakiris (2009). The SDI index is defined as (Nalbantis and Tsakiris 2009):

$$SDI_{i,k} = \frac{y_{i,k} - \bar{y}_k}{s_{y,k}} \qquad i = 1, 2, \ldots, k = 1, 2, 3, 4$$

where

$$y_{i,k} = ln(V_{i,k}) \qquad i = 1, 2, \ldots, k = 1, 2, 3, 4$$

are the natural logarithms of cumulative streamflow with mean $\bar{y}_k$ and standard deviation $s_{y,k}$. The criterion of hydrological drought are identical to those used in the SPI ranging from 0.0 (no drought) to -2.0 (extreme drought) (Nalbantis and Tsakiris 2009).

The SDI allows the computation even if there are missing values. The years with missing values are not considered in the long term statistics (mean and standard deviation), and the SDI is only computed for the years without missing data in the monthly series. In this way, the computed SDI time series will have gaps in the years with missing data but the computation for other years is still possible.

Figure 2-31 presents the results of the computed SDI for both observed and simulated flow for a 6 month time period in Station 24 and Figure 2-32 shows the 6 months SRI results for the simulated flow of Station 24.

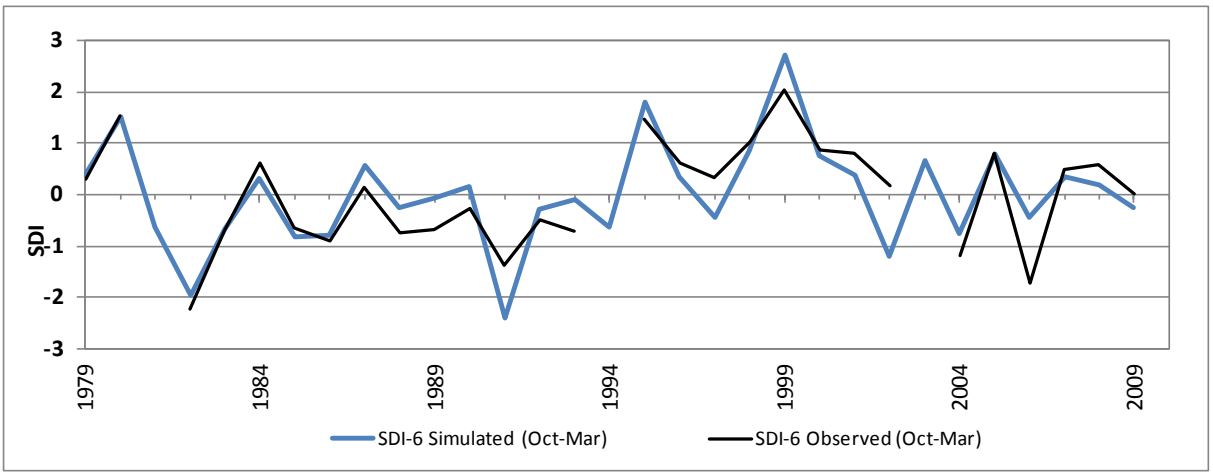

Figure 2-31 6 months SDI for station 24 (ARA- SUL: St No. E35)

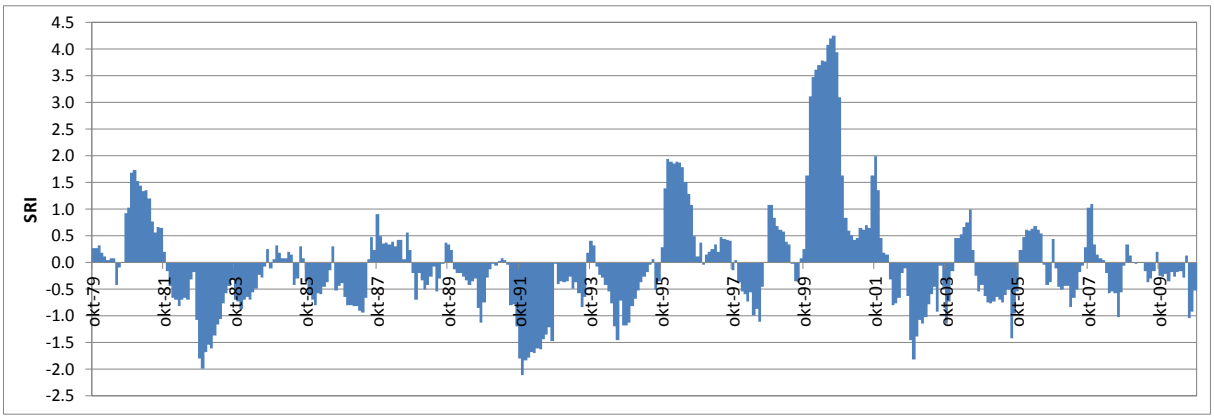

Figure 2-32 6 months simulated SRI for station 24 (ARA- SUL: St No. E35)

In the same way, Figure 2-33 and Figure 2-34 illustrate the results of SDI and SRI respectively for Station 24 for a time period of 12 months.

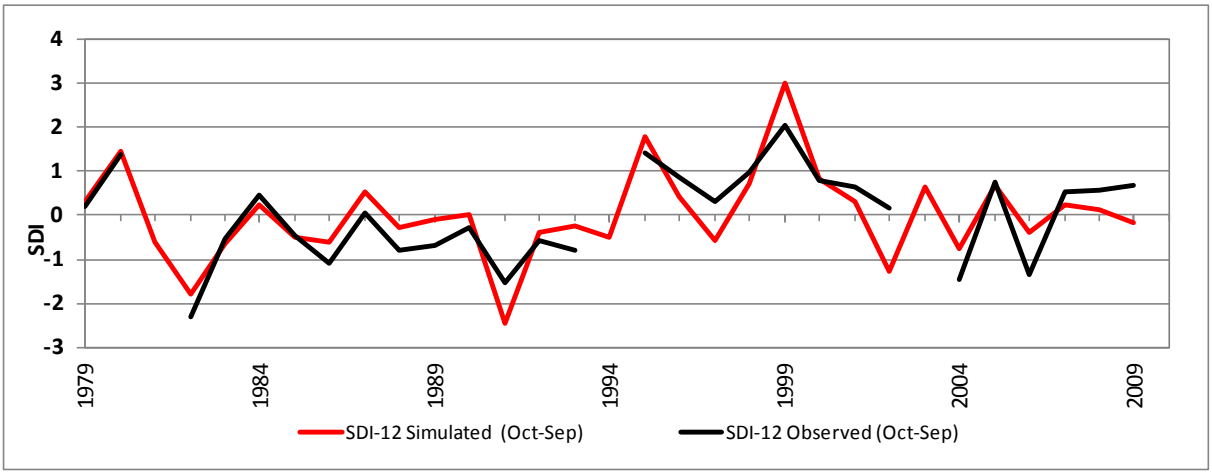

Figure 2-33 12 months SDI for station 24 (ARA- SUL: St No. E35)

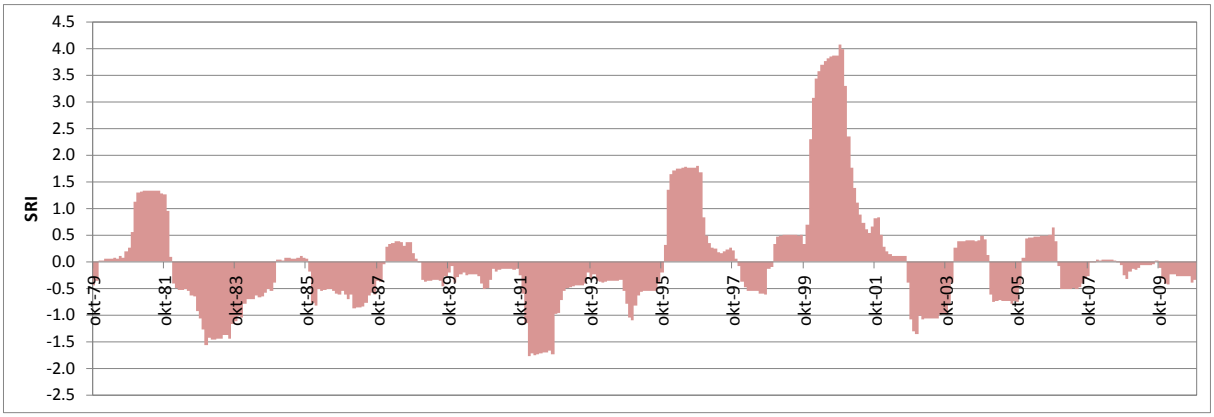

Figure 2-34 12 months simulated SRI for station 24 (ARA- SUL: St No. E35)

The results of both the SDI and SRI for the time periods of 6 and 12 months are very similar given that the majority of the flow occurs in the first 6 wet months of the hydrological year. In both cases the major droughts appear to be identified reasonably well (1982-83, 1991-92) with SDI and SRI values smaller than -1.5. Moreover, the extremely wet year of 2000 is very visible with SDI and SRI higher than 2.0.

3. HYDROLOGICAL MODEL FOR THE NIGER CASE STUDY BASIN

3.1 INTRODUCTION

Since the 1970s, the Sahelian Great Drought has severely and continuously affected regional food security, human societies, economic development and the ecosystem functions of semi-arid and wet ecosystems in Mali. By considering as well the significant demographic growth, it results in an increasing competition and upstream downstream conflicts for water access between vulnerable local stakeholders (rainfed and controlled irrigation farming, nomad pastoralism, traditional fishing) and steers national investments with the construction of dams and diversion channels for the development of hydropower energy and fully governed irrigated agriculture which tend to leave aside the problematic of nature conservation (protection of wetland or forest habitats and of endangered or migratory species) [Andersen et al. 2005; Marie et al., 2007; Moorehead, R. 1997; Zwarts et al., 2005]. At present, the combination of poor rainy season, region-wide high food prices and conflicts between rebelled factions and the Malian army causes massive population displacements, blocks pre-established food aid programs and intensifies the chronic vulnerability and poverty.

To mitigate drought vulnerability and to support preparedness for drought adaptations in regional development strategies, short term weather forecasts and long term dynamical climate projections are thus of paramount importance. Whilst climate change is typically associated with an increase in mean global surface temperature, what matters regionally and still remains uncertain is the change in rainfall, discharge and drought patterns from daily intensity to large inter-annual and multi-decadal variability.

For this propose, the eco-hydrological model SWIM is selected and tailored to reproduce past drought events. SWIM is a daily continuous-time, semi distributed catchment model for the coupled hydrological / vegetation / water quality modelling in mesoscale watersheds. The model is set-up and calibrated to represent region specific processes, stocks and fluxes by using regional ground-truth and remote sensing data. The model enables to consider various water storages and flow components such as soil moisture availability, surface, sub-surface and groundwater flows. Further developments integrate reservoir management, wetlands and inundation plain dynamics to account for specific hydrological patterns encountered in the case study. The model will be then employed to simulate short-term hydrological forecast and long term hydrological projections in order to assess drought persistence and risk under a range of upstream water resources management.

3.2 DESCRIPTION OF THE NIGER CATCHMENT

Stretching between the Sahara desert and the Atlantic coast, the Niger is the third African river according to the length (about 4,200 km) after the Nile and the Congo. The entire basin covers about 2,170,500 km² (7.5% of the continent) across six agro-climatic zones and ten countries while the *active* basin covers 1,272,000 km^2 spread over nine countries: Benin, Burkina Faso, Cameroon, Chad, Ivory Coast, Guinea, Mali, Niger and Nigeria, which are all members of the Niger Basin Authority (NBA). Starting its journey in the Fouta Djallon Massif and the Guinean Dorsale that separates the Middle Guinea and the Guinean forest from Sierra Leone and from Liberia, the river receives consistently high amounts of rainfall which contributes to flow northeast towards Sahelian and sub-desertic regions traversing a vast spreading flood plain in Mali known as the Inner Niger Delta. The course across the Inner Niger Delta dissipates an appreciable portion of its potential hydraulics through absorption and evaporation. Further on, when it reaches the fringes of the Sahara desert, the Niger river turns back by forming a great bend and flowing south and east as the middle Niger river section, then as the lower Niger, to the maritime Niger Delta (20 000 km²) at the Gulf of Guinea, which is reached after being joined by its largest tributary, the Benue River. [Andersen et al., 2005; NBA, PADD, 2007]

DEWFORA project focuses on the Intermediate Niger basin covering an area of about 350,000 km^2 and stretches from south to north over the Soudano-Guinea, Soudan, and Sahel zones (Figure 3-1). The Intermediate Niger basin comprises two specific sub-regions:

- **The Upper Niger Basin** and the Bani Watershed composed the headwaters of the Niger which has an extensive network of steep-sloped tributaries originating in Upper Guinea, whereas the Bani tributary network originates in the low-altitude plateaus of southern Mali and Côte d'Ivoire.
- **The Inner Niger Delta** and Lakes District, entirely situated in Mali, a seasonally inundated floodplain, a network of tributaries, channels, swamps, and lakes providing vital habitats supporting livelihoods in fishing, farming, and stock farming

The catchment is subject to enormous seasonal and interannual variation in rainfall and river flow and rainfall is very unequally distributed in the Upper Niger Basin, where the headwater regions receive up to 2,000 mm of rainfall during the rainy season (July to October) and the northern regions only 200-500 mm. Therefore, the IND ecosystem strongly depends on the surface runoff from its two tributaries: the Niger and the Bani rivers. Because of climatic variations, the annual river flood does not occur at the same intensity and at the same time in different parts of the Basin. Quantitatively, there are usually high flows from the headwaters in Guinea, a decrease in flow caused by evaporation and expansion in the floodplain of the Inner Niger Delta, followed by an increase in flow from tributary input through the Middle and lower reaches as the river enters the Maritime Niger Delta. Concerning the timing, In the

Upper Niger, the high-water discharges generally occur in September, and the low-water season is generally April–May. The Inner Niger Delta with its significant storage capacity has a high rate of loss caused by evaporation over the thousands of square kilometers of its floodplain. This loss is estimated at about 44 percent of the inflow. The peak flow period that arrives in September is delayed as it spreads out, exiting the Inland Delta three months later.

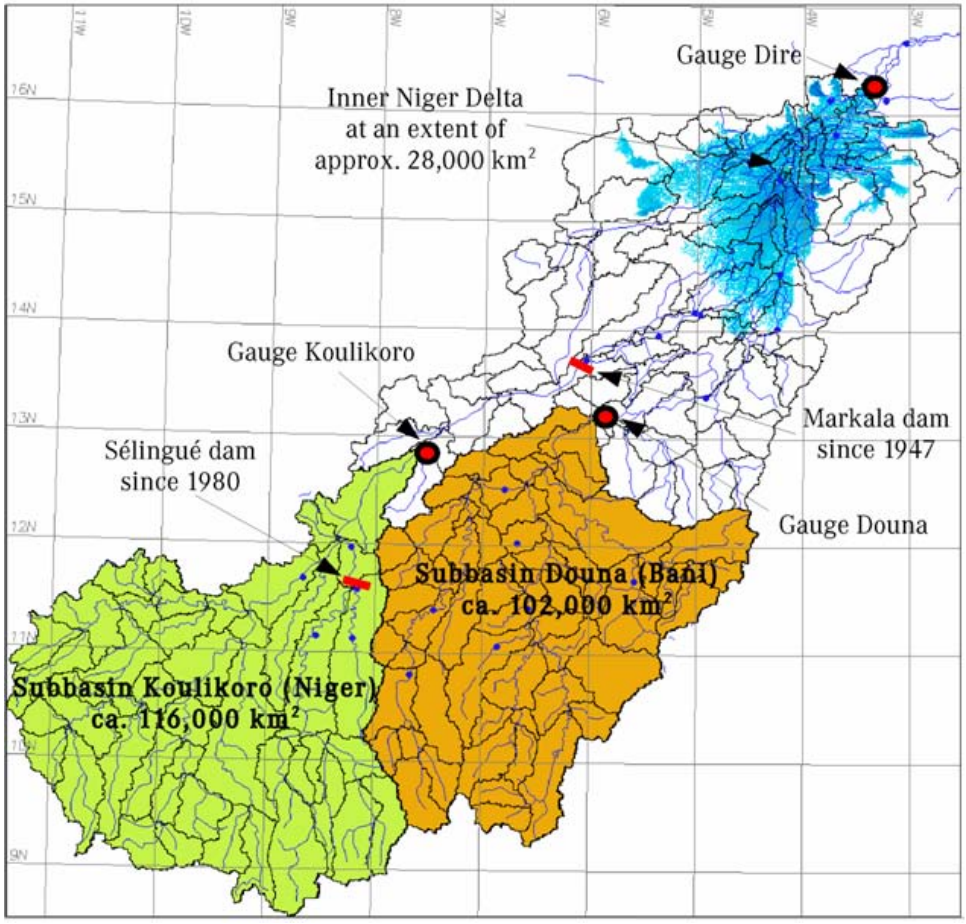

Figure 3-1 The Intermediate Niger Basin in West Africa [Liersch et al., 2012]

For further information, we invite the reader to a detailed description of the case study which was already the object of one section in the Deliverable 6.1 Work Package 6, "Implementation of improved methodologies in comparative case studies – Inception report for each case study" submitted in May 2012.

3.3 DESCRIPTION OF THE HYDROLOGICAL MODEL

Many hydrological models with different degrees of physical background exist; each adopting different approaches to reproduce the spatial heterogeneity and the hydrological processes in a catchment. For this case study the eco-hydrological watershed model SWIM (Soil and Water Integrated Model) had been chosen. The eco-hydrological model SWIM is a daily continuous-time, semi distributed catchment model for the coupled hydrological / vegetation / water quality modelling in mesoscale watersheds (Krysanova et al., 1998, 2000a, 2000b, 2005)**.** SWIM simulates crop and vegetation growth, nutrients dynamics (nitrogen and phosphorous), hydrological and erosion processes at the river basin scale (Figure 3-2).

Hydrotopes or hydrological response units (HRUs), respectively, are the core elements in the model. The HRUs are considered as units with same properties (soil and land use/cover) regarding bio-physical processes. The model is connected to meteorological, land-use, soil, vegetation and agricultural management input data. It was developed from SWAT (Soil and Water Assessment Tool) version '93 (Arnold et al., 1993) and MATSALU models (Krysanova et al., 1989) for climate and land use change impact assessment on hydrology and water quality.

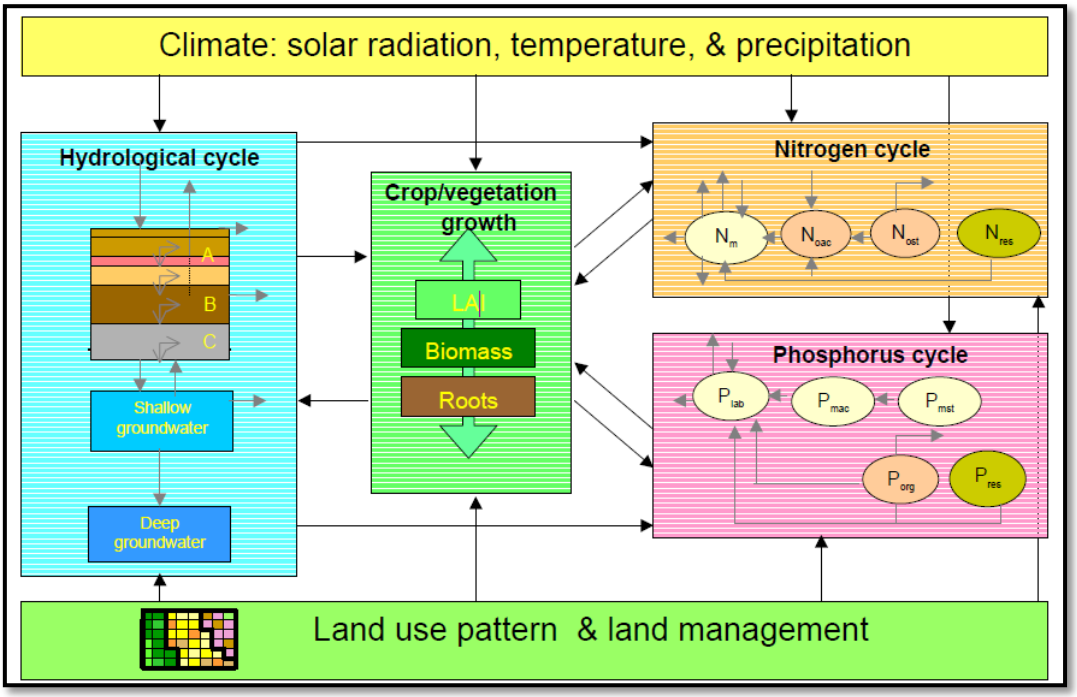

Figure 3-2 Simulation process diagram for the SWIM model in Krysanova et al.,2000a

The hydrological module is based on the water balance equation, taking into account precipitation, evapotranspiration, percolation, surface runoff, and subsurface runoff for the soil column subdivided into several layers (Figure 3-3). The simulated hydrological system consists of four control volumes: the soil surface, the root zone, the shallow aquifer, and the deep aquifer. The percolation from the soil profile is assumed to recharge the shallow aquifer. Return flow from the shallow aquifer contributes to the streamflow. The soil column is subdivided into several layers in accordance with the soil data base. The water balance for the soil column includes precipitation, evapotranspiration, percolation, surface runoff, and subsurface runoff. The water balance for the shallow aquifer includes ground water recharge, capillary rise to the soil profile, lateral flow, and percolation to the deep aquifer.

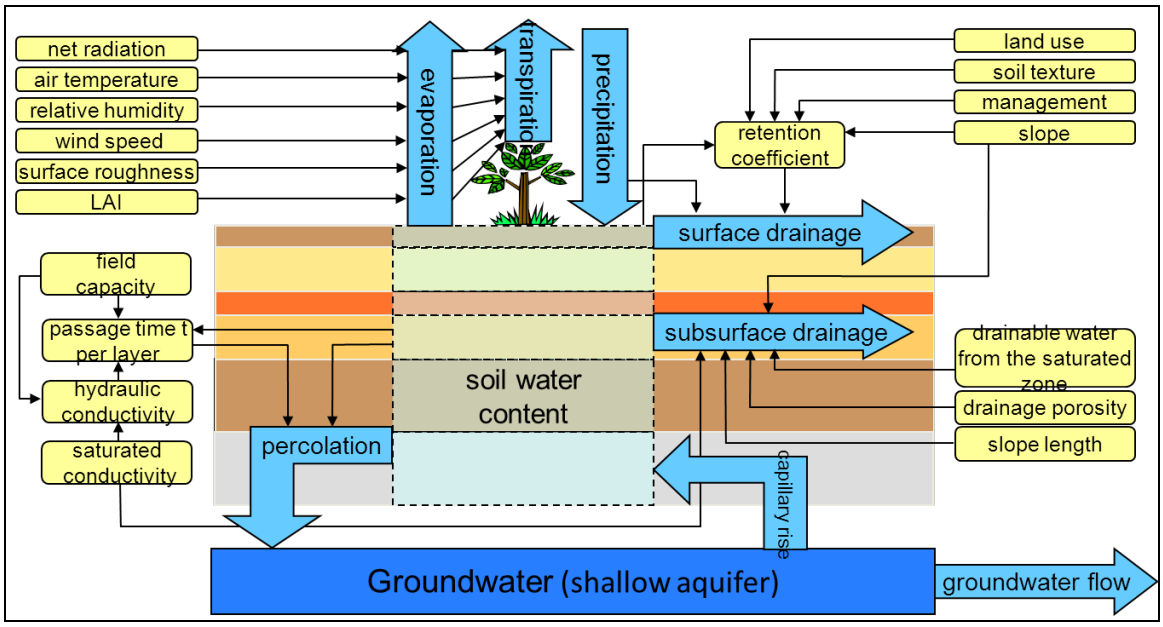

Figure 3-3 The governing processes in SWIM for the simulation in Krysanova et al.,2000a

Reservoir module

A reservoir module (Koch et al., 2011) was developed and integrated into the SWIM model in order to account for impacts of medium to large dams on river discharge. The model provides three different reservoir management options:

1. Variable daily minimum discharge to meet environmental or other targets downstream under consideration of maximum and minimum water levels in the reservoir,
2. Daily release based on firm energy yield by a hydropower plant at the reservoir (the release to produce the required energy is calculated depending on the water level),
3. Daily release depending on water level (rising/falling release with in- creased/falling water level, depending on the objective of reservoir management).

Inundation module

The inundation module, integrated into SWIM, is required to adequately simulate hydrology of the Upper Niger Basin including the Inner Niger Delta (Liersch, 2011). It simulates the flooding dynamics and release, the flooded surface area, inundation depths, and duration, as well as losses due to evapotranspiration and percolation. An important objective was to develop a simple method in order to keep the complexity and data requirements as low as possible. The basis of the wetland module in terms of data requirements are a digital elevation model of adequate resolution, which mainly depends on the wetland area size, and two calibration parameters (the inundation threshold controlling hru-switching *ind_et*, and the recession constant α for the inundation storages). All other parameters can be derived from the DEM or are model parameters anyway. Potentially, the parameters determining the cross-section geometry could be considered as calibration parameters, because they are a source of large uncertainty when they are derived from a DEM. The inundation module is a

semi-explicit process based model. The Inner Niger Delta is divided into sub-basins that respect the routing of the model SWIM. Within the sub-basins and according to a refined digital elevation model, inundation zones are delimited based on the water height and allow to estimate the water volumes stored within the inundation zone and within the ponded area. The flooding simulation encompasses backwater effects, evaporation (water surface), percolation and release.

Delineation of temporarily inundated areas

A first approach to delineate potentially flooded areas can be realized by using GIS functions, such as the GRASS GIS module *r.lake* or the *lake* module in SAGA GIS, respectively. This module simulates the filling of a lake from a seed (reference point) at a given level using a digital elevation model. The reference point should be located at the wetland's outlet and its altitude must be known. By defining a target water level the module fills the area that is (1) below this level, (2) is connected to the reference point or grid cell, and (3) is not a no data value.

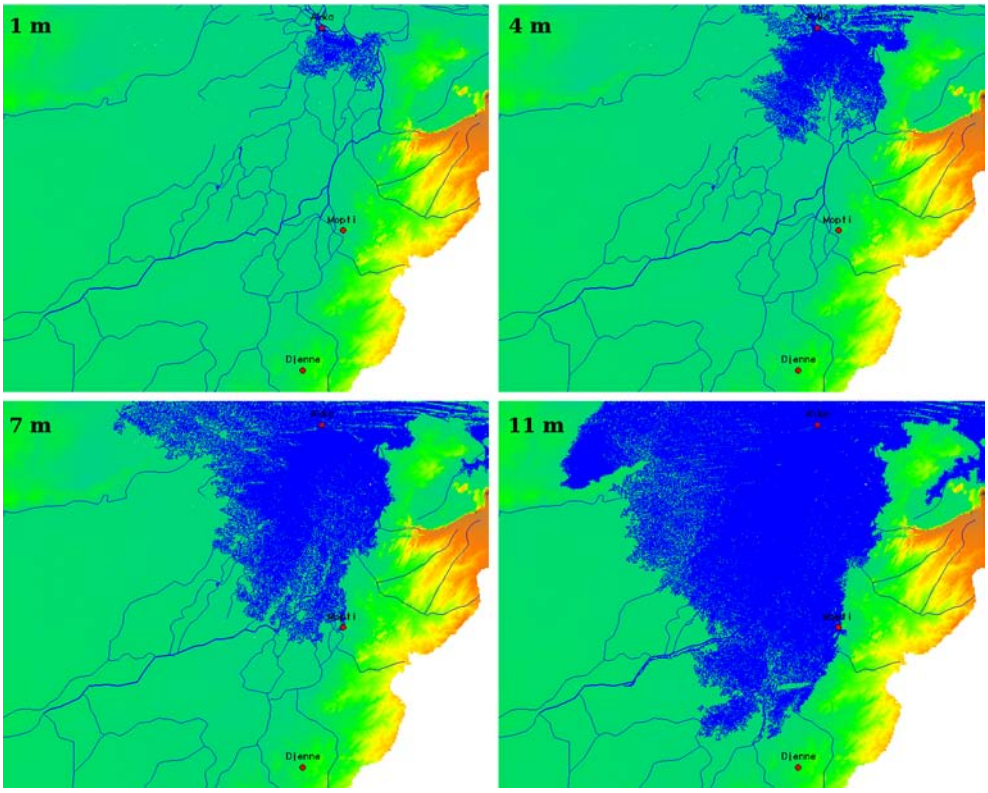

Figure 3-4 Flooding of the Inner Niger Delta using GRASS GIS module r.lake

Figure 3-4 shows an inundation time series from the Inner Niger Delta in Mali (Africa). These maps were created on the basis of SRTM data with a horizontal resolution of 90 meters and a vertical resolution of 1 meter. The reference point was set to a location in the Niger river close to the city of Akka at an altitude of 161 m.a.s.l. The Figures show the extent of the inundated areas when the water level at the reference point reaches the value indicated in the corresponding map (1 to 11m). Please note, the resolution of SRTM data might not be

sufficient for small wetlands. However, in the case of the Inner Niger Delta with an area of approximately 80,000 km^2 (Zwarts et al., 2005) the resolution is adequate. If data about maximum extents of flooded areas are available they could be used as a mask. This information could be estimated from satellite images, for instance. The GRASS GIS module *r.lake* automatically calculates the inundated area and the volume of water for each inundation level. These values are used to define corresponding thresholds in the next steps, the definition of inundation zones and the simulation of flooding processes.

Definition of inundation zones

The number of inundation zones is not fixed but can be determined by the user. In the simple version, the definition of the number of inundation zones basically depends on the vertical resolution of the DEM, the maximum inundation depth, and the level of complexity the user wants to implement. If the maximum inundation depth is 2 meters and the vertical resolution of the DEM is 1 meter, it would be reasonable to assign not more than two classes, or inundation zones, respectively.

In an advanced version of inundation zone delineation, one could further take the flow distance and the surface roughness into account. However, the approach described in this report is only based on inundation extents estimated by the module *r.lake*. In the example above, the maximum water level at the reference point is 11 meter, as shown in the preceding Figure. Hence, we distinguish 11 inundation zones. For each zone the area and the water volume, required for total inundation, was calculated using GIS functionalities.

Wetland HRUs

As mentioned in the description of SWIM model, Hydrologic response units (HRUs) or hydrotopes are portions of a subbasin that possess unique land use and soil properties. Such a map is produced by overlaying the land use, the subbasins, and the soil map. Units with similar land use and soil properties can be scattered throughout a subbasin. Although the geographic location of these units is known, HRUs can be considered as the total area of these units lumped together. Against this background, information about the geographic location of HRUs gets lost. For the implementation of the wetland module in the SWIM model it is necessary to identify unique units that are located inside a certain inundation zone. Therefore, a new model parameter at the HRU level is required (*ind_zone_nbr* = number of the inundation zone where the unit is located in). This parameter is assigned to the units, where units outside the inundation zones obtain the number 0 and all other units their corresponding inundation zone number. Thus, only unique units with similar inundation zone numbers are lumped together to form one HRU. HRUs that are located inside one inundation zone will be called hereafter "Wetland HRUs".

Flooding and release processes

A description of parameters used and processes accounted to simulate the flooding of inundation zones are now given. The general conceptual approach is: If simulated discharge exceeds the maximum water volume that can pass through the channel, it is assumed that the fraction of water volume greater than the maximum possible volume contributes to the flooding of adjacent areas (starting with inundation zone 1). If inundation zone *n* is totally flooded and simulated discharge still exceeds the maximum possible water volume, inundation zone *n+1* will be flooded and so on. The next Figure illustrates the conceptual approach of the flooding process. The release of water from the inundation zones starts, if simulated discharge is below the maximum possible water volume in the channel.

Flooding

The parameters cross section area *cs_area* [m^2] and average flow velocity *flow_vel* [$m*s^{-1}$] determine the maximum possible water volume in the channel. If this value is exceeded by the simulated discharge Q_{sim} [m^3*s^{-1}], the flooding process of adjacent areas (inundation zones) starts. The water volume that contributes per time unit to flooding *flood_flow* [m^3*s^{-1}] is estimated at the daily time step (*t*) using the following equation:

$$flood\_flow_{(t)} = Q_{sim(t)} - cs\_area * flow\_vel_{(t)} \quad (3.1)$$

And consequently $Q_{sim(t)}$ must be updated:

if $flood\_flow_{(t)} > 0$ then $Q_{sim(t)} = Q_{sim(t)} - flood\_flow_{(t)}$ (3.2)

Parameter *cs_area* can be derived from observations, literature or be calculated on the basis of the assumptions made about geometric dimensions of the stream or cross section using the GRASS module *r.stream.att* (Srinivasan & Arnold, 1994), where the width and depth of the stream are exponential functions of drainage area (Rosenthal et al., 1995). The flow velocity is the average channel velocity estimated by applying Manning's equation and assuming a trapezoidal channel with 2:1 side slopes and a 10:1 bottom width to depth ratio (Krysanova et al., 2000).

Each inundation zone is parameterized by its area *ind_area* [m^2] and its maximum storage volume *ind_vol_mx* [m^3]. Both parameters are calculated by the GRASS module *r.lake*. The actual storage volume of an inundation zone *ind_vol_act* [m^3] is calculated at the daily time step:

$$ind\_vol\_act_{(t)} = ind\_vol\_act_{(t-1)} + flood\_flow_{(t)} - ET_{(t)} - PERC_{(t)} + PCP_{(t)} \quad (3.3)$$

if $ind\_vol\_act_{(t)} < 0$ then $ind\_vol\_act_{(t)} = 0$

if $ind\_vol\_act_{(t)} > ind\_vol\_mx$ then see equation 3.4.

The flooding process continues as long as *flood_flow* > 0. If *flood_flow* < 0 then the water storage of the upper inundation zone starts to decrease by flowing back to the channel (release process). Percolation *PERC* [mm] and evapotranspiration *ET* [mm] are reducing the

actual inundation storage whereas rainfall *PCP* [mm] contributes to it. Percolation through the soil layers is only allowed if the respective lower soil layer is not saturated.

If a lower inundation zone is flooded and $flood\_flow_{(t)}$ is greater 0, the next higher inundation zone will be flooded.

$$ind\_vol\_act_{[n+1](t)} = ind\_vol\_act_{[n+1](t-1)} + ind\_vol\_act_{[n](t)} - ind\_vol\_mx_{[n]} \quad (3.4)$$

Due to natural heterogeneity of the land surface the actual inundation depth *ind_depth_act* [m] cannot be calculated by simply dividing volume by area. Instead a normalizing factor *FAC* is used here.

$$ind\_depth\_act_{(t)} = FAC\frac{ind\_vol\_act_{(t)}}{ind\_area} \quad (3.5)$$

With $FAC = ind\_area\frac{h_{[n]}}{ind\_vol\_mx_{[n]}}$ (3.6)

where h[n] is the maximum inundation depth of zone *n*, as illustrated in Figure 3-5.

The method used to estimate evaporation depends on the actual inundation depth. As long as the actual inundation depth is below a user-defined threshold *ind_et* [mm] the predefined evapotranspiration method is used. If the actual inundation depth exceeds this threshold, evaporation will be calculated as following, assuming evaporation from a water surface:

If $ind\_depth\_act_{(t)} > ind\_et$

$$ET_{(t)} = \eta * ET_{pot(t)} * ind\_area \quad (3.7)$$

Where η is an evaporation coefficient (0.6) and ET_{pot} the potential evapotranspiration (Neitsch et al., 2004).

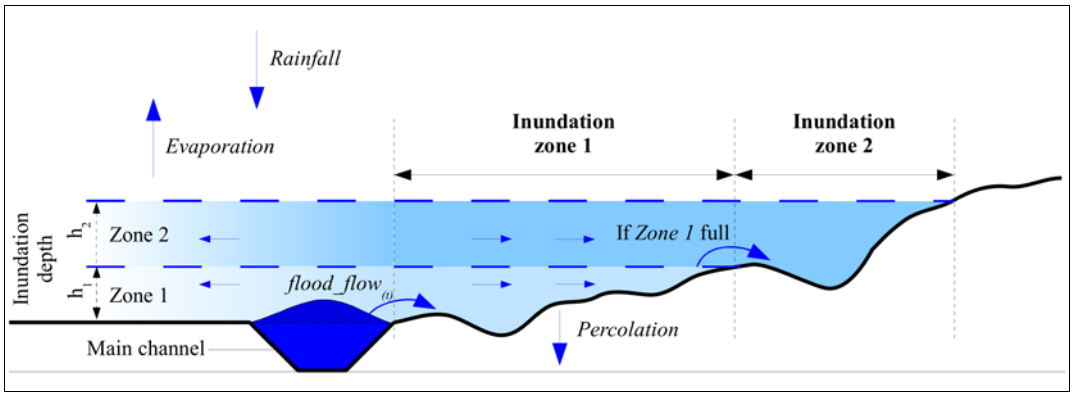

Figure 3-5 Conceptual scheme of the flooding process

Release process

The release process is the reverse function of the flooding process. A fraction of the water volume of the inundation storages will be allowed to contribute to discharge in the main channel at each time step. The process starts with the inundation zone with highest elevation.

In this conceptual approach we assume that the inundation storages have the properties of a linear storage where the outflow is directly proportional to its storage volume. The recession constant α determines the volume that will be released per time step.

$$Q_{storage(t)} = \alpha \frac{ind\_vol\_act_{[n](t)}}{86400} \quad (3.8)$$

Where $Q_{storage(t)}$ is the volume of water contributing to simulated discharge $Q_{sim(t)}$, *n* the number of the inundation storage, and α a value between 0 and 1.

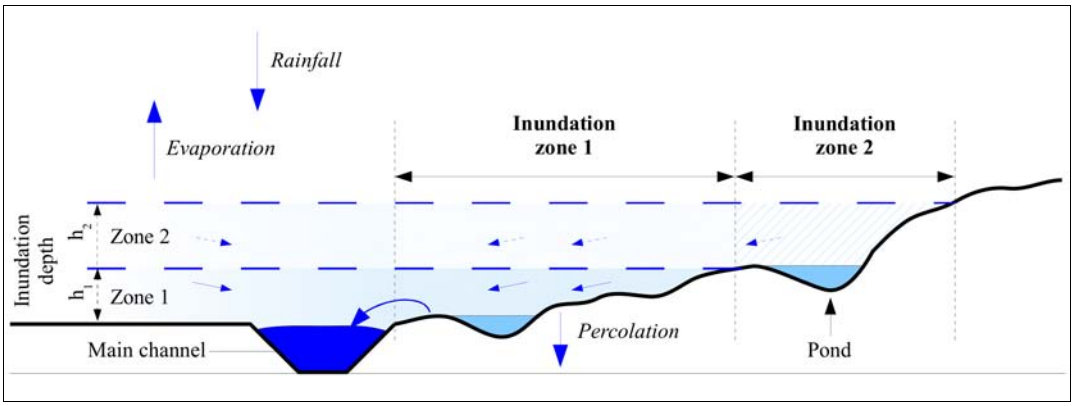

Figure 3-6 Conceptual scheme of the release process

Figure 3-6 shows the conceptual approach of the release process. The blue arrows indicate the main direction of water flows. Depending on the heterogeneity of the wetland's topography, apparently not the total volume of water of an inundation storage will contribute to streamflow. Rather, a fraction of it will remain in lakes and ponds from where it will evaporate or percolate to the shallow aquifer. In order to account for the volume of water stored in such ponds, the volume of the total area that lies below the inundation level inside an inundation zone will be calculated by using GIS and the digital elevation model

Wetland HRU switching

Since, the inundation storage is driven by discharge, rainfall, evaporation, and percolation the status of inundation zones can switch from "flooded" to "not flooded" and vice versa. According to the inundation depth (see equation 3.5), the status of affected Wetland HRUs can switch between the land and the water phase. In equation 3.7 a user-defined threshold *ind_et* was introduced. This threshold can be considered as a switching controller. Assuming a threshold value of 100mm would result in a switching of HRUs from land to water phase if the average inundation depth of an inundation zone is greater than 100mm. If the average inundation depth is below 100mm, the Wetland HRUs would switch back to the land phase. A Wetland HRU in the land phase acts like a "normal" HRU in SWIM. If a Wetland HRU turns to the water (lake) phase, the conditions for several processes (hydrologic and ecologic) change considerably. By switching to the water phase it is possible to change the functions used to simulate these processes. Large effects are expected by changing the evapotranspiration method, such as Penman-Monteith or Turc-Ivanov to a method that

estimates evaporation of a water surface, as shown in equation 3.7. Rainfall in the water phase would not contribute to surface runoff rather to increase the volume of the upper inundation storage.

3.4 DATA COLLECTION

3.4.1 Meteorological data

WATCH is a global sub-daily meteorological forcing dataset provided for use with landsurface- and hydrological-models. The data are derived from the **ERA-40** reanalysis product via sequential interpolation to half-degree resolution, elevation correction and monthly-scale adjustments based on **CRU** (corrected-temperature, diurnal temperature range, cloud-cover) and **GPCC** (precipitation) monthly observations combined with new corrections for varying atmospheric aerosol-loading and separate precipitation gauge corrections for rainfall and snowfall (following table). ERA-40 is the previous generation of global atmospheric reanalysis produced by ECMWF covering the period from mid-1957 to 2001. A new version of WATCH product is under release which are derived from ERA-Interim and covering the period 1979 to 2009.

Table 3-1 Summary of WATCH dataset sources

Dataset	Summary	Location
ERA-40	ECMWF reanalysis product	www.ecmwf.int/research/era/do/get/era-40 Uppala et al., 2005
CRU TS2.1	Climate Research Unit gridded station observations (multiple variables)	www.cru.uea.ac.uk/~timm/grid/CRU_TS_2_1.html
GPCC Full data product v4	Global Precipitation Climatology Centre gridded station precipitation observations	gpcc.dwd.de/ or orias.dwd.de/GPCC/GPCC_Visualiser

A summary of the inter-annual variability (1960-2001) of monthly mean precipitation at different locations in the Niger basin is presented using WATCH forcing dataset in Figure 3-7.

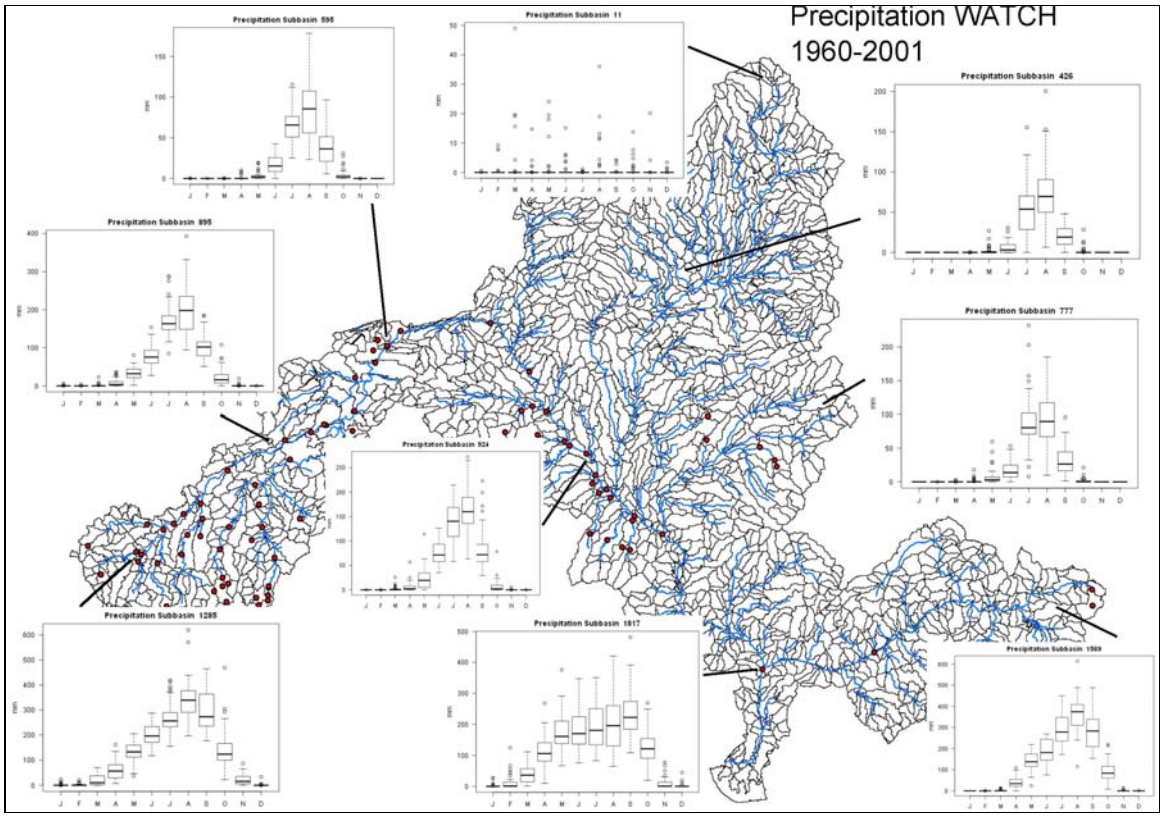

Figure 3-7 Inter-annual variability (1960-2001) of monthly mean precipitation at different locations in the Niger basin, WATCH forcing dataset from Aich, PIK

Climate trends in WATCH (Figure 3-8) show increasing temperatures (0.2°C per decade) and decreasing rainfall (34 mm per decade, although with long-term cyclic behavior) for the time period 1960-2001 in the Upper Niger basin.

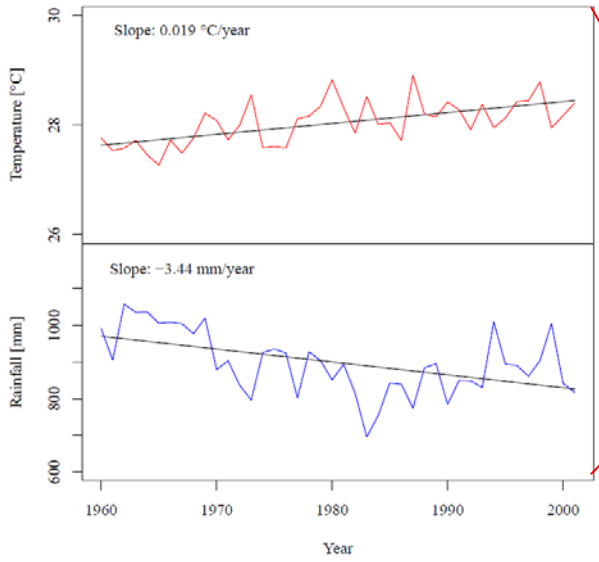

Figure 3-8 Observed temperature and rainfall trends in the Upper Niger Basin, WATCH forcing data, averaged over the Upper Niger region in Liersch et al. 2012

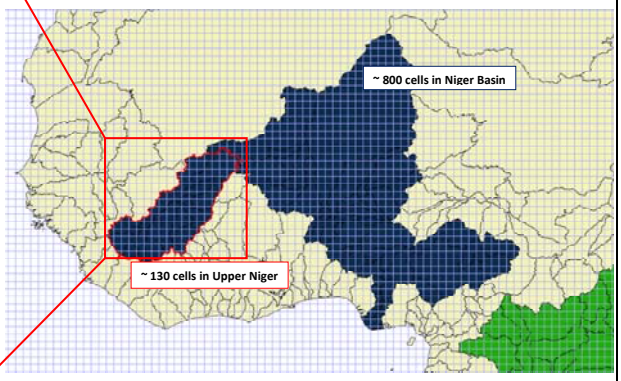

Figure 3-9 Number of cells for WATCH and ERA-I (0.5 degree resolution) for the setup of the Upper Niger region and the full Niger basin, from Liersch, PIK

ERA-Interim (hereafter ERAI) is the latest global atmospheric reanalysis produced by ECMWF. ERAI covers the period from 1 January 1979 onwards, and continues to be extended forward in near-real time. Gridded data products include a large variety of 3-hourly surface parameters, describing weather as well as ocean-wave and land-surface conditions, and 6-hourly upper-air parameters covering the troposphere and stratosphere. Vertical integrals of atmospheric fluxes, various synoptic and daily monthly averages, and other derived fields have also been produced. Berrisford et al. (2009) provide a detailed description of the ERAI product archive. Information about the current status of ERAI production, availability of data online, and near-real time updates of various climate indicators derived from ERAI data, can be found on the internet. Dee et al. (2011) presents a detailed description of the ERAI model and data assimilation system, the observations used, and various performance aspects. For further information, we invite the reader to a detailed description of the product which was already the object of one section in the Deliverable 4.1 Work Package 4, “Meteorological drought forecasting (monthly to seasonal forecasting) at regional and continental scale - ECMWF and CCAM meteorological data description” submitted in August 2011.

A set of 88 rainfall stations from the **DNM** (Direction Nationale de la Météorologie Malienne) is available on a daily basis in the Upper Niger Basin but only for restricted scientific use. Figure 3-10 shows the number of rainfall stations between 1890 and 2010.

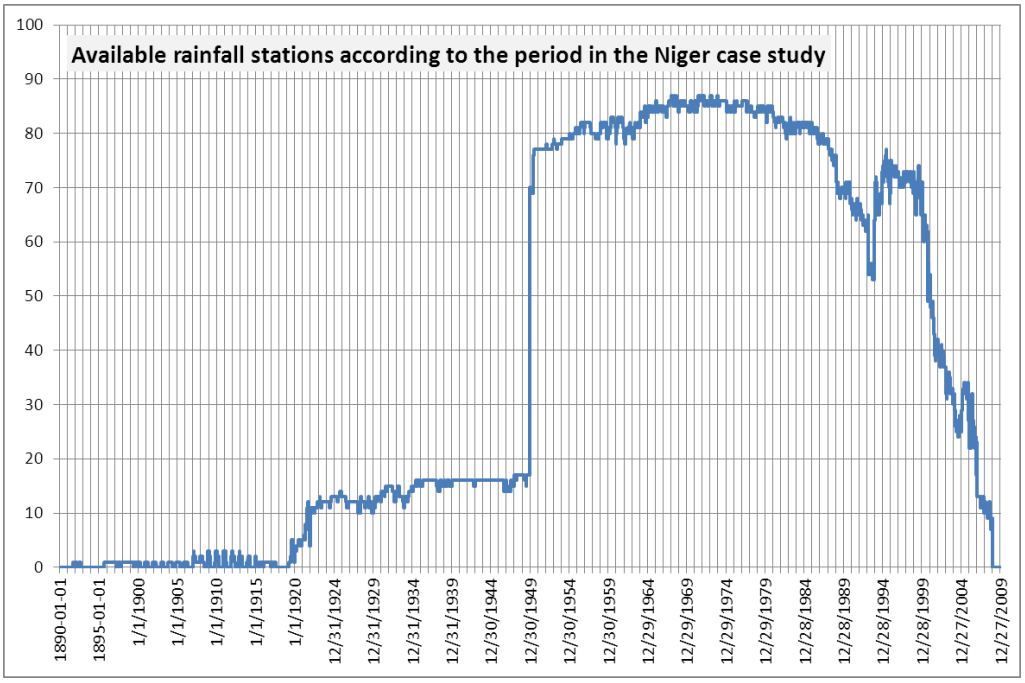

Figure 3-10 Number of available rainfall stations in the Niger case study according to the periods of study, from Fournet, PIK

MONTHLY TO SEASONAL WEATHER FORECAST PREDICTION

ECMWF and **CCAM weather forecast** products will be tested to simulate with SWIM short-term hydrological forecast. For further information, we invite the reader to a detailed description of the products which was already the object of one section in the Deliverable 4.1 Work Package 4, “Meteorological drought forecasting (monthly to seasonal forecasting) at regional and continental scale - ECMWF and CCAM meteorological data description” submitted in August 2011.

LONG TERM DYNAMICAL AND STATISTICAL CLIMATE MODEL PROJECTIONS

DYNAMICAL RCMS

CCAM model is used to simulate long term climate projections. The runs will be used to simulate with SWIM long term hydrological projections. For further information, we invite the reader to a detailed description of the product which was already the object of one section in the Deliverable 4.1 Work Package 4, “Meteorological drought forecasting (monthly to seasonal forecasting) at regional and continental scale - ECMWF and CCAM meteorological data description” submitted in August 2011.

STATISTICAL RCMS

The Statistical Analog Resampling Scheme (**STARS**) generates regional climate projections for the near future (for the next 50-60 years). The approach is based on the assumption that weather states from segments of the observational period may occur again or very similarly during the simulation period (Werner et al., 1997; Orlowsky et al., 2008, 2009, 2010). Hence, simulated series are constructed by resampling from segments of observation series, consisting of daily observations. This methodology thus produces results which can be considered physically consistent, and unlike some other downscaling techniques the STARS model is not driven by GCM-simulated circulation patterns, which are generally considered to lack reliability. STARS instead performs a simplified forcing method which seeks to constrain the simulated series to a pre-described regression line. In practical terms the forcing describes the long-term level and linear increase of a key variable (typically temperature) over the simulation period. As well as forcing, the method incorporates a set of heuristic rules which ensures that the resulting series exhibits properties such as annual cycles and persistence which are coherent with the observed series.

OTHER POSSIBLE RUNS AVAILABILITY

Under the World Climate Research Programme (WCRP) the Working Group on Coupled Modelling (WGCM) established the Coupled Model Intercomparison Project (**CMIP**) as a standard experimental protocol for studying the output of coupled atmosphere-ocean general

circulation models (AOGCMs). The CMIP phase 5 outputs will be normally available under the **ISI-MIP** platform (http://www.pik-potsdam.de/research/climate-impacts-and-vulnerabilities/projects/Externally_RD2/isi-mip). The Inter-Sectoral Impact Model Intercomparison Project is a community-driven modelling effort with the goal of providing cross-sectoral global impact assessments, based on the newly developed climate [Representative Concentration Pathways (RCPs)] and socio-economic [Shared Socio-Economic Pathways (SSPs)] scenarios. Depending on the date of acquisition, the CMIP5 runs would be integrated to the investigations of DEWFORA. The COordinated Regional climate Downscaling Experiment **CORDEX** is an ensemble of multiple dynamical and statistical downscaling models considering multiple forcing GCMs applied to Africa (http://cordex.dmi.dk/joomla/). This product will be normally available within the year 2012. Depending on the date of acquisition, the CORDEX runs would be integrated to the investigations of DEWFORA.

3.4.2 Hydrometric data

Discharge data are provided by the Global Runoff Data Centre (GRDC) which works under the auspices of the World Meteorological Organisation (WMO) (hosted by the German Federal Institute of Hydrology (BFG)). This source is completed with water level information coming from the database archives of Wetlands International. A summary of the inter-annual variability (1960-2001) of monthly mean discharge at different locations in the Niger basin is presented using GRDC dataset in Figure 3-11.

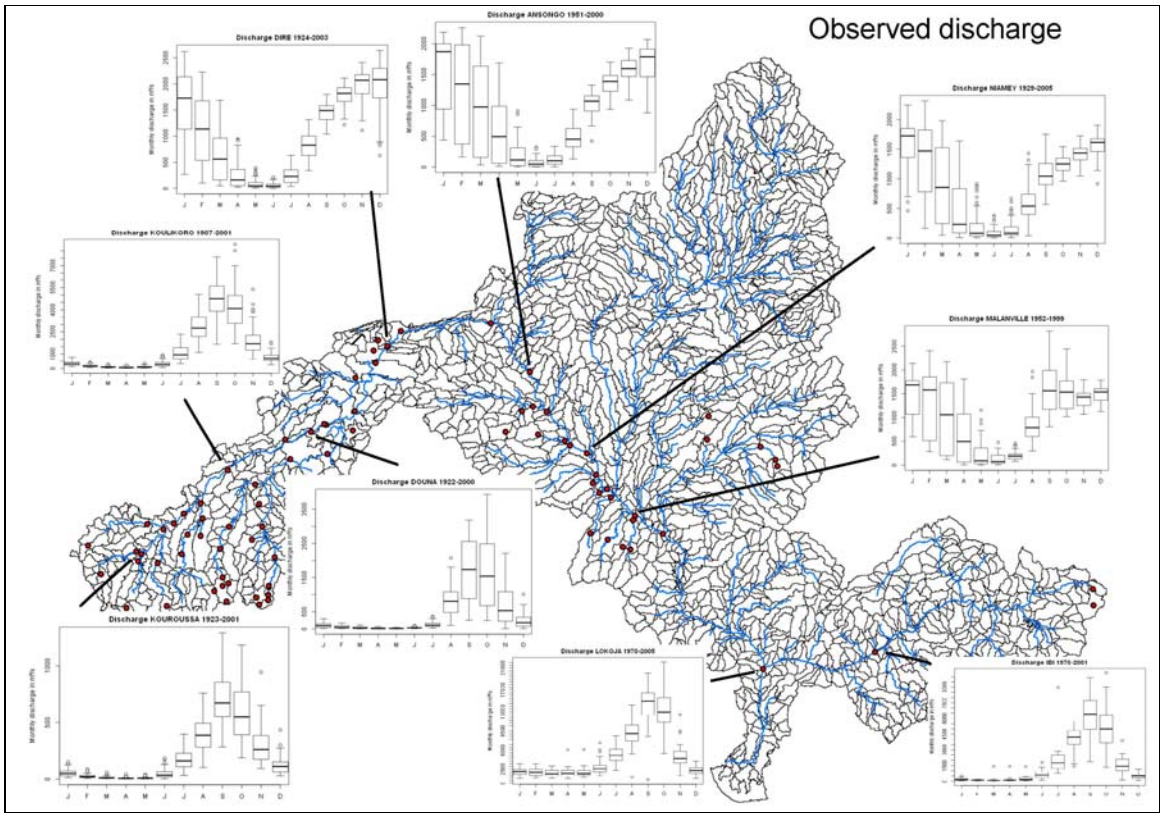

Figure 3-11 Inter-annual variability (period depending on time series availability) of monthly mean precipitation at different locations in the Niger basin, GRDC dataset

3.5 MODEL SET-UP, CALIBRATION AND VALIDATION

3.5.1 Model Set-up

VERSION OF THE MODEL SET-UP

Two model versions for the Niger case study are currently under development and under investigation. The first version called *Upper Niger model* covers the Upper Niger basin and the Inner Niger Delta and was already the object of advanced calibration and validation works. The second model set-up version called *Niger River model* includes as indicated in the name the overall catchment of the Niger River. This version initiated this summer is under the calibration phase. The current advancements of the calibration and validation processes will be then presented for the two model setup versions.

GIS DATA REFINEMENT AND RECLASSIFICATION

SRTM elevation data (Jarvis et al., 2008) served as input for the delineation of sub-basins. Soil classes are taken from the Digital Soil Map of the World (FAO et al., 2009) and the parameters are derived from the Harmonized World Soil Data Base. Finally, land use data were reclassified according to SWIM standard from Global Land Cover (GLC2000). All GIS data refinement and reclassification are summarized in Table 3-2.

Table 3-2 GIS data refinement and reclassification for SWIM setup and parameterization

SWIM referencing GIS inputs	Name	Reference
Digital Elevation Model 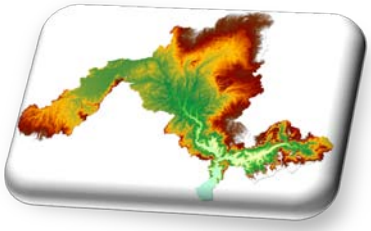	SRTM Version 4, 90m resolution by the Shuttle Radar Topographical Mission	http://bioval.jrc.ec.europa.eu/products/glc2000/glc2000.php
Land-use classification 	Global Land Cover 2000	http://bioval.jrc.ec.europa.eu/products/glc2000/glc2000.php
Soil classification and parameterization 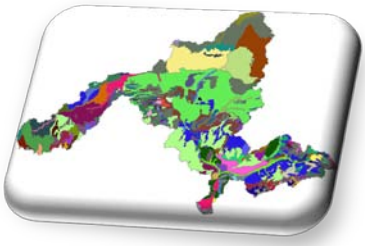	Digital Soil Map of the World	http://www.fao.org/geonetwork/srv/en/metadata.show?id=14116&currTab=distribution
	Harmonized World Soil Data Base v1.1	http://www.iiasa.ac.at/Research/LUC/External-World-soil-database/HTML/index.html
Sub-basin delineation 	**Upper Niger model** Number of sub-basins: Sub-basin average area:	**Niger river model** Number of sub-basins: 1923 Sub-basin average area: 1150km²

3.5.2 Calibration and validation

METHOD

WATCH climate data served as input and daily observed discharge data, provided by the Global Runoff Data Centre (GRDC), were used for calibration and validation. The model PEST (Model-Independent Parameter Estimation and Uncertainty Analysis:

http://www.pesthomepage.org/) was used to calibrate and validate the two model setup versions with the sets of parameters presented in the following table. Further details on the selected calibration/validation parameters and the undergoing related processes operated within SWIM can be found in Krysanova et al., 2000a.

Table 3-3 Summary of the parameters used for calibration in SWIM based on Krysanova et al., 2000a

Main parameters for calibration	Brief explanation
roc2	routing coefficients to calculate the storage time constant for the reach for the surface flow
roc4	routing coefficients to calculate the storage time constant for the reach for the subsurface flow
sccor	correction factor for saturated conductivity (applied for all soils)
bff	baseflow factor for basin, is used to calc return flow travel time. The return flow travel time is then used to calculate percolation in soil from layer to layer
abf	alpha factor for grounwater. This parameter characterizes the groundwater recession (the rate at which groundwater flow is returned to the stream).
delay	groundwater delay (days). The time it takes for water leaving the bottom of the root zone until it reaches the shallow aquifer where it can become groundwater flow.

UPPER NIGER MODEL

SWIM was calibrated for the period 1971-1980 and validated for the period 1982-2000 at several gauges for the Upper Niger model. The 1960s were not included in the calibration-validation process for two main reasons. On one hand, the model needs a relative long period of hot start to generate flood dynamics of the Inner Niger Delta. On the other hand, the region is subject to important inter-decadal climate variability. Also, the end of the 1960s shows an abrupt jump in the precipitation pattern. As a consequence, the 1950s and the 1960s remain exceptionally wet compare to the 1970s and 1980s where a severe and continuous drought is recorded. Following the objective of DEWFORA project to focus on drought pattern, the logic was then to calibrate and validate the model during a drought sensitive period.

Table 3-4 summarizes for seven gauges the final parameterization of the six main parameters used for the calibration and validation of the Upper Niger model. To illustrate, the results of the calibration and validation process, two emblematic gauges are then presented in the two next sub-sections.

Table 3-4 Summary of the optimum PEST parameterization of SWIM in seven gauges (Upper Niger model)

PEST Calibration	Gauge						
Parameter	Dire	Ke-Macina	Koulikoro	Douna	Selingue	Fomi	Tiguibery
roc2	1	0.5	0.5	0.9	10	4	0.93
roc4	1	1.01	1.01	1.64	2	4	1.46
sccor	1	5.41	5.41	5.69	0.97	10	6.38
bff	1	1.206	1.206	0.423	0.1	0.9	0.7
abf	0.005	0.00005	0.00005	0.0114	0.0003	0.0005	0.1999
delay	1	29.1	29.1	21.47	2.6	15.4	10.25

KOULIKORO GAUGE: MODEL VALIDATION UNDER THE IMPACT OF SÉLINGUÉ RESERVOIR MANAGEMENT ON THE HYDROLOGICAL REGIME

During the calibration, the discharges in the Upper Niger Basin were characterized by a natural flow regime not yet affected by the Sélingué dam, which was built in 1982. In the validation period (1982-2000), the Sélingué dam was then also integrated in the model and tested to simulate the management of the reservoir and its effect on the hydrological regime. Therefore, the calibration-validation process enables to analyze the skill of the model to reproduce the hydrological regime under the water management of the Sélingué dam.

From 1971 to 1981, the simulated discharge at gauge Koulikoro fits to the observed discharge reproducing well high peaks and low flow patterns with a respective Nash-Sutcliffe Efficiency (NSE) coefficient of 0.92, a log NSE coefficient of 0.95 and R^2 (applied to the mean annual runoff) equal to 0.996 (see two next Figures). The mean annual runoff shows that high peaks tend to be overestimated over the calibration period.

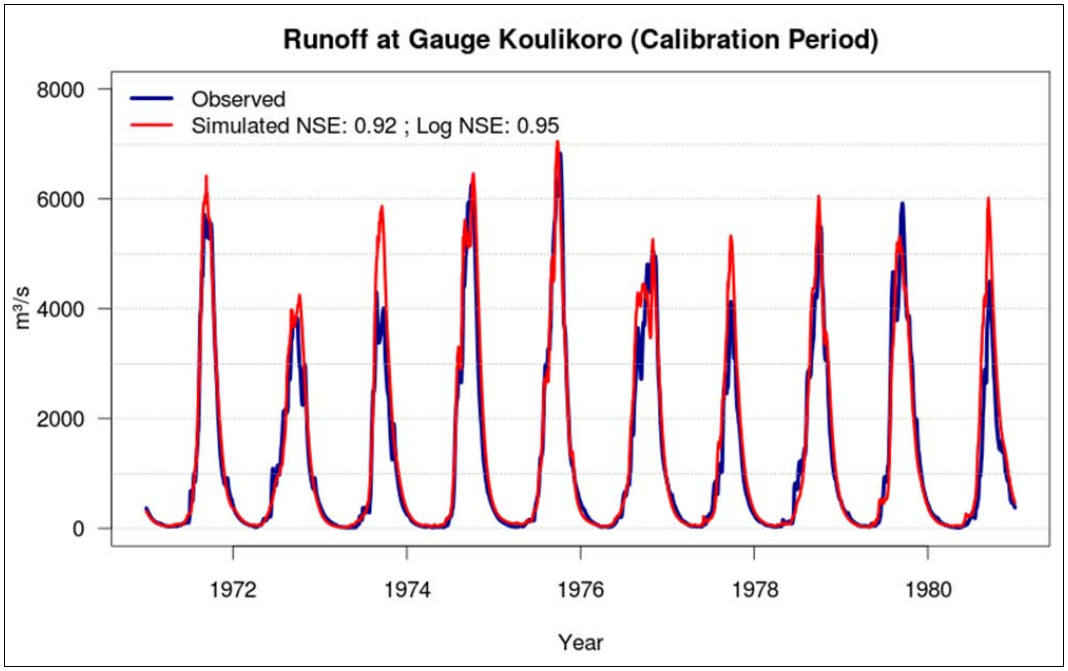

Figure 3-12 Comparison of daily continuous monitored and simulated flow at gauge Koulikoro (1971-1980): calibration phase

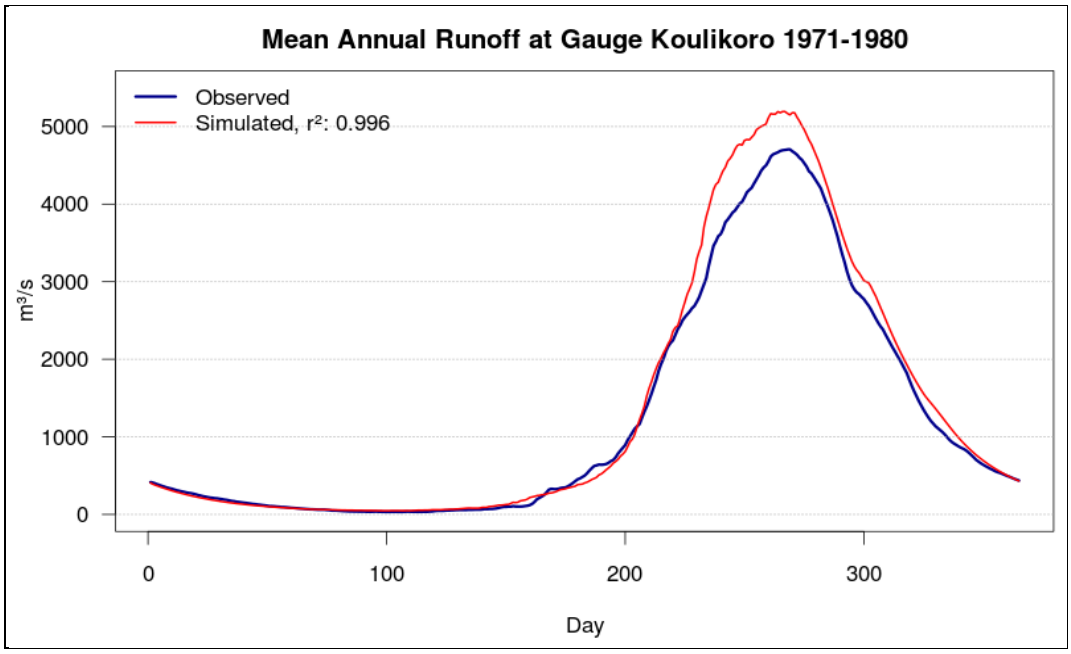

Figure 3-13 Comparison of monitored and simulated flow (mean annual runoff) at gauge Koulikoro (1971-1980): calibration phase

However, the flow duration curve presents a robust trend for the flow exceeding 100 m³/s at the gauge Koulikoro (see Figure 3-14). Below 100 m³/s, a slight shift in the occurrence of low discharge events can be observed. The two biases for high peak and low flow might come from water diversion operated by medium to small irrigation schemes established in the Upper Niger catchment. The irrigation schemes are not yet implemented in the model due to a lack of consistent water management information at this scale for really sporadic and evolutive activites. Large part of the overestimation of the flow especially of the peak seen in the gauge Koulikoro can be then mainly deduced from this factor.

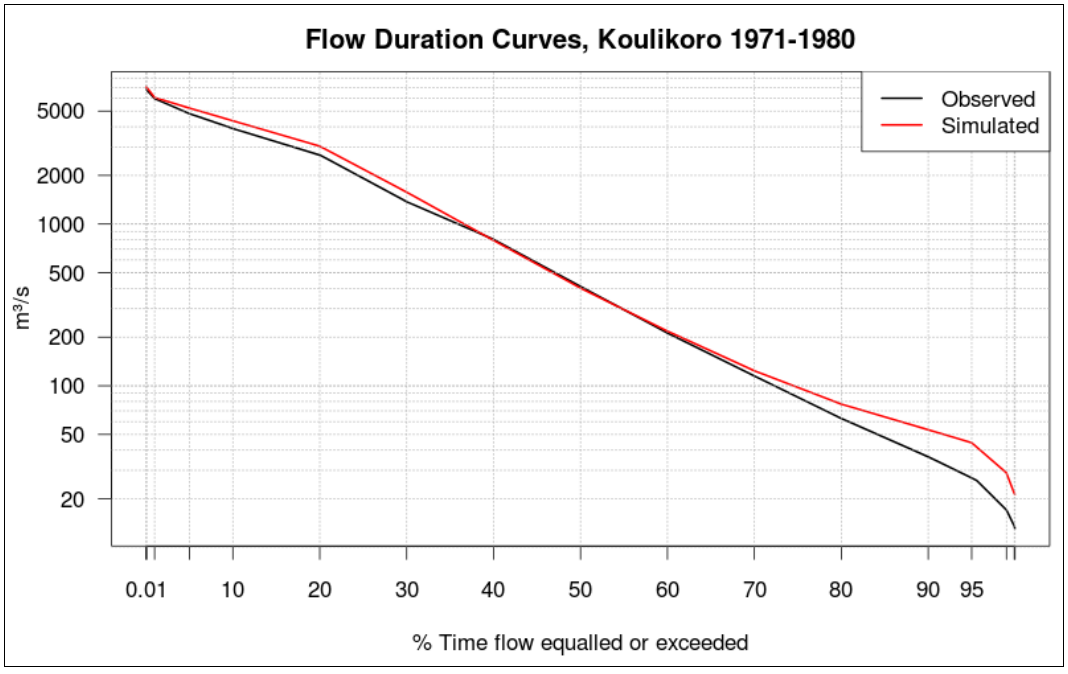

Figure 3-14 Comparison of monitored and simulated flow duration curves at gauge Koulikoro (1971-1980): calibration phase

For the validation period (1982 to 2000), two simulation runs were operated to present the benefits of integrating the reservoir management of Sélingué. Without reservoir, the performance of SWIM present medium skills (NSE: 0.55 and log NSE: 0.78) as the model do not reproduce the effects of the Sélingué dam with a substantial reservoir storage during the annual peak and reversely water release which sustain the volume of discharge during the annual low flow period. When including the reservoir module, the low flow pattern corresponds better to the annual cycle monitored at gauge Koulikoro and gain in performance with a NSE equal to 0.69 and a log NSE equal to 0.89. Also, we can observe a large mismatch for the year 1999 between monitored flow and the simulation including the reservoir module and this year strongly contributes to lower the general performance. Orange et al., 2002 reported for the year 1999 an exceptional mismanagement of the Sélingué reservoir with a release of water starting at an earlier stage than what is normally and originally scheduled and implemented in SWIM model. Consequently, the difference between the simulated and the monitored data in the year 1999 allow pointing out the effects of this specific mismanagement in the Sélingué reservoir.

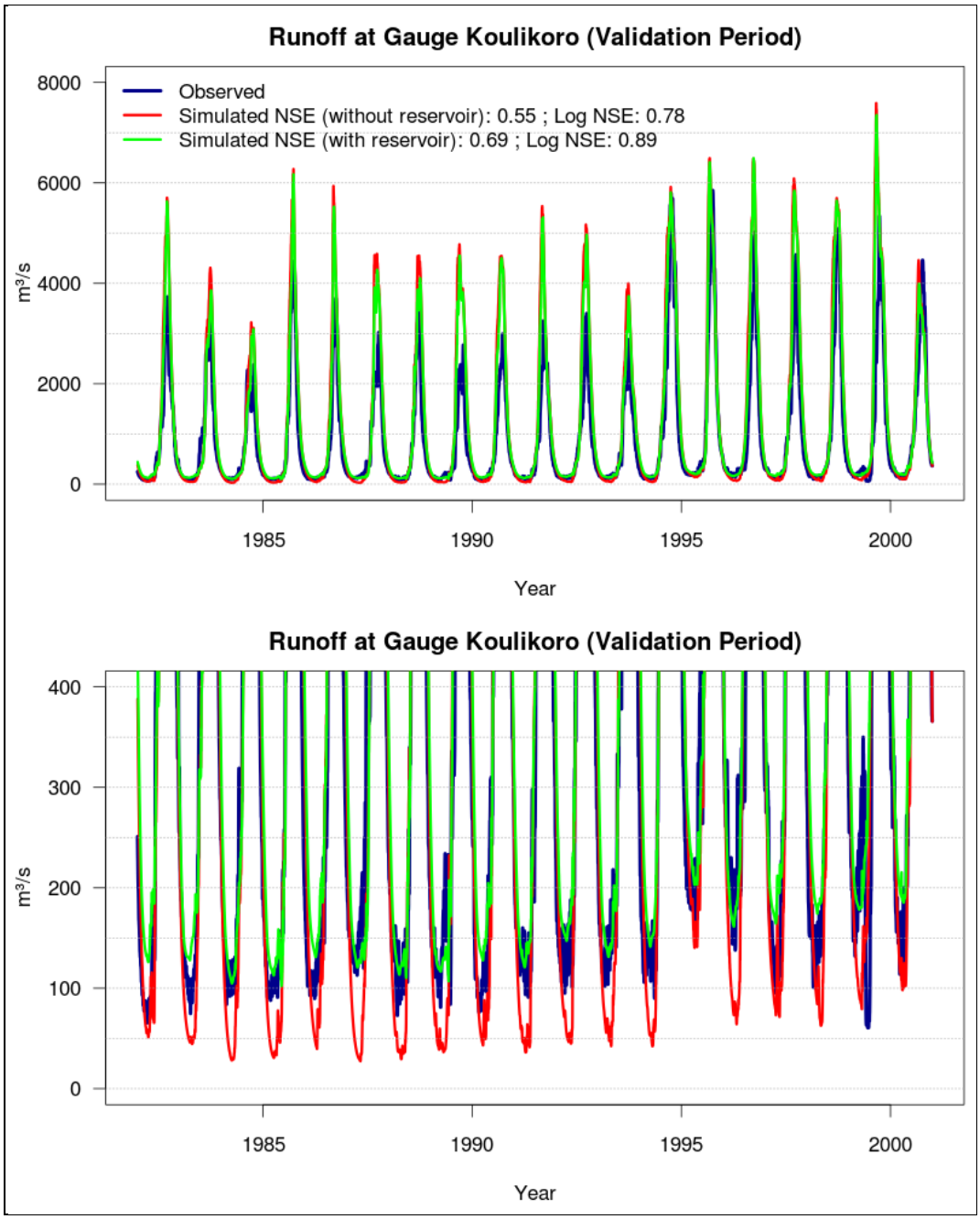

Figure 3-15 and 3-16: Comparison of monitored and simulated flow at gauge Koulikoro (1971-1980) with a focus on low flow pattern: validation phase

In the two following Figures, same remarks outlined in the results for the calibration period can be addressed with even a more pronounced overestimation of the annual peak and with less extend of the low flow period. This behavior can be partly associated to a gradual increase of water diversion initiated by a politic of extension and development of irrigated schemes in the catchments upstream Koulikoro.

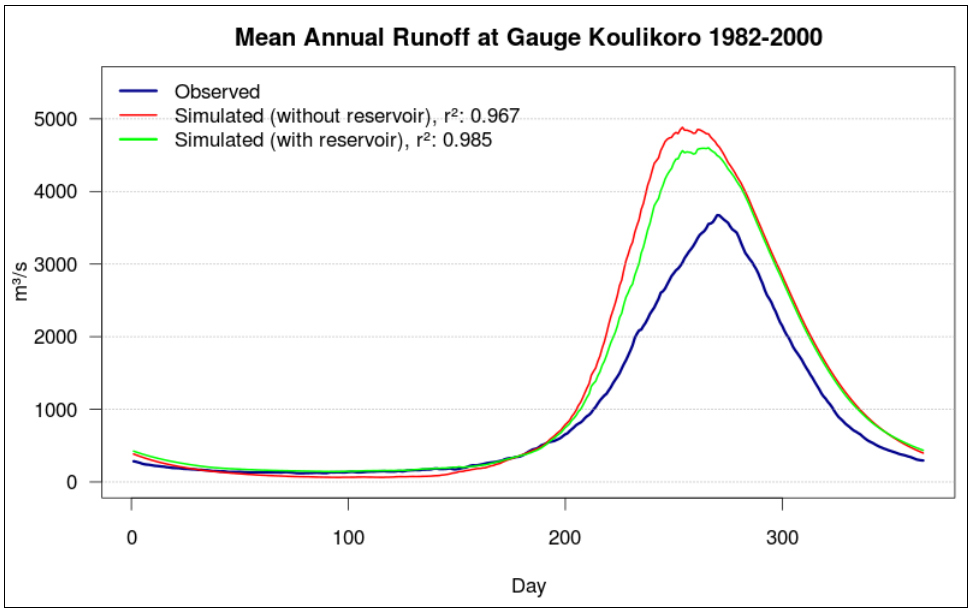

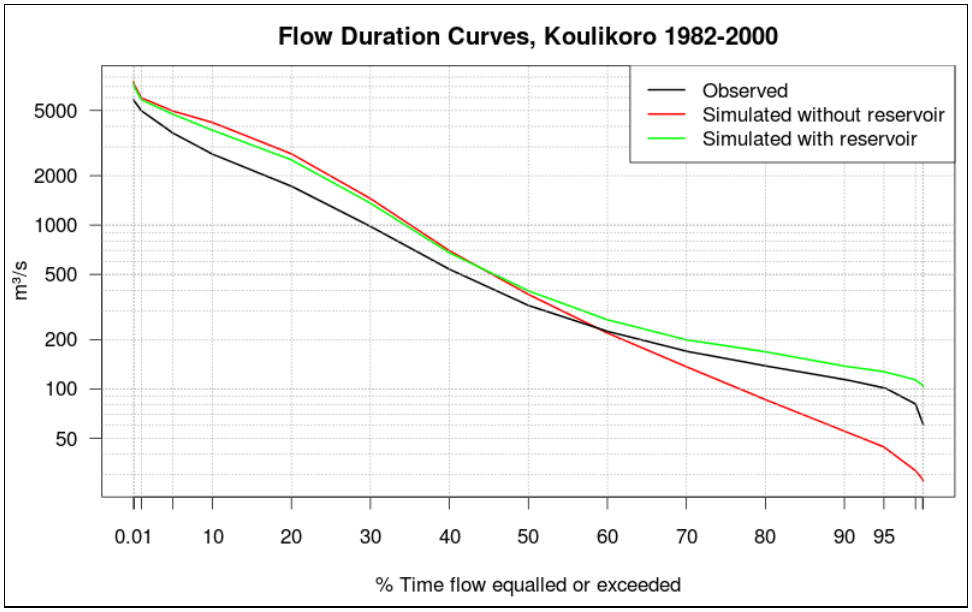

Figure 3-17 and 3-18: Comparison of monitored and simulated flow at gauge Koulikoro (1971-1980) Mean Annual runoff and flow duration curve: validation phase

DIRÉ GAUGE: MODEL VALIDATION UNDER THE IMPACT OF THE INNER NIGER DELTA FLOOD PROPAGATION ON THE HYDROLOGICAL REGIME

Figure 3-19 illustrates the effects of the flood propagation and the water losses in the Inner Niger Delta on the downstream annual flood peak at gauge Diré compared to the two main tributaries represented by the gauges Diré and Koulikouo. We can observe a delay of the flood peak of about two months and mean annual relative water losses corresponding of about 42 % of the total inflows.

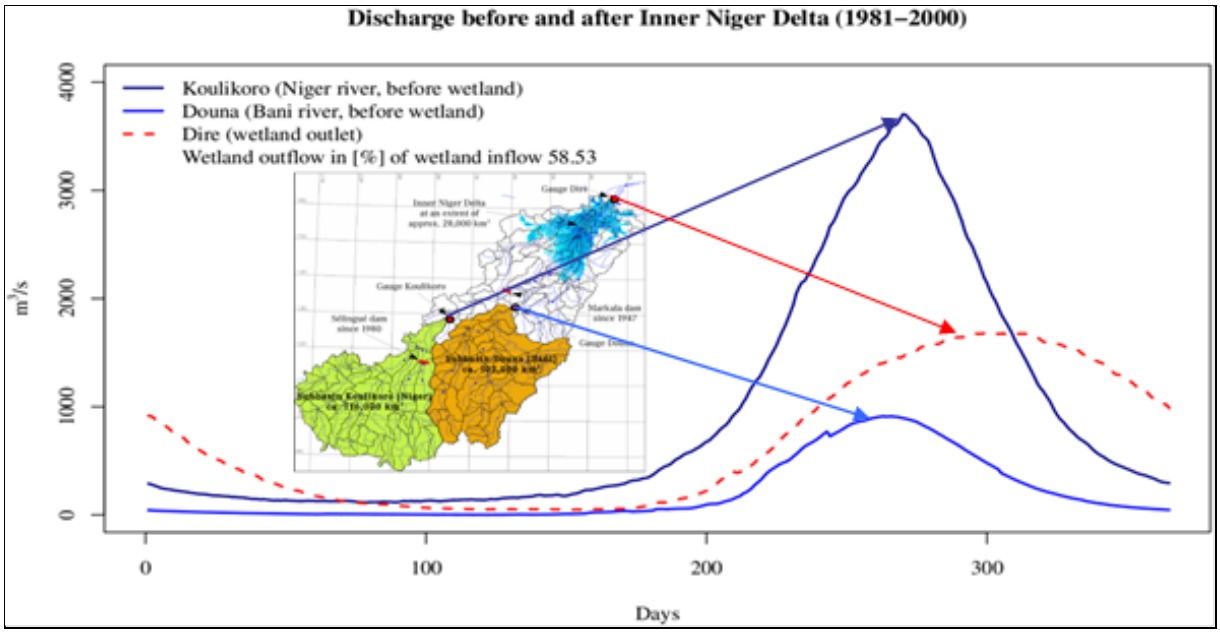

Figure 3-19 Discharge before and after the Inner Niger Delta (1981-2000) in Liersch, 2011

Figure 3-20 shows what SWIM might simulate when the inundation module (described in the previous sub-sections) is not integrated. The simulated discharge at gauge Diré at this step do not incorporate the overflowing processes assuming a fast release of the flood peak with a detrimental effect on the reflectance of the regional water balance. The reproduction of the discharge patterns is then highly compromised.

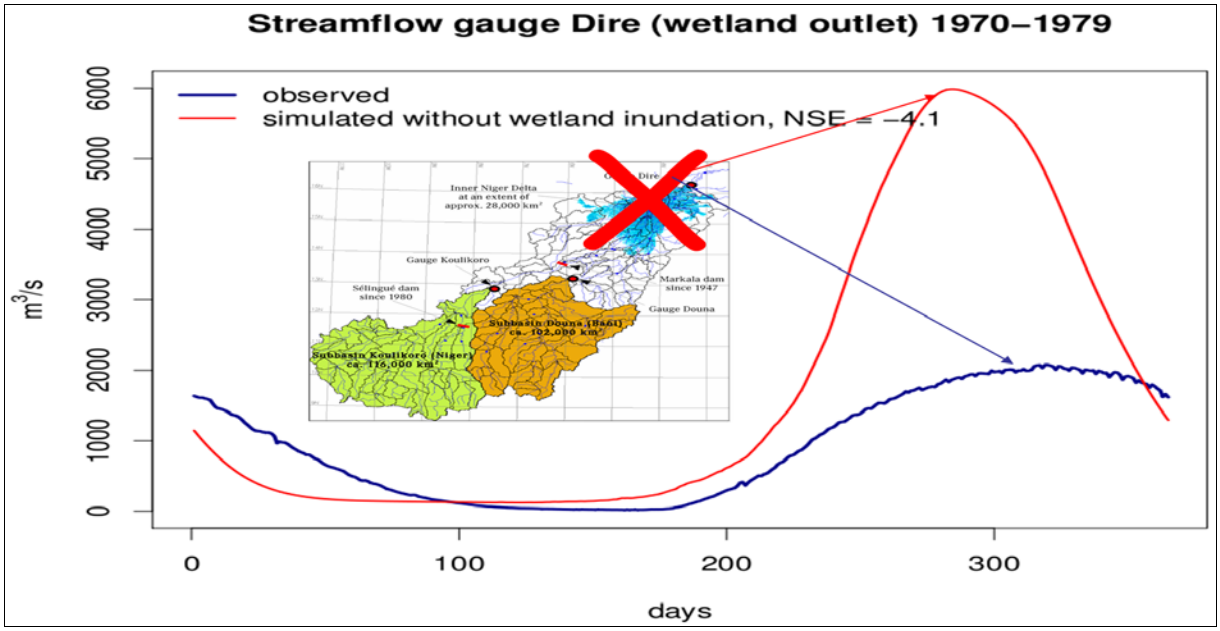

Figure 3-20 Comparison of the monitored and simulated streamflow at Diré gauge without the implementation of the inundation module (1970-1979) in Liersch, 2011

With the inundation module, the model SWIM challenges this problem and obtains a satisfactory Nash-Sutcliffe coefficient equal to 0.77 over the calibration period.

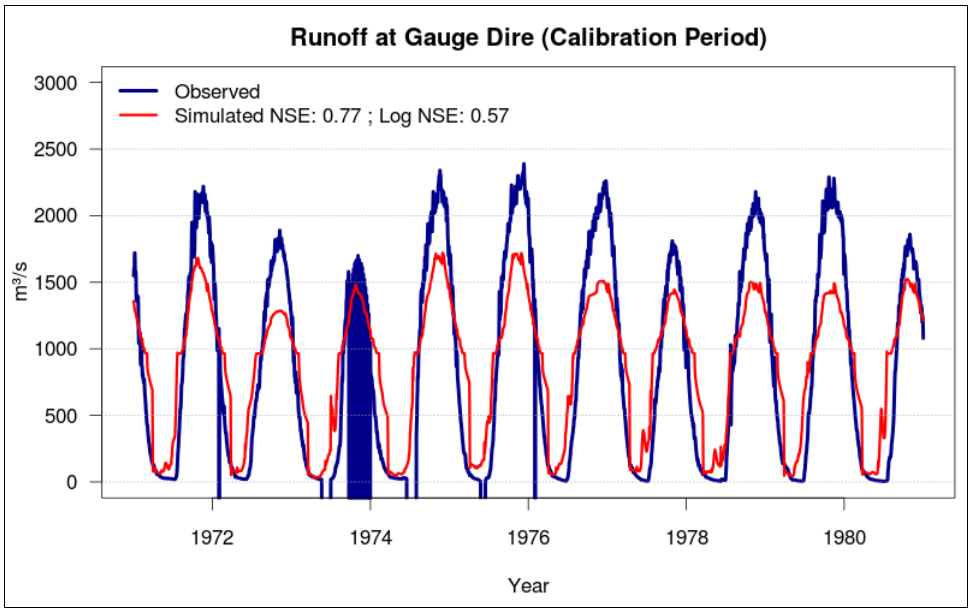

Figure 3-21 Comparison of monitored and simulated flow at gauge Diré (1971-1980): calibration phase

For the validation period, both simulations (incorporating or not Sélingué reservoir management) get a reasonable Nash-Sutcliffe coefficient above 0.7 which demonstrates the skill of the method applied. However, this simple conceptual technic presents naturally some limitations when the objectives would be to analyse the annual discharge peak in absolute values due to an underestimation of this hydrological process or also to analyze the date initiating the discharge increase as the initial and the final dates of the flooding process differ from some days to the monitored which tend to extend the flooding period. We can outline better skills of the model to reproduce low discharge values which is really valuable for the aim of the DEWFORA project. Finally, we can also observe the two main influences of the reservoir management which tend to smooth down the annual peak and artificially maintain higher flow during the dry season.

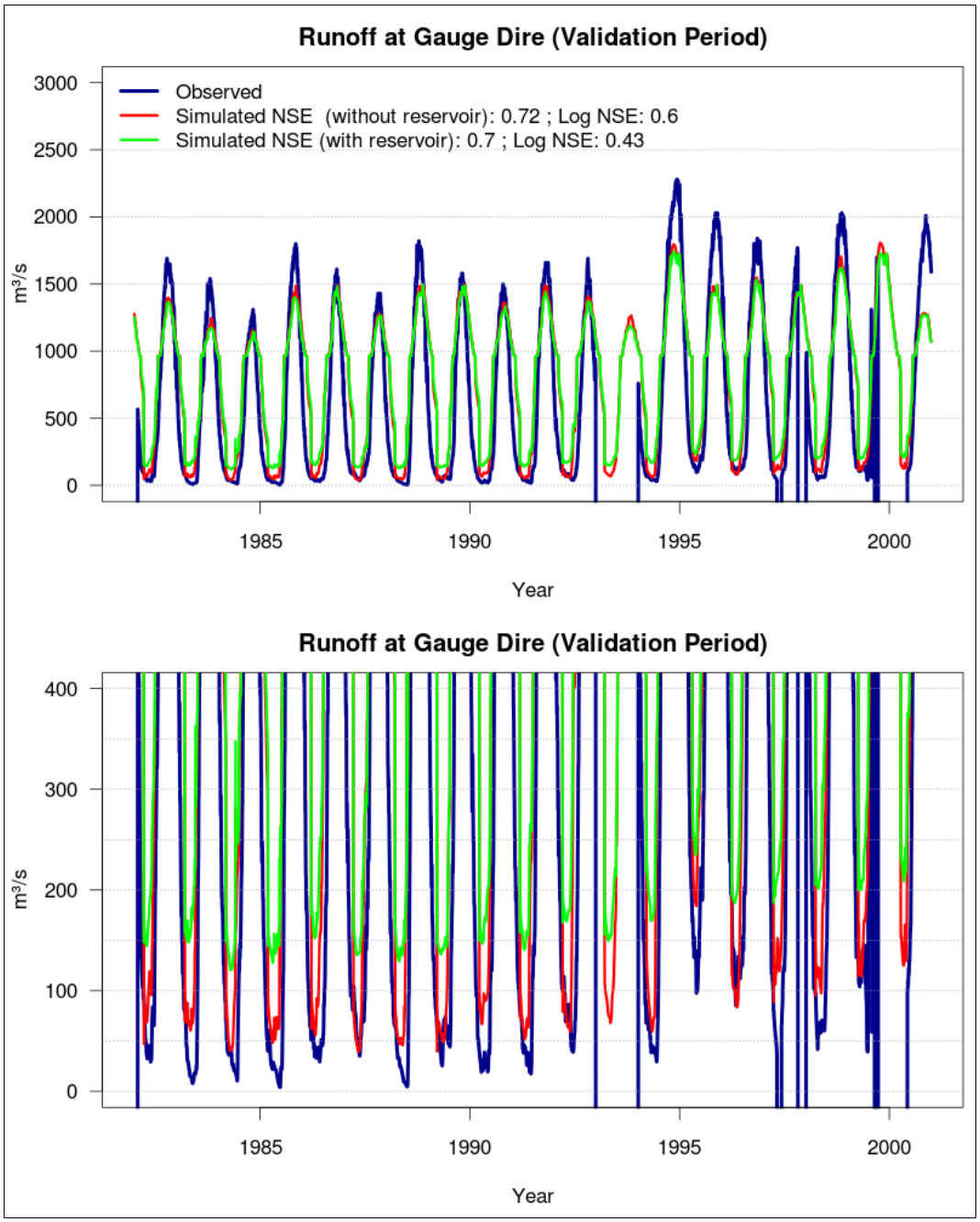

Figure 3-22 and 3-23: Comparison of monitored and simulated flow at gauge Dire (1980-2000) with a focus on low flow pattern: validation phase

The skills of the inundation module enable then to study with more details the general effects of the reservoir management during significant realization (wet and a dry year). The results presented in Figure 3-24 show a general decrease of the flood propagation especially pronounced during the release phase. A small delay can be observed for the propagation which can particularly affect the productivity of free submersion agriculture and the regional food security.

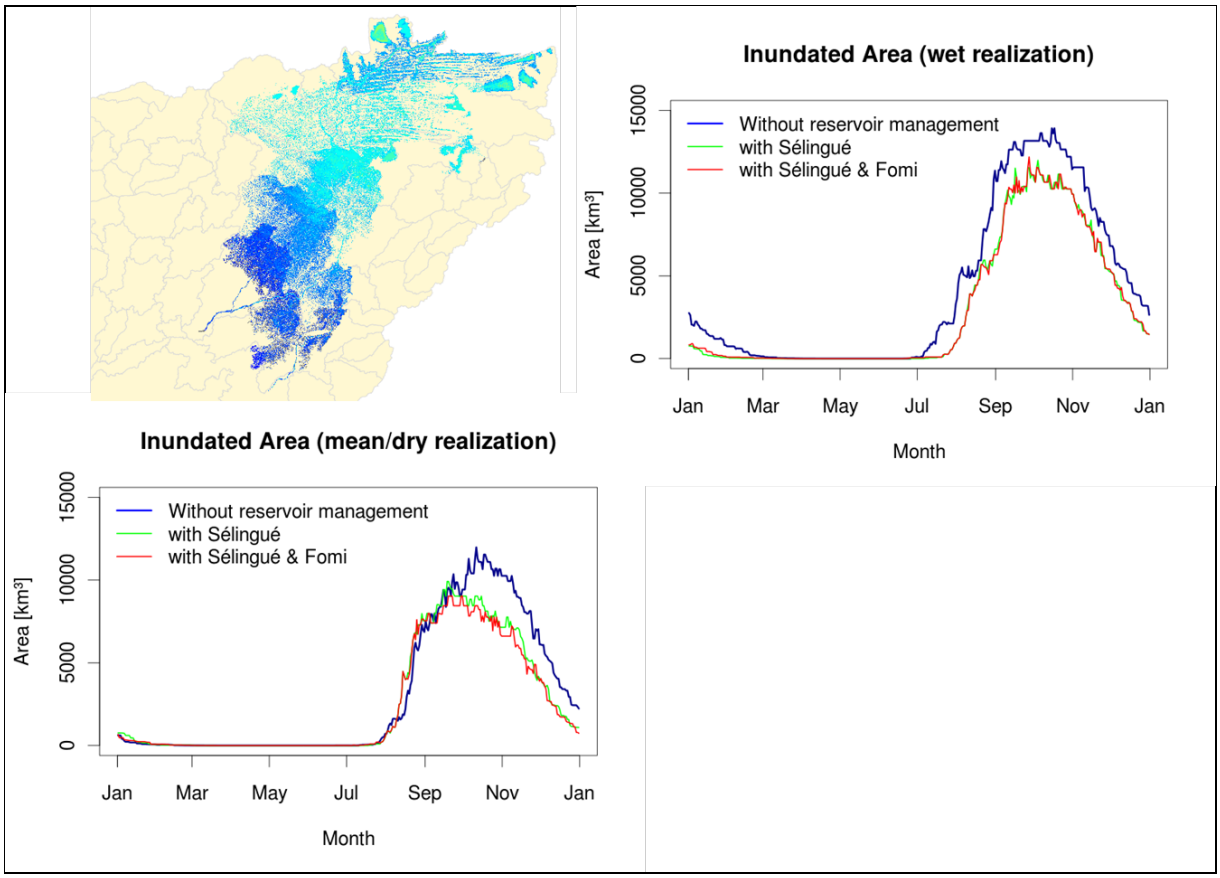

Figure 3-24 Effects of reservoir management on the flood extent of the Inner Niger Delta during a dry and wet year, simulation with inundation module in Koch et al., 2011

To present the current advancement of the Niger River model setup, a summary of the optimum PEST parameterization for the six main parameters are presented in Table 3-5 for two representative gauges influenced by reservoirs. The results of the calibration are then presented in the two following sub-sections.

Table 3-5 Summary of the optimum PEST parameterization of SWIM for the Sélingué and Kouroussa gauges (Niger river model)

PEST calibration	Sélingué gauge			Kouroussa gauge		
Parameter	Min	Max.	Opt.	Min	Max.	Opt.
roc2	100	400	400	10	400	400
roc4	300	100	400	10	400	369.445
sccor	4	55	4	5	55	5.62044
bff	0.005	1.5	0.217373	0.005	1.5	0.670311
abf	0.005	1	1.07E-02	0.005	1	1.22E-02
delay	2	200	4.55532	2	200	1

KOUROUSSA GAUGE: MODEL CALIBRATION

Kouroussa gauge corresponds to the closest gauge influenced by the implementation of the Fomi dam. The Figure 3-25 shows the current advancements for the calibration of this gauge without the influence of the Fomi dam (currently under construction). When comparing the

daily simulated to the discontinuous discharge time series monitored between 1963 and 1974, SWIM fits well to the monitored annual hydrological fluctuations and obtains after calibration a NSE equal to 0.88.

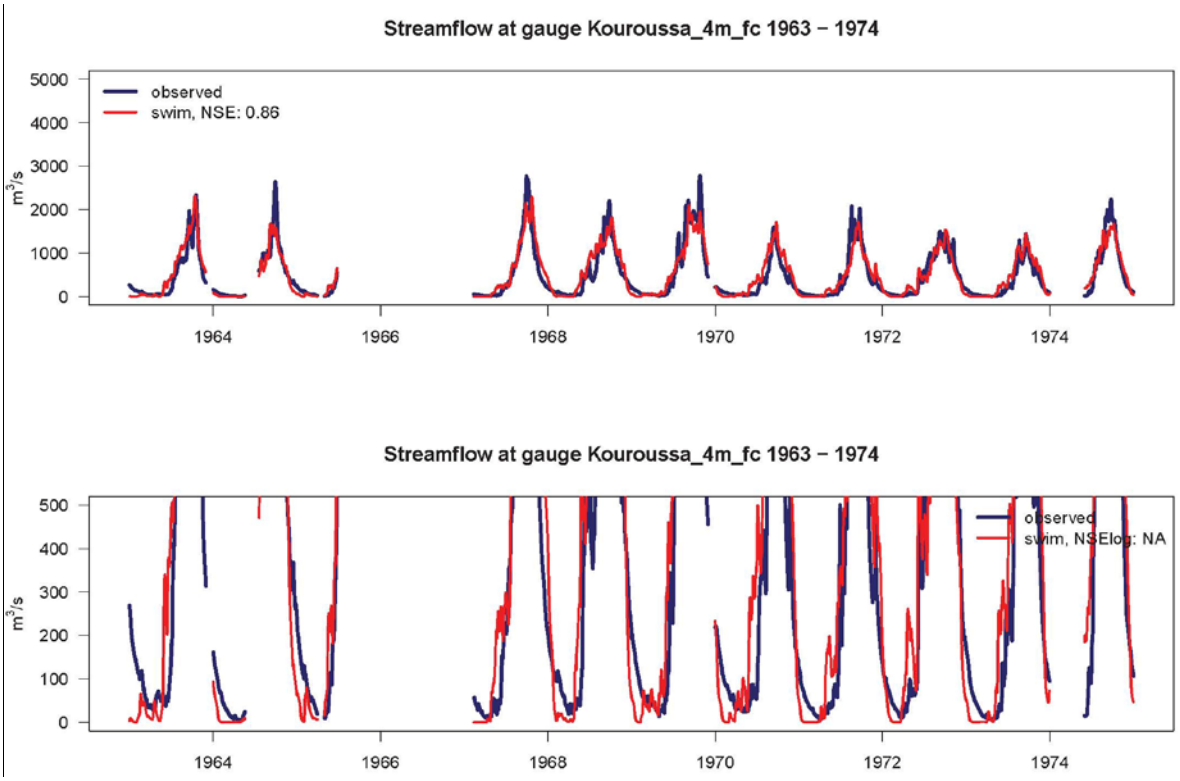

Figure 3-25 and 3-26: Comparison of monitored and simulated flow at gauge Kouroussa (1964-1974) with a focus on low flow pattern: calibration phase

SÉLINGUÉ GAUGE: MODEL CALIBRATION

Sélingué gauge corresponds to the implementation of Sélingué dam. Figure 3-27 shows the current advancements for the calibration of this gauge without the influence of the dam (constructed in 1982). When comparing the simulated to the discontinuous discharge data monitored between 1965 and 1975, SWIM fits well to the monitored annual hydrological fluctuations and obtains after calibration a NSE equal to 0.82.

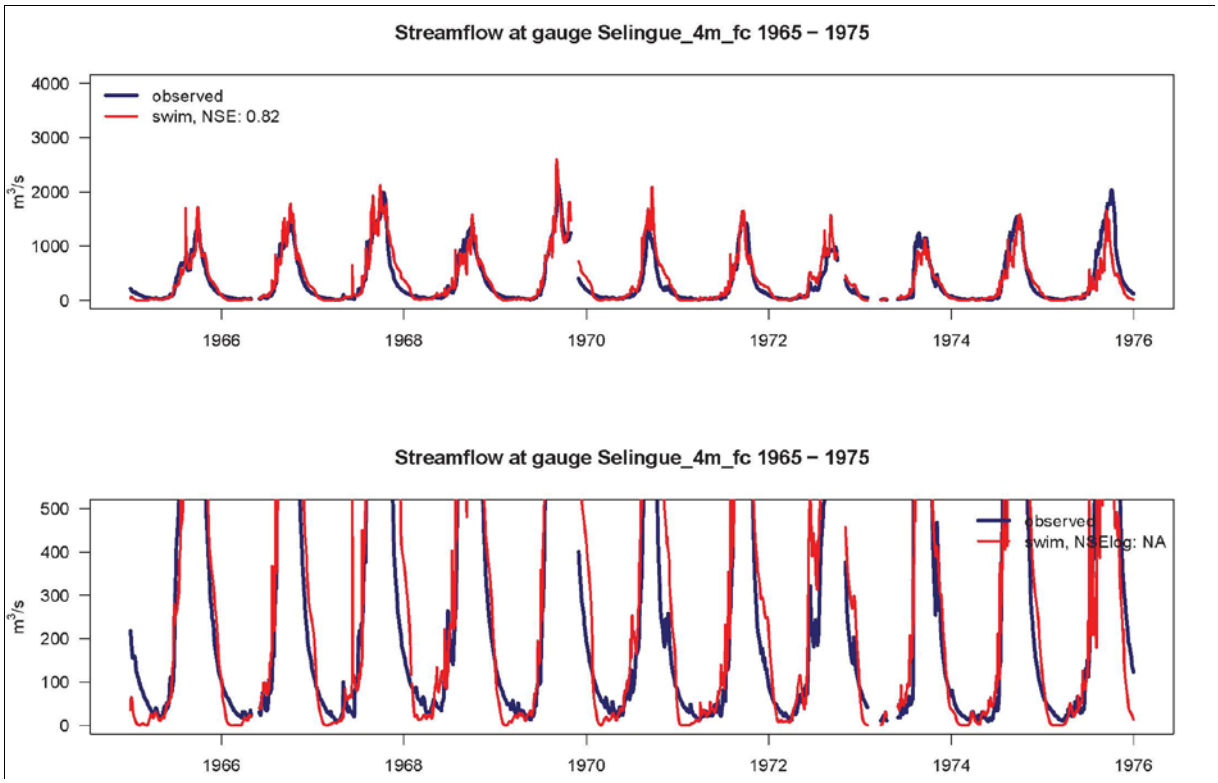

Figure 3-27 and 3-28: Comparison of monitored and simulated flow at gauge Sélingué (1965-1975) with a focus on low flow pattern: calibration phase

3.6 CONCLUSION

The results of the calibration and validation processes of the model SWIM present satisfactory results to further extend analyses of drought variability and impact in the Niger case study. The model will be then employed in the core of DEWFORA project to simulate short-term hydrological forecast and long term hydrological projections in order to assess drought persistence and risk under a range of upstream water resources management. The final objective is to translate modeling results into explicit indices measuring the socioeconomic vulnerability and the potential adaptive capacities of specific water uses in the Inner Niger Delta. Current efforts to setup a model to analyze the entire Niger River are initiated and under process but the main interest for DEWFORA project remain to deliver appropriate answers at the local scale with a focus on the Inner Niger Delta actors. Although the report is based on comprehensive modelling results, many factors were not considered yet. For instance, the existing Talo dam, the Markala barrage, and the planned dam in Djenné at the River Bani were not yet included in the model. The impacts of the extension of irrigation areas in the Upper Niger catchment, which is expected to have impacts on the hydrology, still need to be integrated as well. Moreover, social and environmental consequences of the investigated adaptive measure, proposed by the stakeholder platform and Wetlands International, need to be now considered. Although several integrated studies, such as those by Zwarts et al. (2005); Kuper et al. (2003) have been conducted, there is a need for more detailed studies with specific focuses on the one hand but on the other hand

there is also a need for more process-based and integrated assessments of the highly complex socio-ecological system of the Inner Niger Delta and the Upper Niger Basin as a whole.

4. REFERENCES

Limpopo River Basin

Allen, R. G., L. Pereira, D. Raes & M. Smith (1998) FAO Irrigation and drainage paper No. 56. *Rome: Food and Agriculture Organization of the United Nations*, 26-40.

Balsamo, G., S. Boussetta, P. Lopez & L. Ferranti. 2010. Evaluation of ERA-Interim and ERA-Interim-GPCP-rescaled precipitation over the USA. ed. ECMWF ERA Report Series.

Clapp, R. B. & G. M. Hornberger (1978) Empirical equations for some soil hydraulic properties. *Water Resour. Res.,* 14, 601-604.

Dee, D. P., S. M. Uppala, A. J. Simmons, P. Berrisford, P. Poli, S. Kobayashi, U. Andrae, M. A. Balmaseda, G. Balsamo, P. Bauer, P. Bechtold, A. C. M. Beljaars, L. van de Berg, J. Bidlot, N. Bormann, C. Delsol, R. Dragani, M. Fuentes, A. J. Geer, L. Haimberger, S. B. Healy, H. Hersbach, E. V. Hólm, L. Isaksen, P. Kållberg, M. Köhler, M. Matricardi, A. P. McNally, B. M. Monge-Sanz, J. J. Morcrette, B. K. Park, C. Peubey, P. de Rosnay, C. Tavolato, J. N. Thépaut & F. Vitart (2011) The ERA-Interim reanalysis: configuration and performance of the data assimilation system. *Quarterly Journal of the Royal Meteorological Society,* 137, 553-597.

DEWFORA. 2011. WP4-D4.5 - Available continental scale hydrological models and their suitability for Africa. DEWFORA project - EU FP7.

---. 2012a. WP6-D6.1 - Implementation of improved methodologies in comparative case studies - Inception report for each case study. DEWFORA project - EU FP7.

---. 2012b. WP6-D6.3 - Testing of drought indicators at Pan-African level (Draft version). DEWFORA project - EU FP7.

Dumenil, L. & E. Todini (1992) A rainfall-runoff scheme for use in the Hamburg climate model. *Advances in Theoretical Hydrology, A Tribune to James Dooge*, 129-157.

Dürr, H. H., M. Meybeck & S. H. Dürr (2005) Lithologic composition of the Earth's continental surfaces derived from a new digital map emphasizing riverine material transfer. *Global Biogeochemical Cycles,* 19, GB4S10.

FAO. 1997. *Irrigation Potential in Africa: A Basin Approach*. FAO.

---. 2003. The digital soil map of the world (Version 3.6).

GRDC. The Global Runoff Data Centre, D -56002 Koblenz, Germany.

Hagemann, S. 2002. *An improved land surface parameter dataset for global and regional climate models*. Max-Planck-Institut für Meteorologie.

Hagemann, S., M. Botzet, L. Dümenil & B. Machenhauer. 1999. *Derivation of global GCM boundary conditions from 1 km land use satellite data*. Max-Planck-Institut für Meteorologie.

Huffman, G. J., R. F. Adler, D. T. Bolvin & G. Gu (2009) Improving the global precipitation record: GPCP version 2.1. *Geophys. Res. Lett,* 36, L17.

LBPTC. 2010. Joint Limpopo River Basin Study Scoping Phase. Final Report. BIGCON Consortium. Limpopo Basin Permanent Technical Committee.

Lehner, B. & P. Doll (2004) Development and validation of a global database of lakes, reservoirs and wetlands. *Journal of Hydrology,* 296, 1-22.

Lehner, B. & P. Döll (2004) Global Lakes and Wetlands Database GLWD. *GLWD Docu mentation*.

McKee, T. B., N. J. Doesken & J. Kleist. 1993. The relationship of drought frequency and duration to time scales. 179-183. American Meteorological Society Boston, MA.

Moody, J. A. & B. M. Troutman (2002) Characterization of the spatial variability of channel morphology. *Earth Surface Processes and Landforms,* 27**,** 1251-1266.

Nalbantis, I. & G. Tsakiris (2009) Assessment of Hydrological Drought Revisited. *Water Resources Management,* 23**,** 881-897.

Olson, J. (1994a) Global ecosystem framework-definitions. *USGS EROS Data Center Internal Report, Sioux Falls, SD,* 37.

--- (1994b) Global ecosystem framework-translation strategy. *USGS EROS Data Center Internal Report, Sioux Falls, SD,* 39.

Siebert, S., P. Döll, S. Feick, J. Hoogeveen & K. Frenken 2007. Global Map of Irrigation Areas version 4.0.1. ed. F. a. M. Johann Wolfgang Goethe University, Germany / Food and Agriculture Organization of the United Nations. Rome, Italy.

Sloan, P. G. & I. D. Moore (1984) Modeling subsurface stormflow on steeply sloping forested watersheds. *Water Resour. Res.,* 20**,** 1815-1822.

Sperna Weiland, F. C., C. Tisseuil, H. H. Dürr, M. Vrac & L. P. H. van Beek (2012) Selecting the optimal method to calculate daily global reference potential evaporation from CFSR reanalysis data for application in a hydrological model study. *Hydrol. Earth Syst. Sci.,* 16**,** 983-1000.

Sperna Weiland, F. C., L. P. H. van Beek, J. C. J. Kwadijk & M. F. P. Bierkens (2011) On the Suitability of GCM Runoff Fields for River Discharge Modeling: A Case Study Using Model Output from HadGEM2 and ECHAM5. *Journal of Hydrometeorology,* 13**,** 140-154.

Szczypta, C., J. C. Calvet, C. Albergel, G. Balsamo, S. Boussetta, D. Carrer, S. Lafont & C. Meurey (2011) Verification of the new ECMWF ERA-Interim reanalysis over France. *Hydrology and Earth System Sciences,* 15**,** 647-666.

USGS EROS Data Center. 2002. Africa Land Cover Characteristics Data Base Version 2.0.

---. 2006. Hydro1K Africa

van Beek, L. P. H. 2008. Forcing PCR-GLOBWB with CRU data. Utrecht University.

van Beek, L. P. H. & M. F. P. Bierkens. 2009. The Global Hydrological Model PCR-GLOBWB: Conceptualization, Parameterization and Verification. Utrecht, The Netherlands: Utrecht University, Faculty of Earth Sciences, Department of Physical Geography.

Water Affairs Republic of South Africa. Hydrological Services - Surface Water (Data, Dams, Floods and Flows).

Niger river basin

Andersen, I., Dione, O., Jarosewich-Holder, M., Olivry, J. 2005. The Niger River Basin, A Vision for Sustainable Management. Edited by K.G. Golitzen. Washington D.C.; The World Bank.

Berrisford, P., D. Dee, M. Fielding, M. Fuentes, P. Kallberg, S. Kobayashi, and S. M. Uppala, 2009: The ERA-Interim Archive, *ERA Report Series*, **No. 1**, ECMWF, Shinfield Park, Reading, UK.

BRL, and DHI. 2007a. *Etudes Sur L'élaboration Du Plan d'Action De Développement Durable (PADD) Du Bassin Du Niger: Phase 1: Bilan Diagnostic*. NIGER BASIN AUTHORITY (NBA).

BRL, and DHI. 2007b *Etudes Sur L'élaboration Du Plan d'Action De Développement Durable (PADD) Du Bassin Du Niger: Phase II : Schéma Directeur D'aménagement Et De Gestion*. NIGER BASIN AUTHORITY (NBA). 2007.

Dee, D. P., and Coauthors, 2011: The ERA-Interim reanalysis: configuration and performance of the data assimilation system, *Quart. J. Roy. Meteor. Soc.*, **137**(656), 553-597, doi: 10.1002/qj.828.dee

FAO, IIASA, ISRIC, ISSCAS, & JRC (2009). Harmonized world soil database (version 1.1). FAO, Rome, Italy and IIASA, Laxenburg, Austria , .

Jarvis, A., Reuter, H., Nelson, A., & Guevara, E. (2008). Hole-filled seamless srtm data v4, international centre for tropical agriculture (ciat), available from http://srtm.csi.cgiar.org.

Koch, Hagen, Stefan Liersch, Fred Hattermann, Jan Cools, and Bakary Kone. 2011. "Vulnerability of Agricultural Production in the Inner Niger Delta to Water Resources Management Under Climate Variability and Change" presented at the World Water Week, August, Stockholm.

Kuper, M., C. Mullon, Y. Poncet, and E. Benga. 2003. "Integrated Modelling of the Ecosystem of the Niger River Inland Delta in Mali." *Ecological Modelling* 164 (1): 83–102.

Krysanova, V., Meiner, A., Roosaare, J., & Vasilyev, A. (1989). Simulation modelling of the coastal waters pollution from agricultural watershed. Ecological Modelling , 49 , 7–29.

Krysanova , V., Müller-Wohlfeil, D.I. and Becker, A., 1998, Development and test of a spatially distributed hydrological water quality model for mesoscale watersheds, Ecological Modeling 106,p. 261–289.

Krysanova, V., Wechsung, F., Arnold, J., Srinivasan, R., Williams, J., 2000a, PIK Report No.69: SWIM (Soil and Water Integrated Model), User Manual, Potsdam Institüt für Klimafolgenforschung.

Krysanova, V., Becker, A., 2000b, Integrated modeling of hydrological processes and nutrient dynamics at the river basin scale, Hydrobiologia 410, p. 131–138.

Krysanova, V. Hattermann, F., Wechsung, F., 2005, Development of the ecohydrological model SWIM for regional impact studies and vulnerability assessment, Hydrological Processes 19, p.763–783

Liersch, Stefan. 2011. "How to Integrate Wetland Processes ?" presented at the SWAT conference 2011, June, Toledo, Spain.

Liersch, S., Koch, H., Aich, V., Reinhardt J., Fournet S., Hattermann F.F., 2012a, Constraints of future freshwater resources in the Upper Niger Basin – Has the human-environmental system of the Inner Niger Delta a chance to survive?, 6th International Congress on Environmental Modelling and Software (iEMSs), Leipzig, Germany

Liersch, S., Cools, J., Kone, B., Koch, H., Diallo, M., Reinhardt J., Fournet S., Aich V., Hattermann F.F., 2012b, Vulnerability of rice production in the Inner Niger Delta to water resources management under climate variability and change, Environmental Science & Policy, under review.

Marie, J., Pierre Morand, and H. N'Djim, eds. 2007. *The Niger River's Future : Synthesis and Recommendations, Analytical Chapters*. Expertise Collégiale. IRD ; IER. http://www.documentation.ird.fr/hor/fdi:010041819.

Orange, Didier, Robert Arfi, Marcel Kuper, Pierre Morand, and Yveline Poncet, eds. 2002. *Gestion Intégrée Des Ressources Naturelles En Zones Inondables Tropicales*. Colloques Et Séminaires. IRD ; CNRST. http://www.documentation.ird.fr/hor/fdi:010030354.

Orlowsky, B., Bothe, O., Fraedrich, K., Gerstengarbe, F.-W. & Zhu, X. (2010). Future climates from bootstrapped weather analogues: an application to the Yangtze river basin. Journal of Climate, 23: 3509-3524

Orlowsky, B. & Fraedrich, K. (2009). Up-scaling European surface temperatures to North-Atlantic circulation pattern statistics. International Journal of Climatology, 29: 839-849

Orlowsky, B., Gerstengarbe, F.-W. & Werner, P. (2008). A resampling scheme for regional climate simulations and its performance compared to a dynamical RCM. Theoretical and Applied Climatology, 92: 209-223

Uppala, S.M., Kållberg, P.W., Simmons, A.J., Andrae, U., da Costa Bechtold, V., Fiorino, M., Gibson, J.K., Haseler, J., Hernandez, A., Kelly, G.A., Li, X., Onogi, K., Saarinen, S., Sokka, N., Allan, R.P., Andersson, E., Arpe, K., Balmaseda, M.A., Beljaars, A.C.M., van de Berg, L., Bidlot, J., Bormann, N., Caires, S., Chevallier, F., Dethof, A., Dragosavac, M., Fisher, M., Fuentes, M., Hagemann, S., Hólm, E., Hoskins, B.J., Isaksen, L., Janssen, P.A.E.M., Jenne, R., McNally, A.P., Mahfouf, J.-F., Morcrette, J.-J., Rayner, N.A., Saunders, R.W., Simon, P., Sterl, A., Trenberth, K.E., Untch, A., Vasiljevic, D., Viterbo, P., and Woollen, J. 2005: The ERA-40 re-analysis. Quart. J. R. Meteorol. Soc., 131, 2961-3012.doi:10.1256/qj.04.176

Werner, P. & Gerstengarbe, F.-W. (1997). Proposal for the development of climate scenarios. Climate Research, 8: 171-182

Zwarts, L., P. van Beukering, B. Kone, and E. Wymenga. 2005. *The Niger, a lifeline, Effective water management in the Upper Niger Basin*. RIZA IVM / WISO / A&W. http://www.altwym.nl/uploads/file/133Executive%20summary%20-%20The%20Niger,%20a%20lifeline.pdf.

5. APPENDICES

5.1 USER MANUAL FOR THE LIMPOPO HYDROLOGICAL MODEL

The hydrological model PCR-GLOBWB is a script coded in Python-PCRaster. The user manuals of both Python and PCRaster are available online and can be found at:

- Python: http://docs.python.org/release/2.5/
- PCRaster: http://pcraster.geo.uu.nl/support/documentation/

To run the tailored hydrological model for the Limpopo river basin go through the following steps:

0. Before getting started

0.1 Installing python and PCRaster

Python 2.5 and PCRaster should be installed in your PC before you can run the model.

1. Download PCRaster from http://pcraster.geo.uu.nl/downloads/ and read the prerequisites and installation procedure.
2. Install PC-Raster in C:\PCRaster
3. Go to the python webpage indicated in "Prerequisites" and download Python 2.5.4. Newer versions of python do not work with PCRaster.
4. Install Python 2.5 in C:\python25
5. Install python libraries: numpy and scipy in C:\python25
6. Download from http://pypi.python.org/pypi/ and install:
    - matplotlib for python 2.5
    - pyreadline
    - ipython
    - pyqt
    - spyder

I. Getting started

I.1 Create a directory for the Limpopo Model

The directory or folder for the model should be organized as showed in the following figure.

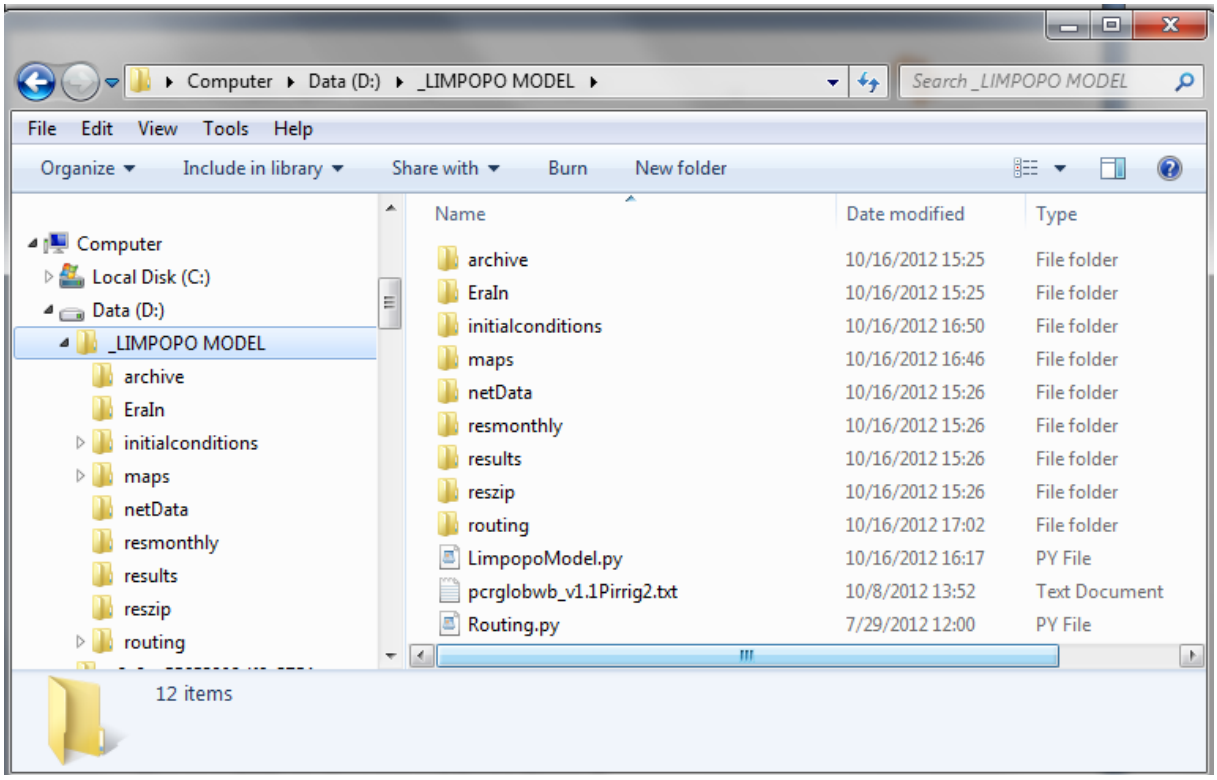

The folder "archive" contains a folder for each year named: ERA_year with all the meteorological forcing data for that year. Each year's folder contains evapotranspiration data (EVyear00.day), temperature data (tayear00.day) and precipitation data (rayear00.day). The files are in PCRaster format (see following figure).

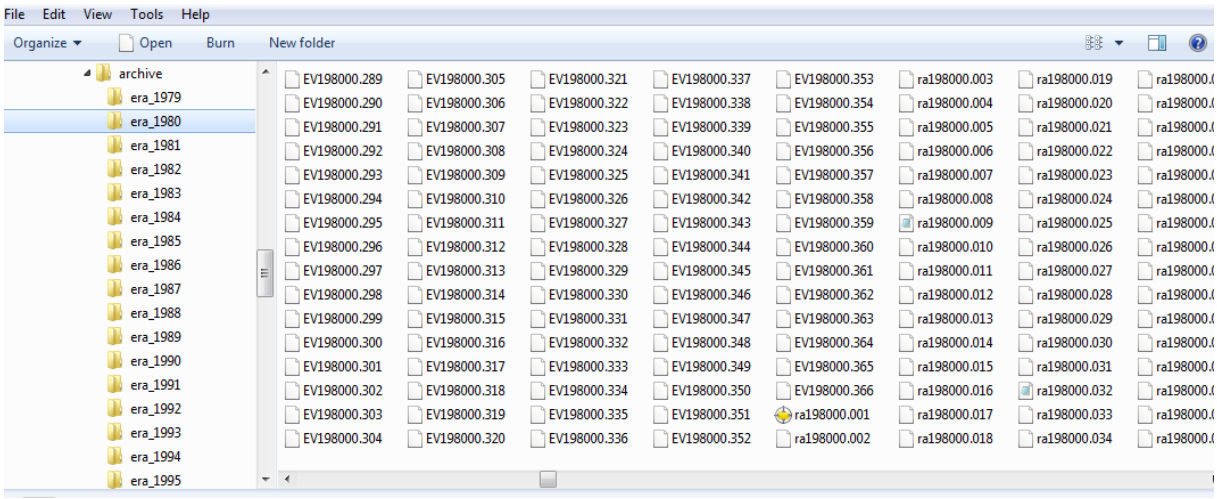

The folder "EraIn" should remain empty as the model uses this folder to copy the meteorological data from each year before running the yearly water balance model.
In the same way, the folders "netData", "results", "resmonthly" and "reszip" are empty and should remain that way as the model uses these folders while is running. The results of the model will be in the folder "netData".
The folder "maps" contain all the input parameter maps and tables required by the hydrological model (see following figure).

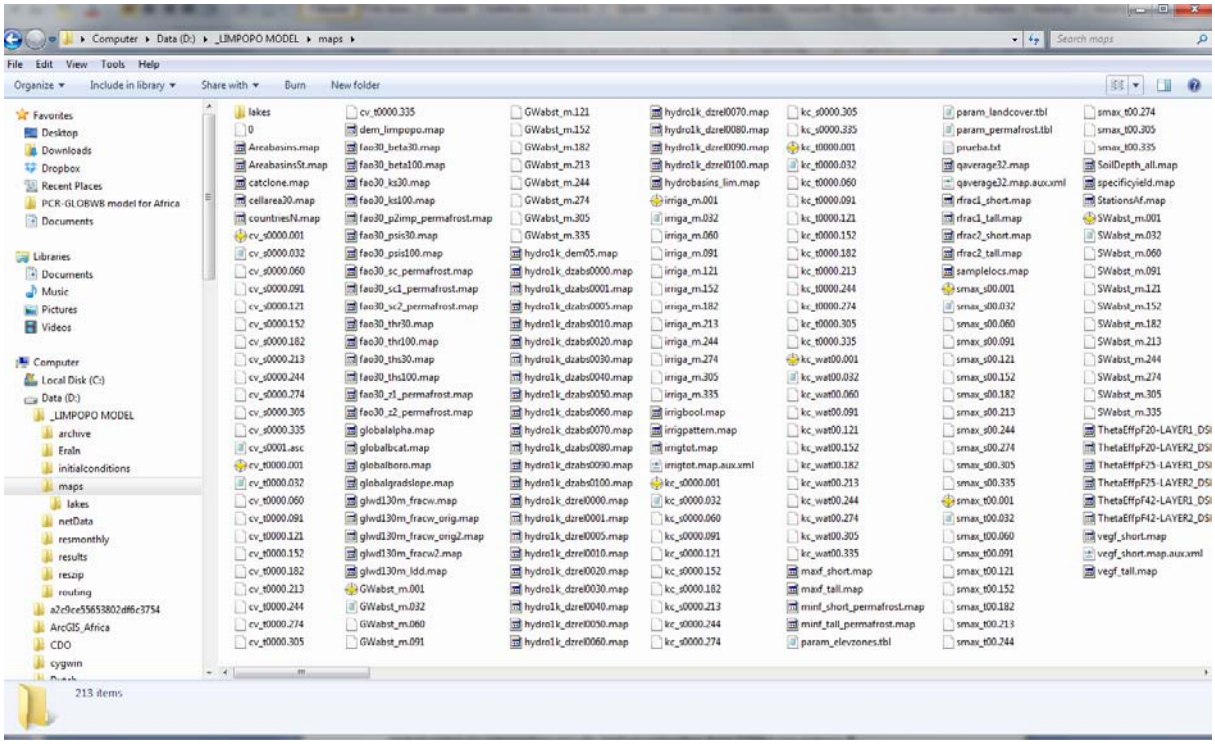

The folder "intitialconditions" contains only one folder named "startrun" with some initial maps for the model to run. Folders for each year's initial conditions will be created during the model run.

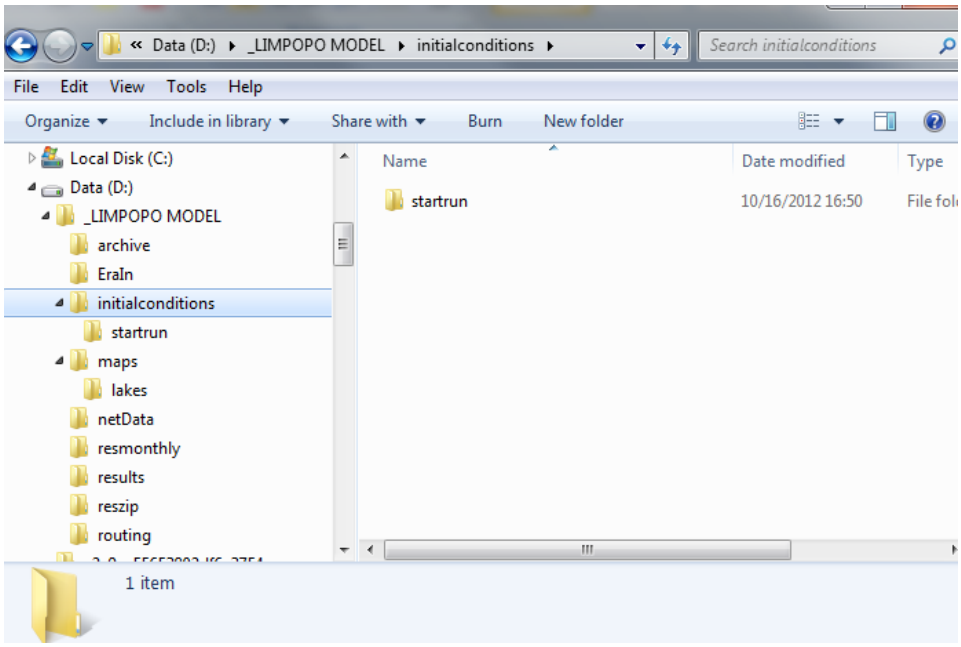

The folder "routing" contains only two folders: "maps" and "results". The folder "maps" contain some maps necessary for the routing module such as channel width and depth, lakes volumes, etc. (see following figure). The folder "results" is initially empty.

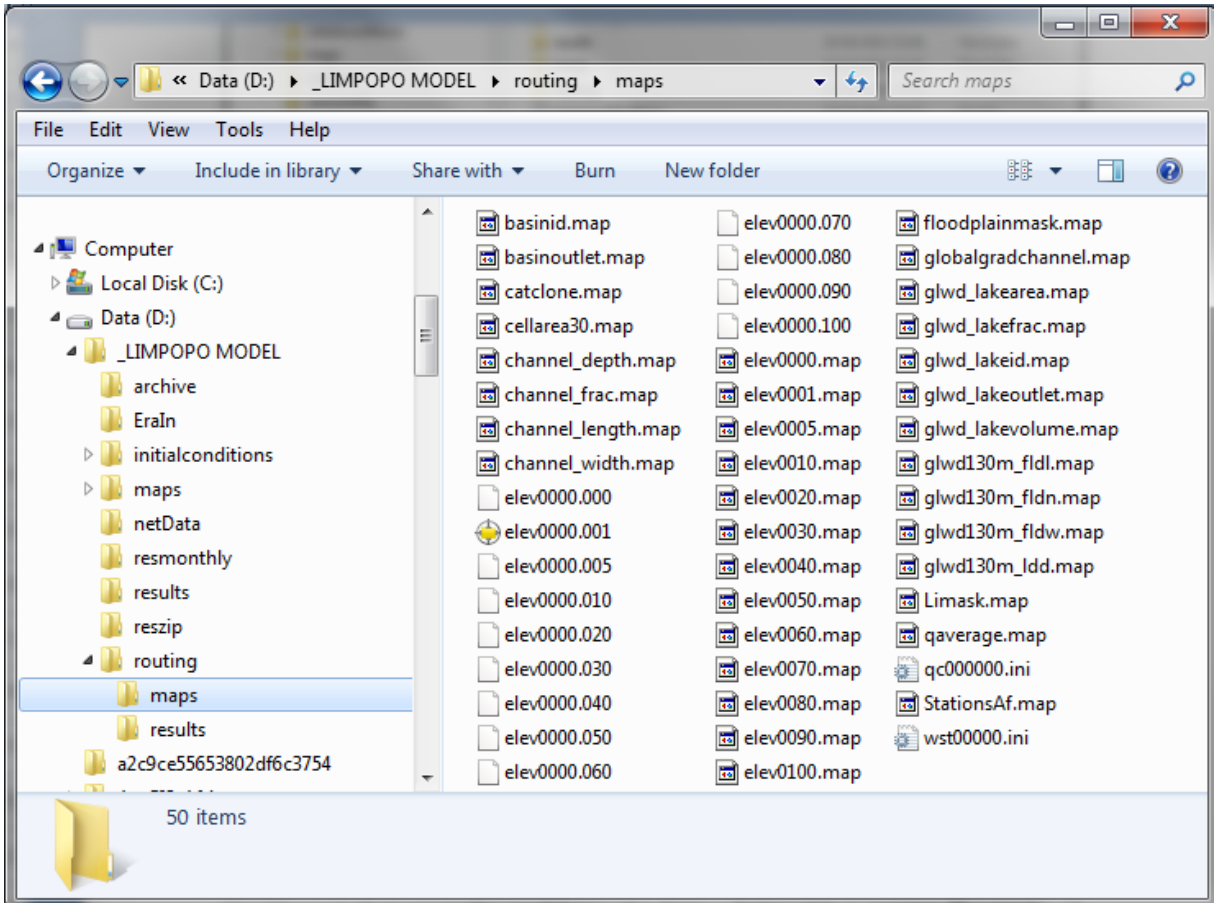

II. Run the Limpopo model

II.1 Run the Hydrological Model

Open the script "LimpopoModel.py" in Spyder or any other Python interface and run it. This run takes approximately 10 hours and produce PCRaster result maps including runoff, soil moisture, actual evaporation, root stress and others in a daily time step. Other result maps are produced in an annual time step. The results are located in the folder "netData".

II.2 Run the Routing Model

Open the script "Routing.py" in Spyder or any other Python interface and run it. This run takes approximately 10 hours and produces the routed channel runoff result maps in a daily time step. The results are located in the folder "routing/results".

5.2 USER MANUAL FOR THE NIGER HYDROLOGICAL MODEL

The user manual delivered for the Niger hydrological model comprises the materials from the SWIM workshop 2010 hold in the Potsdam Institute for Climate Impact Research in Germany. One of the objectives of the workshop was to train Karamoko SANOGO, a hydrologist from Wetlands International, the Malian partner in DEWFORA project in order to make accessible scientific outcomes to a large stakeholder audience. The aim was also that the Malian agency of Wetlands International, first, understands the processes governing the eco-hydrological SWIM, second, benefits from a transfer of capacity building directly applied to the case study by having the skills to use SWIM and, third, disseminate results to the stakeholders by interpreting results and uncertainties from SWIM simulations.